

**On the Genetic Basis of Pigment Pattern
Diversification in *Danio* Fish**

Dissertation

der Mathematisch-Naturwissenschaftlichen Fakultät
der Eberhard Karls Universität Tübingen
zur Erlangung des Grades eines
Doktors der Naturwissenschaften
(Dr. rer. nat.)

vorgelegt von
Marco Podobnik
aus Kelheim

Tübingen
2022

Gedruckt mit Genehmigung der Mathematisch-Naturwissenschaftlichen Fakultät der
Eberhard Karls Universität Tübingen.

Tag der mündlichen Qualifikation: 09.02.2023

Dekan: Prof. Dr. Thilo Stehle

1. Berichterstatter: PD Dr. Uwe Irion

2. Berichterstatter: Prof. Dr. Nico Michiels

CONTENTS

PREAMBLE.....	1
SUMMARY.....	1
ZUSAMMENFASSUNG	2
PUBLICATIONS.....	4
INTRODUCTION.....	5
Pigment pattern variation in teleost fish.....	5
Neural crest as the source of pigment cell type diversity.....	9
Development of the stripe pattern in <i>D. rerio</i>	12
Identification of genetic evolution and its molecular basis	17
Evolution of pigment patterning in <i>Danio</i> species	19
Objectives.....	21
RESULTS.....	23
CHAPTER ONE.....	23
Complementation tests for pattern diversification in <i>Danio</i> fish.....	23
CHAPTER TWO	24
Cis-regulatory evolution in <i>kcnj13</i> during pattern variation in <i>Danio</i> fish	24
DISCUSSION.....	25
Evolutionary developmental biology	25
Pigment pattern diversification in <i>Danio</i> fish.....	26
Genetic basis of pigment cell interactions in stripes and bars	26
Complementation tests in hybrids identify diverged genes.....	27
Cell-autonomy and endogenous expression of <i>kcnj13</i>	28
Pigment cell shape acquisition by <i>kcnj13</i> function.....	29
Cis-regulatory evolution in <i>kcnj13</i>	31
Closing remarks.....	32
GLOSSARY	33
ACKNOWLEDGMENTS.....	34
THESIS APPENDIX I.I	35
THESIS APPENDIX I.II	65
THESIS APPENDIX II	77
REFERENCES.....	112

PREAMBLE

The 21st century offers the opportunity to follow development as a concerted action at many levels of biological organization, from molecules, to cells, tissues and organs within the individual organism. An evolutionary context for development is increasingly provided by a zoo of currently studied species. Methods such as genetic screens, sequencing, mapping and genetic engineering, primarily using CRISPR/Cas systems, are being performed to uncover the genetic basis of morphological variation during natural speciation or domestication. Advances in molecular, genetic and imaging technologies allow to understand the cellular basis of development by labelling and tracking of individual cell populations. Computational and “omics” approaches along with classical techniques give new insights and provide promising directions. The future of evolutionary developmental biology is bright. Teleost fishes, especially the *Danio* species, are excellent models to study pigment pattern formation and evolution in vertebrates using a power battery of available methods.

SUMMARY

The genetic basis of morphological variation provides a major topic in evolutionary developmental biology. Fish of the genus *Danio*, containing the model species zebrafish, *Danio rerio*, represent a system to study pigment pattern diversification as they display amazingly different patterns ranging from horizontal stripes, to vertical bars or spots. Stripe formation in *D. rerio* is a self-organizing process based on cell-contact mediated interactions between melanophores, xanthophores and iridophores. Little is known about the genetic and cellular basis of pigment pattern formation and evolution in other *Danio* species. Genes known to be involved in stripe formation in *D. rerio* might have functionally diverged to produce a pattern of vertical bars in its sibling species, *Danio aesculapii*. In collaboration with my colleagues, I showed by mutant analysis that the same three pigment cell types are required for bar formation. Reciprocal hemizyosity tests with genes, which are known to be involved in interactions between the pigment cells in *D. rerio*, identified the potassium channel gene *kcnj13*, but not the gap junction genes, *gja4* and *gja5b*, or the adhesion molecule gene *igsf11* as diverged between the two species. Further complementation tests with eight additional *Danio* species suggested evolutionary change in pigment patterns

through repeated and independent functional divergences in *kcnj13*, *gja5b* and *igsf11* across the genus. Focusing on *kcnj13*, we used in vivo imaging of transgenic reporters, transplantation experiments and lineage tracing of pigment cell population in chimeras and found that the shapes of all three types of pigment cells are affected in the *D. rerio* mutants, although the gene function is only required in melanophores. These differences, similar to the ones in *D. rerio* mutants, were also partly observed between *D. rerio* and *D. aesculapii*, might therefore underlie the evolutionary change of the divergent patterns. Using molecular, biochemical and bioinformatic analyses we confirmed the homo-tetrameric structure of the channel, which explains the dominant phenotype of most known mutations. A transcriptome-wide allele-specific expression analysis indicated higher expression of the *D. rerio* allele in hybrids between the two species. Together with our findings that the protein from both species are able to rescue the stripe phenotype in transgenic rescue lines, this confirmed cis-regulatory evolution of *kcnj13*. Species-specific pigment cell interactions could be important factors contributing to the variation in pigment patterns. This work highlights the genetic complexity underlying the diversification of pigment patterning and shows that the evolutionary history of biodiversity can be reconstructed in *Danio* fish.

ZUSAMMENFASSUNG

Die genetische Grundlage der morphologischen Variation ist ein wichtiges Thema in der evolutionären Entwicklungsbiologie. Fische der Gattung *Danio*, zu der auch der Modellorganismus Zebrafisch, *Danio rerio* (auch: Zebrafisch), gehört, stellen ein System zur Untersuchung der Diversifizierung von Pigmentmustern dar, da sie erstaunlich unterschiedliche Muster aufweisen, die von horizontalen Streifen bis zu vertikalen Balken oder Tupfen reichen. Die Streifenbildung in *D. rerio* ist ein selbstorganisierender Prozess, der auf durch Zellkontakte vermittelten Wechselwirkungen zwischen Melanophoren, Xanthophoren und Iridophoren beruht. Über die genetischen und zellulären Grundlagen der Bildung und Entwicklung von Pigmentmustern bei anderen *Danio*-Arten ist wenig bekannt. Gene, von denen bekannt ist, dass sie bei *D. rerio* an der Streifenbildung beteiligt sind, könnten sich funktionell divergierthaben, dass sie bei der Geschwisterart *Danio aesculapii* ein Muster aus vertikalen Balken erzeugen. In Zusammenarbeit mit meinen KollegInnen zeigte ich mithilfe einer Mutantanalyse, dass die gleichen drei Pigmentzelltypen für

die Balkenbildung erforderlich sind. Reziproke Hemizygotestests mit Genen, von denen bekannt ist, dass sie an den Interaktionen zwischen den Pigmentzellen in *D. rerio* beteiligt sind, zeigten, dass das Kaliumkanal-Gen *kcnj13*, aber nicht die Gap Junction-Gene *gja4* und *gja5b* oder das Adhäsionsmolekül-Gen *igsf11* zwischen den beiden Arten divergiert ist. Ausgedehntere Komplementierungstests mit acht weiteren *Danio*-Arten deuteten darauf hin, dass sich die Pigmentmuster durch wiederholte und unabhängige funktionelle Divergenzen in *kcnj13*, *gja5b* und *igsf11* innerhalb der Gattung evolutionär verändert haben. Wir konzentrierten uns auf *kcnj13* und verwenden In-vivo-Bildgebung von transgenen Reportern, Transplantationsexperimente und die Verfolgung von Pigmentzellenpopulation in Chimären und stellten fest, dass die Formen aller drei Arten von Pigmentzellen in den *D. rerio*-Mutanten beeinträchtigt sind, obwohl die Genfunktion nur in Melanophoren erforderlich ist. Diese Unterschiede, die denen in *D. rerio*-Mutanten ähneln, wurden teilweise auch zwischen *D. rerio* und *D. aesculapii* beobachtet und könnten daher dem evolutionären Wandel der divergenten Muster zugrunde liegen. Durch molekulare, biochemische und bioinformatische Analysen bestätigten wir die homo-tetramerische Struktur des Kanals, die den dominanten Phänotyp der meisten bekannten Mutationen erklärt. Eine transkriptomweite allelspezifische Expressionsanalyse zeigte eine höhere Expression des *D. rerio*-Allels in Hybriden zwischen den beiden Arten. Zusammen mit unseren Erkenntnissen, dass das Protein beider Arten in der Lage ist, den Streifenphänotyp in transgenen Rettungslinien zu retten, bestätigte dies die cis-regulatorische Evolution von *kcnj13*. Speziesspezifische Zell-Zell-Interaktionen könnten daher wichtige Faktoren sein, die zur Variation der Pigmentmuster beitragen. Diese Arbeit verdeutlicht die genetische Komplexität, die der Diversifizierung der Pigmentmusterung zugrunde liegt, und zeigt, dass die Evolutionsgeschichte der Artenvielfalt im *Danio*-Genus rekonstruiert werden kann.

PUBLICATIONS

Unpublished:

Podobnik, M., Nüsslein-Volhard, C. and Irion U. (2022a) Genus-wide complementation tests for pigment pattern diversification.

Published:

Podobnik, M., Frohnhöfer, H.G., Dooley, C.M., Eskova, A., Nüsslein-Volhard, C., and Irion, U. (2020) Evolution of the potassium channel gene *kcnj13* underlies colour pattern diversification in *Danio* fish.

Nature communications, [<https://doi.org/10.1038/s41467-020-20021-6>]

Podobnik, M., Singh, A.P., Zu, F., Dooley, C.M., Frohnhöfer, H.G., Firlej, M., Elhabashy, H., Weyand, S., Weir, J.R., Lu, J., Nüsslein-Volhard, C., Irion, U. (2022b) Cis-regulatory evolution in the potassium channel gene *kcnj13* during pigment pattern diversification in *Danio* fish.

bioRxiv, [<https://doi.org/10.1101/2022.12.05.519077>]

Not included in this manuscript:

Arndt, H., Ahlers, J., Amano, C., Augustin, N., Dangl, G., Feuling, Y., Herrero, T., Hohlfeld, M., Jeuck, A., Marx, M., Mähner, B., Meißner, R., Meyer, C., **Podobnik, M.**, Palgan, D., Paulmann, C., Prausse, D., Romankiewicz, T., Schade, M., Scherwaß, A., Schiwitza, S., Schoenle, A., Schuffenhauer, I., Sintes, E., Stefanschitz, J., Werner, J., Wildermuth, B., Zivaljić, S. (2017) DEEP MICROBES - Deep-sea Microbial Food Webs of the Atlantic and Caribbean, BRIGHT FLOWS - Investigation of Young Non-hotspot and Non-MOR-related Volcanism on 20 Ma Crust South of Kane Fracture Zone, Cruise No. M139, July 7 - August 8, 2017, Cristóbal (Panamá) - Mindelo (Cabo Verde).

METEOR-Berichte (Vol. M139, pp. 1-90) Gutachterpanel Forschungsschiffe.

[https://doi.org/10.2312/cr_m139]

INTRODUCTION

The diversity of pigment patterns in teleost fish is a beautiful example of natural morphological variation, commonly known as a form of biodiversity. The patterns are important targets for natural and sexual selection. They are readily visible and therefore provide an excellent opportunity to study the genetic and cellular basis of morphological variation. Teleost species of the genus *Danio*, including the model species zebrafish, *Danio rerio*, form amazingly different pigment patterns. In this thesis, I use *D. rerio* to ask what is the molecular, genetic and cellular basis for pattern diversification in the *Danio* genus. To contextualize my work, I will first introduce concepts required in the field of pigment pattern variation in teleosts. Briefly, the patterns are composed of different types of pigment cells, which arose through the evolutionary innovation of the neural crest in vertebrates. Stripe formation in *D. rerio* depends on differentiation and migration of pigment cells and interactions among them. Little is known about these developmental processes in other *Danio* species, but they might have diverged to diversify the patterns across the genus. I describe general approaches, e.g. interspecific complementation tests, to identify functionally diverged genes and which of these methods have already been applied in the context of pigment pattern variation in *Danio* species. In Chapter One I report the identification of diverged genes through complementation tests between ten different *Danio* species. In Chapter Two I describe a novel function in pigment cell behaviour for one of these genes in the striped *D. rerio* and characterize the molecular basis for its functional divergence in the barred sister species *D. aesculapii*. I argue that *Danio* species provide a unique opportunity to reconstruct the evolutionary history of pigment pattern variation in vertebrates.

Pigment pattern variation in teleost fish

Teleosts (Teleostei) belong to the Neopterygii subclass of ray-finned fishes (Actinopterygii). Actinopterygians are occasionally introduced as the largest and most successful group of fishes in terms of number of species; but it is specifically the teleosts, which comprise over half of all living vertebrate species, or contribute 23,000 of 24,000 actinopterygians, i.e. 96 % of all living fish species. Teleosts show an amazing variation in a multitude of traits including diverse pigment patterns, which are adaptive with many functions such as photoprotection, thermoregulation, and visual

communication within and across species^{1,2}. Chromatophores, or pigment cells, contain the pigments or crystalline structures. Pigments change the colour of reflected light as the result of wavelength-dependent absorption. Structural colouration is due to the selective reflectance of incident light caused by the physical nature of a structure. The latter unfolds in wide areas of the available colour space, whereas pigments are more restricted due to their chemical nature. Physiological cues, which can act quickly over short or long distances in the animals, control body colouration through reversible changes of the intracellular localization of pigments, the configuration of crystalline units, and alterations of cell shapes. Pigment aggregation or cellular contraction render affected body regions light, while pigment dispersal or cellular expansion darken the area. Alterations in the configurations of crystalline structures may change hue and/or brightness. This context-dependent plasticity enables rapid switching between conspicuous and inconspicuous appearance for communication and camouflage, respectively^{3,4}. The patterns are also used for visual crypsis to avoid interactions between prey and predators. Countershading is a common camouflage strategy in animals. By contrast, conspicuous patterns are displayed by prey to advertise their toxicity (aposematism) or to imitate dangerous species (mimicry). The patterns are also used for social signalling, like in kin recognition or mate choice. While different functions of patterns are appreciated, little is still known about how the perception and cognition systems of interacting individuals integrate visual and other ethologically relevant cues such as touch and odours. Patterns are evolutionarily highly significant, although even their complete loss is not necessarily lethal but can be due to regressive adaptation. Cavefish populations differ in the expression of pigmentation, visual sensory systems and sleep behaviour dependent on dark or light habitats^{5,6}. Such evolutionary targets can (co-)evolve rapidly. They vary extensively within a single genus or resemble distant genera with similar ecological niches. As “deep genetic homology” and “selection’s capacity for iterating nearly identical adaptations from scratch” are often difficult to differentiate⁷, it often remains unclear to which extent similar patterns evolved in parallel or convergently within or across genera. In summary, patterns have many different functions, are trade-offs between opposing evolutionary drivers, and are important for survival and speciation.

So far, only a small fraction of teleost species is used to study the variation in pigment patterning. They were often selected for a variety of reasons⁸, mostly favouring species that show remarkable features of development or behaviour, and are genetically tractable or optically transparent. Some of them are situated in a phylogeny of closely related species, or subspecies, which vary tremendously in pigmentation and pigment patterning. Teleosts in which these traits are studied are cichlids⁹⁻¹¹, goldfish¹², cavefish^{5,6}, anemonefish^{13,14}, guppies¹⁵, swordtail^{16,17}, fighting fish^{18,19}, medaka²⁰ and *D. rerio*²¹⁻²⁴. *D. rerio*, is an established model organism for biomedical research and provides the opportunity to study the genetic and cellular basis of pigment pattern formation. They have been domesticated for over a century and mating pairs reliably produce large quantities of fertilized eggs for stock maintenance and experiments under laboratory conditions^{25,26}. A number of ENU mutagenesis (forward) screens²⁷⁻³¹, spontaneous mutations appearing in stocks^{32,33}, and targeted mutations of specific genes (reverse screens) led to the identification of many genes involved in pigmentation and pigment pattern formation in larval and adult fish. Optical transparency for fluorescence imaging is given in embryos and viable mutants of larval and adult fish lacking pigment cells. More than 20 *Danio* species with distinct pigment patterns diversified within the *Danioninae* subfamily across Southeast Asia, from India over Pakistan, Nepal and Bangladesh to Myanmar. Horizontal stripes develop in *D. rerio* and *D. quagga* (formerly the striped *D. aff. kyathit*), vertical bars are formed in *D. aesculapii*, *D. choprae* and *D. erythromicron*, and spots are displayed in (the spotted) *D. kyathit*, *D. tinwini* and *D. margaritatus*. Mixed patterns of stripes, spots or bars are present in *D. nigrofasciatus* and *D. dangila*. In *D. albolineatus* pigment cells intermingle in the trunk, although a horizontal xanthophore stripe is visible towards the posterior end of the tail. The distribution of species with similar patterns does not align with the phylogenetic relationship among the species, i.e., species that develop a similar pattern are not necessarily most closely related. In fact, similar patterns must have evolved repeatedly and independently in the genus. These observations suggest a complex genetic basis underlying the pattern diversification between the species. The two sister species *D. rerio* and *D. aesculapii* seem to overlap in their biodistribution, but are separated from other relatives by the Arakan Mountains of Myanmar. The exact phylogenetic position of *D. kyathit*, a member of the *D. rerio* species group, has not yet been completely resolved, possibly due to gene flow before speciation and introgression afterwards^{34,35}. A few species can be maintained in the

laboratory similar to *D. rerio* or propagated using in vitro fertilization. Although hybrids between species are virtually sterile, they can be produced in the laboratory and used for genetic tests. Whether the genes, which are known to regulate stripe formation in *D. rerio*, are also involved in pattern formation and variation in other *Danio* species is only recently being explored³⁶⁻³⁹.

Orthologs of pigmentation and patterning genes identified in mice⁴⁰ and *D. rerio*^{41,42} frequently appear as candidate genes in studies investigating pattern variation in distantly related teleosts species⁴³. Cichlids are especially suitable to study the repeated association of loci with pigment pattern variation as they form a large family of more than 2,000 species with diverse pigment patterns due to several events of adaptive radiation during the last 5-7 million years in East Africa⁹. Accumulating evidence from studies investigating pattern variation across natural or domesticated populations of teleost species argues for the existence of evolutionary hotspot genes⁴⁴⁻⁴⁶, which have been postulated for diverse morphological traits in different organisms. Rapid evolutionary changes are associated with duplications of genes or entire genomes, that produces new genes (ohnologs)⁴⁷ with novel functions. The explosive increase of speciation and morphological diversification in the teleosts followed a whole-genome duplication (WGD) after the split between Teleostei and Holostei⁴⁸, represented by gar⁴⁹ and bowfin⁵⁰. In addition to the WGD at the base of teleost evolution, more recent genome duplications have occurred in salmonids, common carp and goldfish. Inactivating mutations or loss of redundant copies are most likely to occur after WGDs, although many duplicated genes are retained after rediploidization. In teleosts, pigmentation genes have been preferentially retained suggesting that the duplicated genes share only low functional redundancy⁴¹. Pigmentation genes therefore appear to be biased towards reuse throughout evolution, perhaps because they present an opportunity for mutations with small pleiotropic effects. Sub- and neofunctionalization of paralogs might have led to the diversification of pigment cell types and pigment patterns. Broad phylogenetic sampling in combination with genetic screens in model organisms has successfully driven the study of pattern variation in teleost fish and functionally diverged loci have been identified. Given the findings from *D. rerio* research, genetic and genomic studies across teleosts will continue to provide new insights into the genetic basis of pattern variation. How genetic evolution is translated into the evolutionary change of

development and behaviour of pigment cell types during pattern formation in the many species studied is then the crucial question.

Neural crest as the source of pigment cell type diversity

Vertebrates develop a specific transient embryonic population of migratory cells, the neural crest (NC) cells. They are multipotent and not germ layer-restricted, giving rise to a variety of cell types during embryogenesis including all pigment cells with the exception of the retinal pigment epithelium. An ancestral form of the NC exists in chordates⁵¹, but it evolved, as an often called “fourth germ layer”, specifically in the vertebrate lineage⁵². Embryonic NC cells, specified in part by the Sox10 transcription factor, develop from the ectoderm, at the boundary between neural tube and epidermis. NC cells form different cranial, trunk, vagal and sacral lineages along the anterior-posterior axis of the developing embryo. Then they delaminate from the neural tube, thereby exiting the neural epithelium to become mesenchymal, a gradual process called epithelial-to-mesenchymal transition (EMT). Depending on the axial position of their origin, they give rise to distinct cell types. In the trunk lineage in *D. rerio*, three subpopulations consist of premigratory cells located in the dorsal region as well as a chain of leader and follower cells⁵³, whose migratory identity is autonomously controlled by Notch signalling⁵⁴. Migratory NC cells travel along the medial pathway between the somites and the neural tube/notochord and give rise to diverse cell types, including pigment cells, neurons of the sensory and sympathetic ganglia and Schwann cells (glia), the latter two cell types forming the dorsal root ganglia (DRG, or spinal ganglion) at the peripheral nervous system (PNS). NC cells located in the dorsal most region of the neural tube enter the lateral pathway between the ectoderm and the somites, and differentiate only into pigment cells. Premigratory NC cells already express genes associated with differentiated derivatives, specifically the transcription factors Pax3/7 (*pax3/pax7*) for the xanthophore lineage^{55,56}. Some transcription factors specifying NC cells remain active and are involved in the subsequent specification of NC derivatives, e.g. Sox10 drives *mitfa* (*nacre*) expression for fate specification of melanoblasts^{29,57}. Expression of *mitfa* is repressed by Foxd3⁵⁸ and Tfec⁵⁹ in the common precursors of melanoblasts and iridoblasts, that specifies the iridophore lineage in concert with Alx4a⁶⁰. Iridophores are maintained by the function of the mitochondrial protein Mpv17 (*mpv17/transparent/roy-orbison*)⁶¹. NC

derivatives are committed to their final fate before reaching their ultimate location, involving receptor-ligand interactions such as Csf1a-Csfr1a (*csfr1a/pfeffer*) in xanthoblasts⁶², Kitlga (*kitlga/sparse-like*)-Kita (*kita/sparse*)⁶³⁻⁶⁵ and WntL-WntR⁶⁶ in melanoblasts, and Alkal2a/2b-Ltk (*ltk/shady*)^{67,68} and Edn3b-Ednrb1a (*ednrba/rose*)^{69,70} in iridoblasts. The larval pigment cells form a simple pattern, with black melanophores forming rudimentary stripes occasionally associated with iridophores, whereas yellow/orange xanthophores are mostly scattered over the body. NC-derived stem cells (NCSCs), originally called melanophore stem cells (MSCs), are set aside during embryonic development. Some of them require ErbB and Kit signalling and are used as postembryonic progenitors⁶⁵, with their niche established at the DRGs (specified by Crestin and Tfap2b expression⁷¹), and function as tissue-resident multipotent stem cells throughout life^{72,73}, giving rise to derivatives including all three pigment cell types, neurons and glia of the DRG and the PNS.

The early larval pattern is largely replaced during metamorphosis to generate the adult form. The horizontal stripes, formed by black melanophores, yellow/orange xanthophores and blue/silvery iridophores, develop in parallel to the growth of the fish. Most adult melanoblasts and iridoblasts develop from the same NCSCs and migrate along the nerves into the hypodermis, their larval counterparts do not contribute to the adult pattern. By contrast, most adult xanthophores are directly derived from the larval xanthophores, which persist during metamorphosis supported by Csf1 signalling. Few xanthophores of the adult pattern derive from the same NCSCs as the melanophores and iridophores⁷³. At the onset of metamorphosis, after three weeks of development, larval xanthophores dedifferentiate and proliferate to cover the trunk. They subsequently redifferentiate into two populations with differences in shape and hue. Yellow xanthophores are compact in the interstripe, while stellate xanthophores (often referred to as cryptic or undifferentiated xanthoblasts) remain very light or unpigmented in the stripe⁷⁴. Their differentiation is dependent on thyroid hormone (TH), as hypothyroid fish only develop unpigmented xanthophores^{75,76}. *Mitfa* is required for the differentiation of postembryonic melanophores²⁹, of which two differentiable populations contribute to the adult stripes. Most melanophores are Kit signalling-dependent⁶³⁻⁶⁵ and Kit-independent melanophores seem to be indirectly maintained by Endothelin and Csf1a signalling^{32,63,69,77,78}. Similar to xanthophores, terminal maturation of melanophores is dependent on TH signalling, as hypothyroid

fish develop excess melanophores⁷⁵. Once in the hypodermis, iridoblasts, clonally related with the same stem cells as the melanophores, give rise to two distinct populations of iridophores^{79,80}, similar to xanthophores, with a stellate-shaped, loose population in the stripes (blue iridophores) and a reflective, dense-shaped population in the interstripes (surface (S) or dense iridophores). These subtypes differentiate, proliferate and undergo patterned aggregation in situ within stripes or interstripes spanning the entire dorsoventral axis. L-iridophores, a third type of iridophores, localize underneath the melanophores. Loss of *Alkal2a/b-Ltk* signalling^{67,68} and *Mpv17*⁶¹ affect both S- and L-iridophores. Although hypodermal and peritoneal S-iridophores have distinct requirements for the two ligands *Edn3a* and *Edn3b*, respectively, they both depend on the *Ednrb1a* receptor^{38,69}. Mutants that exclusively lack blue or L-iridophore types have not been identified yet. Iridophore differentiation is seemingly independent of TH but their numbers change as an indirect response to altered numbers of melanophores and xanthophores in hypothyroid fish⁷⁵. TH actions in the hypodermis are regulated by galanin hormone produced in the pituitary gland³³. Galanin signalling is a negative regulator of TH signalling, loss of either signalling component results in hyperthyroid (in *tshr/opallus* or *galanin receptor 1a/nepomuk* mutants) or hypothyroid fish, respectively, with defects in melanophore and xanthophore differentiation. The Galanin/TH axis is therefore non-cell-autonomously required for the differentiation of melanophores and xanthophores, and indirectly important for pigment cell interactions involving iridophores during stripe patterning. Unknown non-pigment cells in the tissue environment require the function of *aquaporin3a (mau)* for larval xanthophore development, although specific influences of water homeostasis on xanthophores is unclear⁸¹. Another genetic requirement in non-pigment cells is demonstrated by *basonuclin-2 (bnc2/bonaparte)*, coding for a zinc finger protein^{82,83}. Transplantation experiments indicate a functional requirement for *bsn2* in the dermis, where it regulates the differentiation pathways of melanophores, xanthophores, and possibly iridophores.

The three pigment cell types are also present in the anal, caudal and dorsal fins. They are derived from the same NCSCs as the pigment cells migrating into the hypodermis. The homologs of these pigment cell types are present in skin and fins across the *Danio* genus. In *D. rerio*, *D. aesculapii* and *D. albolineatus*, *Kit*, *Csf1* and *Edn/Ltk* signalling pathways are required for melanophore, xanthophore and

iridophore development, respectively, although to different degrees among pigment cell type populations⁸⁴. Another pigment cell type, widespread in the *Danio* genus, is the white leucophore located at the tips of anal and dorsal fins. This cell type arises through trans-differentiation, indirectly from other adult NC-derived cells, in the anal and dorsal fins of *D. rerio*. In these fins, melanophores can transition directly into melano-leucophores, and xanthophores or their progenitors can transdifferentiate into xantho-leucophores⁸⁵. These trans-differentiated populations depend on Kit and Csf1 signalling, respectively, thereby remaining faithful to their origin. Melano-leucophores are present in dorsal fins across species, except in *D. erythromicron*, and xantho-leucophores mostly develop in anal fins, except in *D. albolineatus* and *D. erythromicron*. Melano-leucophores only form in the anal fins in *D. nigrofasciatus* and *D. choprae*, xantho-leucophores only develop in the dorsal fins in the spotted *D. kyathit* and *D. tinwini*. Red erythrophores in the fins are also common among *Danio* species⁸⁶, likely lost in *D. rerio*, *D. nigrofasciatus* and *D. tinwini*. In *D. albolineatus*, fin erythrophores and xanthophores arise from a common progenitor, probably derived from NCSCs, and remain plastic after differentiation. The presence, absence or modification of the many different pigment cell types in the *Danio* genus provide an outstanding venue to study NC cell type diversification. A wider view into the teleost phylogeny shows the presence of eight different pigment cell types^{4,87-89}, including electric-blue cyanophores, dichromatic erythro-iridophores, cyano-erythrophores and highly fluorescent pigment cells. How the cell types generate different pigments is an exciting question, especially suitable to address with *Danio* species, but will not be discussed in this manuscript.

Development of the stripe pattern in *D. rerio*

D. rerio is an excellent model to investigate pigment pattern formation in teleosts, and in vertebrates in general. Mutant analyses, transplantations, and lineage tracing have revealed distinct genetic requirements for individual pigment cell types and their local and distant interactions with tissue environments during growth. Careful imaging series throughout metamorphosis have shown the behaviours and shapes of the pigment cells that generates colour and contrast. However, there is little understanding of how the different pigment cells interact to form the stripes.

At the onset of metamorphosis, the NCSCs at the DRGs produce melanoblasts and iridoblasts, which migrate along peripheral neurons that innervate the skin via the dorsal, horizontal and ventral myosepta. At the horizontal myoseptum (HM), iridoblasts differentiate into iridophores to form the first interstripe as a coherent, dense sheet along the anterior-posterior body axis^{79,80}. Xanthophores derived from their larval progenitors already populate the hypodermis and respond via Csf1 signalling^{62,77} to the arrival of iridophores with changes in shape and density to form compact cells on top of the iridophores in the developing interstripe^{74,83,90}. As indicated by transplantation and mutant analyses, the acquisition of the compact form, is dependent on positive short-range interactions between iridophores and xanthophores, and requires heteromeric gap junctions composed of Gja4 and Gja5b (also known as Connexin 39.4 (*luchs*) and Connexin 41.8 (*leopard*), respectively) in xanthophores, which argues for direct homotypic and heterotypic cell-to-cell communication^{30,91-94}. Xanthophores remain faint and stellate on top of melanophores in the developing stripe region, where iridophores with loose morphology also develop^{79,83,90}.

Once melanoblasts enter the skin, presumably guided by neuronal migration and partially by Kit signalling⁹⁵, they localize to presumptive stripe regions dorsally and ventrally to the developing first interstripe and differentiate as they acquire melanin pigment. It is unclear how the two distinct melanophore populations, Kit-dependent or independent, specifically participate in the aspects of stripe formation. Melanophores have to limit their response to the global rise of proliferative insulin signalling derived from the brain during metamorphosis⁹⁶. They fill vacant space in the stripes by size expansion rather than proliferation and move little. Their confluence is dependent on the function of the adhesion molecules Igsf11 (*igsf11/seurat*)⁹⁷ and Jam3b (*jam3b/pissarro*)⁹⁸, which induce spotted patterns in mutants. A similar phenotype is observed in *gja4* and *gja5b* mutants. An allele of *gja5b* exerting a strong dominant negative-effect on *gja4* in combination with mutants lacking xanthophores or iridophores led to the assumption that gap junctions or their individual connexin components are required for homotypic interactions between melanophores. Dense iridophores strictly separate from melanophores locally, although melanophore aggregation is supported by the presence of dense iridophores, but not xanthophores, as indicated by mutants lacking Csf1 signalling and therefore also xanthophores.

Mutants deficient in Endothelin and Ltk signalling, and therefore lacking iridophores, develop fewer melanophores^{83,90}. Thus, dense iridophores maintain positive long-range interactions with melanophores. Tight junction protein 1a, a scaffolding protein, is required in dense iridophores to prevent their spread as coherent sheets into the stripe region, which is strictly separated from the interstripe even in *tjpa1a* (*schachbrett*) mutants⁹⁹.

During the consolidation of the stripe-interstripe boundary, larval melanophores die in the developing interstripe and late-arriving cells are excluded from this region by cell death or migration towards the prospective stripe^{79,100}. Survival and migration of melanophores is promoted by unpigmented xanthophores (xanthoblasts), which form rare and temporary contacts with melanophores through cellular projections, termed airinemes¹⁰¹. These contacts enable DeltaC (*deltac/beamter*)-Notch1a (*notch1a*)¹⁰² signalling from xanthoblasts to melanophores and are relayed via macrophages, which control specificity and duration of these interactions¹⁰³. Stripes expand when Delta-Notch signalling is overactive. When the airineme-mediated survival signalling from xanthophores to melanophores are long gone, melanophores establish permanent protrusions towards interstripe xanthophores at the consolidated stripe-interstripe boundary in adult fish¹⁰². These protrusions are rare in xanthophore mutants deficient for Csf1 signalling with low melanophore numbers. The function of these interactions has not been investigated. Mutations in the inwardly rectifying potassium channel *Kcnj13* (*obelix/jaguar*), expressed and required in melanophores, cause fewer and wider stripes, which are frequently interrupted and melanophores and pigmented xanthophores mix^{104,105}. In vitro experiments with pigment cells isolated from the fins suggest that melanophore membranes depolarize upon contact with pigmented xanthophores, and this causes melanophores to migrate away from xanthophores¹⁰⁶. A dominant missense mutation in the potassium/chloride cotransporter gene *kcc4a* (*slc12a7a/schleier*) causes fewer and interrupted stripes in homozygous fish; homozygous fish for a nonsense mutation are phenotypically normal, possibly due to a functional redundancy with its paralogue *kcc4b*¹⁰⁷. Whether *kcc4a/b* and *kcnj13* have overlapping functions in stripe formation remains to be investigated. Stripe expansion and defects in melanophore-xanthophore interactions are observed in mutants carrying dominant alleles of the membrane scaffold protein Tspan3c (*tspan3c/dali*)¹⁰⁸. It is unknown whether Delta-Notch signalling components, *Kcnj13*, *Kcc4a/b* and

Tspan3c interact genetically or physically with each other to affect the same outcome. While Gja4/Gja5b gap junctions are involved in homotypic interactions between melanophores and xanthophores, respectively, they are likely not directly involved in the short-range repulsive interactions between melanophores and xanthophores. Mutants in the *spermidine synthase* gene (*srm/idefix*) develop defects in stripe width and display some spots. The gene codes for an enzyme in the biosynthesis pathway of polyamines (spermidine and spermine); transplantation experiments suggest that *srm* function is not required in pigment cells but influences their behaviour indirectly¹⁰⁹. Gja4 and Gja5b contain a putative polyamine-binding motif and rectification Kcnj13 is regulated by binding polyamine to the pore domain of the channel¹¹⁰. A joint regulation of Gja4, Gja5b and Kcnj13 might be therefore mediated by the polyamine spermidine^{109,110}. Taken together, integral membrane proteins are autonomously required in the pigment cells for their interactions, which controls the robust formation of the boundary between the dark and light stripes, the layer-specific, location-dependent acquisition of pigment cell shapes, induces stripe reiteration and maintains the stripe pattern throughout life.

In summary, the dark-blue stripes and golden-light interstripes develop in the hypodermis^{111,112}, the innermost skin layer between epidermis and the underlying myotome. The stripes consist of one-cell thick sheets of melanophores at the innermost level, stellate xanthophores on top and loose iridophores in between, while interstripes contain dense iridophores covered by compact xanthophores but no melanophores. Precise superposition of the pigment cells within the dark and light stripes creates the blue and golden colours, respectively. The HM provides cues for the horizontal orientation of the stripes, as its absence in *meox1* (*choker*) mutants leads to meandering stripes of normal width and composition⁹⁰. Mutants lacking individual adult pigment cell types fail to form stripes, indicating that all three cell types are required for their assembly into stripes of horizontal orientation. These observations led to the working hypothesis that stripe patterning is a Turing-like process of self-organization¹¹³ of the pigment cells, which receive positional cues for their horizontal orientation from the HM as anatomical prepattern. Melanophore shapes remain robust in their organization in the stripes. The organization of xanthophore and iridophore shapes is dependent on their location within a stripe or interstripe, which indicates cell-cell communication in the hypodermis. Mutants

allowing xanthophores or iridophores to develop in the absence of the other two cell types show that these cells have the tendency to spread over the entire body, whereas melanophores remain rather localized. Transplantation experiments reveal that the different pigment cells are derived from stem cells segmentally positioned along the anterior-posterior body axis. Xanthophores and iridophores compete with their relatives from clones in neighbouring segments, thus effectively restricting migration along the anterior-posterior axis. Accordingly, heterotypic interactions between pigment cell types are required for cell shape changes, direction of migration, and assembly into the striped pattern, homotypic interactions regulate number, direction of migration and individual spacing of the cells in the trunk¹¹⁴.

Stripes do not form in the dorsal fin, whereas anal and caudal fins are striped. Stripe formation in these fins is fundamentally different compared to stripe patterning in the trunk. Melanophores and xanthophores are required and sufficient for stripe formation in these fins, as stripes still form in the absence of iridophores in mutants deficient in Endothelin and Ltk signalling^{83,90}. Mutant analysis and transplantation experiments indicate that interactions between melanophores and xanthophores require *gja5a*, rather than *gja4*³⁰. This suggests that *gja5b* is almost exclusively required and sufficient for interactions between these cells through homomeric Gja5b-based gap junctions or hemichannels. Similar to stripe patterning in the trunk, these interactions might also depend upon the setting of distinct membrane potentials and regulation via spermidine, as stripes in anal and caudal fins lack completely in *kcnj13*^{104,106}, *tspan36*¹⁰⁸ and *srm* mutants¹⁰⁹. Homotypic interactions between melanophores require autonomous and cooperative functions of the adhesion molecule genes *igsf11*⁹⁷ and *jam3b*⁹⁸, as double-heterozygotes develop defective body and fin patterns. Anatomical prepatterns providing cues for the orientation of the stripes in anal and caudal fins have not been identified and non-cell-autonomous factors regulating interactions between melanophores and xanthophores in the striped fins are unknown. Whether stripe formation is actively suppressed in the dorsal fin or whether positive signals are lacking remains an open question. Our understanding of the genetic and cellular bases of stripe formation in trunk and fins in *D. rerio* is far from complete, yet the next questions have emerged how the identified genes and mechanisms are involved in pattern variation across closely related *Danio* species.

Identification of genetic evolution and its molecular basis

Powerful methods that exist to identify functionally diverged genes have been used in a small number of studies on pigment pattern variation in mice and teleosts. Statistical methods as well as analyses of genetic crosses between species and segregating populations within interspecific hybrids can identify genomic regions that are linked to quantitative traits, termed quantitative trait loci (QTLs) in an unbiased manner. Association mapping (scanning) involving a set of genetic markers, such as single-nucleotide polymorphisms (SNPs), or in the form of genome-wide association studies (GWAS) can provide further resolution to identify candidate regions or even individual genes. A major limitation is that QTL analysis is impossible if hybrids are sterile, which is the case for many species. Strong evidence of causal genetic evolution can be obtained by genomic allele exchanges via homologous recombination (HR), transgenic assays, and reciprocal hemizyosity tests (RHTs)¹¹⁵. Unmapped or complex genomes, the lack of precise gene editing methods and low efficiency for HR have impeded the generation of mutants and allele exchanges. The reciprocal hemizyosity test requires only the generation of reciprocal F1 hybrids between species, which carry null alleles from either parental species in the same genetic background. Although different strategies for transgenesis and mutagenesis have existed for the last two decades, the advent of precise and straightforward gene editing using the CRISPR/Cas9 system in 2012¹¹⁶ provided a broad accessibility of methods to derive causality of QTLs also in non-model species.

I want to cite three studies carried out in *Drosophila*, mouse and cichlids to show current depth of insights into the evolutionary process. A QTL study from 2016 used the CRISPR/Cas9 system for the generation of null mutants for RHT and genomic allele exchange by HR to identify a causal mutation in an ion channel gene contributing to song divergence between two closely related *Drosophila* species¹¹⁷. An evolutionary recent integration of an intronic retroelement was identified as causal mutation in one of the two species tested. Another QTL analysis from 2019 on differently pigmented and closely related deer mice populations in the Sand Hills of Nebraska identified *Agouti* as a known adaptive locus of major effect¹¹⁸. Differences in colour were observed in transgenic mice with single-copy insertions of species-specific *Agouti* alleles into a presumably neutral locus using the PhiC31 integrase system in a strain with no endogenous *Agouti* expression. QTL mapping in combination with association

scans in 2018 led to the identification of regulatory changes in *agouti-related peptide 2* (*agrp2*) as being linked to the convergent evolution of stripes in cichlids in all three African Great Lakes⁴³. The negative effect of an enhancer on *agrp2* expression was linked to suppression of stripe formation in Lake Victoria cichlids. Although *agrp2* seems not to be directly involved in pigment cell interactions in *D. rerio*, it regulates an ancient dorso-ventral countershading mechanism in fish^{119,120}. Stripe development in CRISPR/Cas9-induced F0 *agrp2* mutants in a barred species from the same lake confirmed the causality of the QTL. Expressing stripe or bar alleles of homologous intronic elements identified by association scans yielded strong reporter expression only with the bar allele in transgenic larval *D. rerio*. This result suggests that the cis-regulatory “bar” element causes suppression of *agrp2* expression in the skin, which underlies the development of bars. Similar to the practical limitations in mice, higher HR efficiency will facilitate genomic allele exchanges in cichlids.

Models and hypotheses about stripe formation in trunk and fins in *D. rerio* can be tested in other *Danio* species to understand the genetic basis underlying pattern variation across the genus. Evolutionary change of pigment patterns might arise through divergence in gene function involved in pigment cell differentiation, migration and interactions, although non-cell-autonomous factors in the tissue environment or global signals regulating pattern formation might have functionally diverged as well to mediate pattern variation. Hybridization between different *Danio* species has been observed in aquaria for about 100 years¹²¹. Most crosses between *Danio* species produce infertile hybrids, in part owing to aneuploidies¹²², which prohibit further hybrid crosses and QTL analysis to identify candidate genes. One-way interspecific complementation tests, in contrast to RHTs, however, can be used to screen for such candidates mediating pattern evolution. A handful of genes known to regulate stripe formation in *D. rerio* have been successfully tested in hybrids between *D. rerio* mutants and other *Danio* species³⁶. Although genomic allele exchanges (in an evolutionary context) or reciprocal hemizyosity tests have not yet been performed, the *Danio* genus including *D. rerio*, with all the benefits of a model species, has now fully emerged as a model system for evolutionary developmental biology in vertebrates.

Evolution of pigment patterning in *Danio* species

Pigment cell types homologous to melanophores, xanthophores and iridophores in *D. rerio* are present in the skin and fin patterns in all *Danio* species. The genes, which are involved in stripe formation in *D. rerio*, have therefore been tested in other species for their role in producing divergent patterns. In *D. aesculapii*, the direct sister species to *D. rerio*, Kit, Csf1 and Ltk signalling pathways are required for melanophore, xanthophore and iridophore development, respectively⁸⁴. A Kit signalling-independent melanophore population also develops in this species. Rudimentary bars form in the absence of Kit and Ltk signalling given a sufficient number of melanophores, which develop variably in quantity and then spread loosely across the dorsoventral axis in the respective mutants. Bars fail to develop upon loss of xanthophores in mutants deficient for Csf1 signalling. This suggests that melanophores and xanthophores are essential for bar patterning, whereas the absence of iridophores still allows for bar patterning to occur. Whether the genes required for pigment cell interactions in *D. rerio* are also required for bar patterning in *D. aesculapii* is unknown.

Closest related to *D. rerio* and *D. aesculapii* are *D. kyathit* and *D. quagga*³⁵, which also develop divergent pigment patterns, with stripes similar to *D. rerio* in *D. kyathit* and spots similar to *D. tinwini* in *D. quagga*. Iridophores of stripes and spots appear earlier in *D. kyathit* than *D. quagga* during development. Only one QTL study from 2021 used quantitative approaches⁸⁴ to investigate pigment pattern variation in *Danio* species³⁹. Two separate hybrid crosses between the striped *D. quagga* and the spotted *D. kyathit* yielded non-overlapping QTLs, with regions containing candidate genes known to be required for stripe formation in *D. rerio*, such as *tjp1a*, required in dense iridophores to inhibit an invasion of interstripes into stripe regions, and *gja4*, required for homotypic interactions between melanophores and xanthophores, respectively. Apparent epistatic interactions between loci and segregating variation within species suggest a polygenic and still-evolving genetic basis of stripe and spot development in these species. The QTLs remained candidates as they were not further investigated using functional assays, possibly due to difficulties with obtaining mutants in these species.

Two other sister species are *D. nigrofasciatus*, which develops a prominent stripe with ventral spots, and the broadly spotted *D. tinwini*. They are part of the *D.*

rerio species group within the phylogeny³⁵. One-way interspecific complementation experiments identified *edn3* as candidate for mediating pattern evolution between *D. rerio* and *D. nigrofasciatus*³⁸. Hemizygous hybrids carrying only the functional allele from *D. nigrofasciatus* developed fewer melanophores in response to a reduction in iridophore numbers, that was attributed to lower expression of *edn3b*. Overexpression of *edn3b* in led to increased melanophore and iridophore numbers in transgenic *D. rerio* and *D. nigrofasciatus*, but not in *ltk* mutants in *D. rerio*. Thus, both cases highlight cis-regulatory evolution underlying pattern evolution between *Danio* species. A similar mechanism, but more broadly active over the flanks, might underlie the evolution of the spotted pattern in *D. tinwini*, thus regulatory evolution in *edn3* likely occurred before both species diverged.

The *D. rerio* species group (*D. rerio*, *D. aesculapii*, *D. kyathit*, *D. quagga*, *D. nigrofasciatus* and *D. tinwini*) and *D. albolineatus* belong to phylogenetic branches, which are separate from the *D. choprae* groups (*D. choprae*, *D. margaritatus*, *D. erythromicron*)³⁵. Distinct patterns are almost absent in *D. albolineatus*, as melanophores, xanthophores and iridophores intermingle in the trunk. CRISPR/Cas9-induced loss-of-function mutants in Kit signalling lead to a lack of all melanophores in this species^{78,84}, suggesting that NCSC progenitors have lost the potential to differentiate into separate melanophore lineages. One-way interspecific complementation tests identified candidate genes, such as *csf1a* in hybrids between *D. rerio* mutants and *D. albolineatus*, in which xanthophores develop earlier. Transgenic *D. rerio* carrying non-coding elements of *csf1a* from *D. albolineatus* showed early and high reporter expression in the hypodermis. Consistently, early stimulation of Csf1a signalling in *D. rerio* led to the intermingling of melanophores and xanthophores in ventral regions, similar to the aspects of the *D. albolineatus* wild-type pattern³⁷. These results suggest that regulatory changes in Csf1 signalling underlie early differentiation and proliferation of xanthophores in *D. albolineatus*, potentially also in *D. choprae*, but not in *D. kyathit* or *D. dangila*¹²³. The mixing of xanthophores and melanophores might be partly due to the reduction of airinemes, and therefore DeltaC-Notch1a-mediated signalling from xanthophores towards melanophores in *D. albolineatus*¹⁰¹. Little is known about the development and evolution of the small sister species *D. erythromicron* and *D. margaritatus* or the giant *D. dangila*, possibly due to difficulties with their maintenance under laboratory conditions. The *Danio* species vary

considerably in pigment patterning in the fins, but how species other than *D. rerio* even develop fin patterns has not been investigated so far.

Objectives

The study of pigment cells and patterns in *Danio* species sheds light on some of the oldest questions in evolutionary developmental biology. In this thesis, I have applied concepts from evolutionary genetics to ask how variation in pigment patterning arose in the *Danio* genus. Which genes are involved in pattern development and which have permitted modification during pattern evolution? Which steps during development, i.e. differentiation, migration or patterning of the pigment cells, change to for pattern diversification?

In my dissertation project, I have systematically investigated whether genes known to be involved in stripe formation in *D. rerio* are required for the pigment pattern development of other *Danio* species, and whether these genes might have also functionally diverged to contribute to patterning differences between species. For Chapter One, I present the utilization of interspecific complementation tests in hybrids between *D. rerio* mutants and nine different *Danio* species to identify potentially diverged genes (*kcnj13*, *gja4*, *gja5b* and *igsf11*). I used the CRISPR/Cas9 system to generate loss-of-function mutants in *D. rerio* and its sister species *D. aesculapii*, which were crossed to generate reciprocal hybrids. These approaches led to the identification of the causal evolution in *kcnj13* between the two sister species and the notion that this gene might represent an “evolutionary hotspot” for pattern diversification as it has probably functionally diverged repeatedly across the genus (Podobnik et al. 2022a, Podobnik et al. 2020). I then continued to focus on the role of *kcnj13* in pattern formation and evolution.

For Chapter Two, I describe blastula transplantation experiments confirming cell autonomy for *kcnj13* function only in melanophores. Using a CRISPR/Cas9-mediated knock-in reporter for endogenous *kcnj13* expression I found expression of *kcnj13* in melanophores during development in *D. rerio*. Surprisingly, loss-of-function mutations in *kcnj13* have effects on the shape of all three pigment cell types. Evolution in *kcnj13* might have led to patterning differences between *D. rerio* and *D. aesculapii*, which are reminiscent of the mutant phenotypes in *D. rerio*. In the case of *kcnj13*, evolution likely occurred through cis-regulatory rather than protein changes, as

investigated by allele-specific expression analysis of transcriptomes derived from hybrids between the two species, biochemical and bioinformatic approaches, and transgenic rescue experiments in *D. rerio* mutants (Podobnik et al. 2022b).

The findings presented in Chapter One and Two will be recapitulated in the Discussion, where I describe the impact of the findings on the current understanding of pigment pattern diversification in teleosts and propose future directions and technologies that will help to explore the *Danio* genus as a model for morphological variation in vertebrates.

RESULTS

CHAPTER ONE

Complementation tests for pattern diversification in *Danio* fish

Podobnik, M., Frohnhöfer, H.G., Dooley C.M., Eskova, A., Nüsslein-Volhard, C., and Irion, U. (2020). Nature communications, <https://doi.org/10.1038/s41467-020-20021-6>. see *Thesis Appendix I.I*

Podobnik, M., Nüsslein-Volhard, C., and Irion, U. (2022a). In Preparation. see *Thesis Appendix I.II*

Abstract

The genetic basis of morphological variation provides a major topic in evolutionary developmental biology. Fish of the genus *Danio* display colour patterns ranging from horizontal stripes, to vertical bars or spots. Stripe formation in zebrafish, *Danio rerio*, is a self-organizing process based on cell–contact mediated interactions between three types of pigment cells with a leading role of iridophores. Here we investigate genes known to regulate pigment cell interactions in *D. rerio* that might have functionally diverged to produce a pattern of vertical bars in its sibling species, *Danio aesculapii*. Mutant *D. aesculapii* indicate a lower complexity in pigment cell interactions and a minor role of iridophores in patterning. Reciprocal hemizyosity tests identify the potassium channel gene *obelix/kcnj13* as diverged between the two species. One-way complementation tests suggest evolutionary change in patterning through divergence in *kcnj13*, the gap junction gene *gja5b* and the adhesion molecule gene *igsf11* functions in at least three additional *Danio* species. Thus, our results point towards repeated and independent evolution of these genes during pigment pattern diversification.

Contributions

All authors were involved in the design of the experiments. M.P. U.I. and H.G.F. performed the experiments. U.I., C.N.V., M.P., H.G.F. and C.M.D. analysed the data with support of A.E.; M.P. made the figures with contributions from U.I. and C.N.V.; U.I., C.N.V. and M.P. wrote the manuscript. C.N.V. and U.I. acquired funding.

CHAPTER TWO

Cis-regulatory evolution in *kcnj13* during pattern variation in *Danio* fish

Podobnik, M., Singh, A.P., Fu, Z., Dooley, C.M., Frohnhöfer, H.G., Firlej, M., Elhabashy, H., Weyand, S., Weir, J.R., Lu, J., Nüsslein-Volhard, C., Irion, U. (2022b) Cis-regulatory evolution in the potassium channel gene *kcnj13* during pigment pattern diversification in *Danio* fish. see *Thesis Appendix II*

Abstract

Teleost fish of the genus *Danio* are excellent models to study the genetic and cellular bases of pigment pattern variation in vertebrates. The two sister species *Danio rerio* and *Danio aesculapii* show divergent patterns of horizontal stripes and vertical bars that are partly caused by the evolution of the potassium channel gene *kcnj13*. In *D. rerio*, *kcnj13* is required in melanophores for interactions with xanthophores and iridophores, which cause location-specific pigment cell shapes and thereby influence colour pattern and contrast. Here, we show that cis-regulatory rather than protein coding changes underlie *kcnj13* evolution between the two species. *D. aesculapii* express lower *kcnj13* levels and exhibit low-contrast patterns similar to *D. rerio* mutants. Our results suggest that homotypic and heterotypic interactions between the pigment cells and their shapes diverged between species by quantitative changes in *kcnj13* expression during pigment pattern diversification.

Contributions

M.P., A.P.S., C.M.D., H.G.F., S.W., C.N.V. and U.I. were involved in the design of the experiments. M.P., A.P.S., U.I., H.G.F., and M.F. performed the experiments. U.I., M.P., C.N.V., A.P.S., J.L., Z.F., C.M.D., H.E., S.W., J.R.W. and analysed the data. M.P. made the figures with help from U.I. and C.N.V.; M.P., U.I., A.P.S. and C.N.V. wrote the manuscript. C.N.V. and J.R.W. acquired funding.

DISCUSSION

Evolutionary developmental biology

The neural crest as a vertebrate synapomorphy has inspired developmental biologists since its discovery as the *Zwischenstrang* in chicken in 1868 by Wilhelm Hiss (1831-1904). The morphological term “neural crest” was invented a few years later in 1879 by Arthur Milnes Marshall (1852-1893). However, the origin of the NC is rooted deeper in evolutionary history. Its appearance roughly coincided with the transition from protochordates to vertebrates. These fish evolved a “new head” with a protective skull, a jaw for prey capture and gills as respiratory organ, where the NC contributes many cell types during development (Mongera et al. 2013). Basal vertebrates, such as fish, amphibians and reptiles, have evolved and retained a multipotency in the NC and its derived adult stem cells to also differentiate into multiple pigment cell types. Mammals and birds, however, lost all pigment cell types except the melanophores (mostly called “melanocytes”). Amazing examples for complex patterns exist in species of all these animals. I have introduced concepts of how the different pigment cell types assemble into stripes in *D. rerio*. The developmental mechanisms that underlie patterning in *D. rerio* might act in a similar way in other *Danio* species with divergent patterns or evolved to allow or constrain the diversification of patterns^{121,124}.

The concepts of heterochrony and heterotopy originally by Ernst Haeckel, but later reformed by Karl Ernst von Baer and popularized in “*Ontogeny and Phylogeny*” by Stephen J. Gould¹²⁵, were progressively devised to explain how development can be changed during evolution. Heterochrony describes a change in the timing of development, e.g. the onset, offset or rate of differentiation, migration and interactions between pigment cells. A change in the spatial pattern of development is described as heterotopy, which can result from heterochrony. It has been a historical challenge to discriminate heterochrony and heterotopy, as each mode can be sometimes interpreted as the consequence of the other. However, the latter mode of evolution has been more often overlooked in the history of evolutionary biology¹²⁶. It is a fascinating question which developmental mechanisms are used to vary specific characteristics, size and shape of pigment patterns and how synergy of both heterochrony and heterotopy contributes to the overall change.

Pigment pattern diversification in *Danio* fish

In *D. rerio* the characteristic stripe pattern forms by a presumably self-organising process of the three pigment cell types, melanophores, xanthophores and iridophores. The “same”, i.e. homologous, pigment cell types form very different patterns in other *Danio* species. Given that these pigment cells could conceivably behave in the same way in all *Danio* species, the differences between the patterns might arise from heterochrony. Evidence for this mode of evolution comes from studies on the patterning differences between *D. rerio* and *D. albolineatus*, where the pigment cells mix in the skin. One-way complementation tests have suggested evolution in the xanthophore-specific Csf1 signalling pathway between the two species. Csf1 signalling levels in the skin rise earlier and higher in *D. albolineatus* compared to *D. rerio*. Stimulating early Csf1 signalling in *D. rerio* increased the number of xanthophores, which led to the mixing between xanthophores and melanophores^{36,37,123}. Another example for heterochrony might be the patterning differences between *D. rerio* and *D. nigrofasciatus*, which develop fewer stripes. This difference seems to be caused by evolution in the Endothelin signalling pathway and a premature termination of interactions between iridophores and melanophores³⁸. Alternatively, or concurrently, heterotopy, the evolutionary change through variation in spatial arrangement of the pigment cells due to intrinsic differences, might also affect the interactions of the pigment cells and thereby patterns.

Genetic basis of pigment cell interactions in stripes and bars

In a first set of experiments, we focused on the divergent patterns of the sister species *D. rerio* and *D. aesculapii*. All three pigment cell types are essential for stripe formation in *D. rerio*. Single mutants deficient in one of the three pigment cell types develop residual patterns, while double mutants lack any pattern. This mutant analysis indicates that two of the three pigment cell types are still able to interact, seemingly due to a high degree of redundancy in their interactions. To study the requirement of individual pigment cell types for bar formation in *D. aesculapii*, we used the CRISPR/Cas9 system to generate mutants in the known pigment cell differentiation pathways, i.e. melanophore-specific *mitfa*, xanthophore-specific *csf1ra* and iridophore-specific *mpv17*. We found that mutants deficient in melanophore or xanthophore development lack any pattern, while iridophore mutants still formed

remnants of bars. These results suggest that melanophores and xanthophores are essential, while iridophores are rather dispensable for bar formation. This points to a lower degree of redundancy in pigment cell interactions during bar formation, which could be therefore characterized as less complex than stripe formation in *D. rerio*.

We focussed on four genes, *kcnj13*, *gja4*, *gja5b* and *igsf11*, which encode integral membrane proteins and are all known to be autonomously required in the pigment cells, presumably for direct cell-cell interactions during stripe formation in *D. rerio*. Mutations in the potassium channel gene *kcnj13* cause fewer, larger and interrupted stripes, whereas mutations in the gap junction genes *gja4* and *gja5b* as well as the adhesion molecule gene *igsf11* lead to spotted patterns. These genes might also be required for the formation of different patterns in other *Danio* species. The CRISPR/Cas9 system allowed us to test the requirement of the four genes for bar formation in *D. aesculapii*. While mutants in *kcnj13*, *gja4*, *gja5b* and *igsf11* in *D. rerio* still permit some interactions between the pigment cells to occur, i.e. the formation of spots or fewer and interrupted striped, mutants in the four genes in *D. aesculapii* lack any pattern. These mutant phenotypes were similar to the ones observed in single mutants deficient for individual pigment cell types. These results demonstrate that all four genes are required for pattern formation in *D. aesculapii*. Stripe patterning in *D. rerio* seems to be based upon a partial redundancy in pigment cell interactions, as uncovered in the mutants, which still form a residual pattern. This mutant analysis also suggests that there might be lower redundancy in the way the pigment cells interact in *D. aesculapii*, where the bar pattern is completely lost in the mutants. We continued to test the hypothesis that variation in pigment cell distribution arises from evolution of interactions between the pigment cells, i.e. the four genes could have conserved functions or have diverged to cause patterning differences between species.

Complementation tests in hybrids identify diverged genes

We used genus-wide complementation tests to compare the patterning functions of *kcnj13*, *gja4*, *gja5b* and *igsf11* in hybrids between the four *D. rerio* mutants and nine other *Danio* species. We minimized phenotypic variation that typically arises from the different genetic backgrounds by generating new loss-of-function mutations in the four genes in our wild-type TU stock. In most cases (25 out of 36, 69.4 %) we found conserved functions of the tested alleles. In six cases (16.7 %) hemizygous hybrids

showed pattern phenotypes, which overlapped with pattern defects observed in the wild-type hybrids. We assume that the outcome of these tests was strongly influenced by the genetic background. In five cases (13.9 %) hemizygous hybrids differed significantly from the control hybrids; these cases were hybrids between *D. rerio gja5b* or *igsf11* mutants and *D. margaritatus* as well as hybrids between *D. rerio kcnj13* and *D. aesculapii*, *D. tinwini* and *D. choprae*. These results suggest that these genes have potentially functionally diverged to contribute to patterning differences between the species.

The hemizygous hybrids never showed complete non-complementation, i.e. phenotypes similar to *D. rerio* mutants, suggesting that the diverged alleles still provide a patterning function in the parental species. This notion is supported by the loss-of-function phenotypes of the four mutants in *D. aesculapii*. We tested if we could establish complete non-complementation in hybrids by crossing *kcnj13* and *gja5b* mutants of *D. rerio* and *D. aesculapii*. These mutant hybrids resembled the *D. rerio* mutants, showing that the genetic background in the hybrids is similar to the one in *D. rerio*. Comparing phenotypes in reciprocal hemizygous hybrids accounts for effects caused by a novel genetic background in hybrids (Stern 2014). Hemizygous hybrids between *D. rerio* and the four *D. aesculapii* mutants all developed patterns indistinguishable from wild-type hybrids, indicating that the *D. rerio* alleles complemented the loss of functions from the *D. aesculapii* alleles. Thus, the reciprocal hemizygosity tests ruled out evolution in *gja4*, *gja5b* and *igsf11*, but confirmed functional divergence in *kcnj13* between the two species. We therefore continued to focus on the role of *kcnj13* in pigment pattern formation and evolution.

Cell-autonomy and endogenous expression of *kcnj13*

We used blastula transplantations to test the requirement of *kcnj13* function in the individual pigment cell types for stripe formation in *D. rerio* chimeras. Corroborating previous studies (Maderspacher & Nüsslein-Volhard 2003, Iwashita et al. 2006, Inaba et al. 2012), we demonstrated that *kcnj13* is autonomously required in melanophores but not in xanthophores. Additionally, we ruled out a requirement of *kcnj13* function in iridophores. Further transplantations of pigmented *kcnj13* mutants into *albino/slc45a2* hosts suggested that pigmented, i.e. mutant, melanophores, but no other non-pigment cell type, induce pattern defects in the unpigmented host. The hypothesis that *kcnj13*

function is required only in melanophores is further supported by a partial rescue of the mutant phenotype by expressing the wild-type form of *kcnj13* under the control of the melanophore-specific promoter *mitfa* (Inaba et al. 2012). These findings indicate that *kcnj13* function is required only in melanophores or their progenitors.

Larval melanophores persist until early metamorphosis, when new cells develop from the postembryonic stem cells. The melanophore progenitors then migrate into the skin and differentiate into melanophores, i.e. they acquire melanin pigment. There they are directly and indirectly involved in short- and long-range interactions among all pigment cell types during stripe formation (Frohnhofer et al. 2013, Patterson et al. 2013). We generated the reporter line *Tg(kcnj13::venus)* and conducted live imaging during development. We found expression patterns in larval fish, which are similar to previously published results obtained with in situ hybridization (Silic et al. 2020). In this reporter line, which most likely faithfully recapitulates endogenous *kcnj13* expression, we found persistent signals in the spinal cord during and after stripe formation. We imaged this line in combination with the *Tg(sox10::mrfp)* line, which labels NC-derivates, including the pigment cell stem cells at the DRGs. Expression of *kcnj13* and *sox10* never overlapped at the DRGs, suggesting that *kcnj13* is not expressed and required in the pigment cell stem cells. We also did not observe expression in presumed progenitor cells, which follow the nerve tracks between the myosepta. However, expression could be consistently found in a few pigmented melanophores and xanthophores in the skin. A published data set obtained by scRNA-seq of *sox10*-positive cells during stripe formation indicates expression of *kcnj13* in a small subset of melanophores and xanthophores (Saunders et al. 2019). Based on the tests regarding the cell autonomy of *kcnj13* function, expression of *kcnj13* in xanthophores or in cells of the spinal cord might be genuine but functionally irrelevant for stripe formation. Our results indicate that *kcnj13* is expressed and functionally required in differentiated melanophores for stripe formation.

Pigment cell shape acquisition by *kcnj13* function

A key mechanism in stripe formation is the location-specific shape acquisition of the different pigment cell types. We performed live imaging of wild-type and *kcnj13* mutant fish carrying *Tg(kita::mcherry)*, which labels both melanophores and xanthophores. Similar to previous findings in wild-type fish (Singh et al. 2014, Hamada et al. 2014),

we observed tight nets of melanophores. They form long protrusions at the boundary towards the light stripes, presumably directly interacting with xanthophores. Xanthophores show compact shapes in the light stripe and stellate forms in the dark stripes. In the *kcnj13* mutants, melanophores are less densely packed and lack the long protrusions towards the light stripes. These protrusions are short and sprawl out without clear polarity. To test mutant effects on xanthophores, we transplanted wild-type cells carrying *Tg(sox10:mrfp)* into *kcnj13* mutants, thereby placing labelled wild-type xanthophores next to mutant melanophores. Wild-type xanthophores acquired an ectopic compact form in the dark stripes, suggesting that mutant melanophores are unable to interact with wild-type xanthophores. This is similar to the in vitro experiments, where mutant melanophores and xanthophore fail to elicit contact-dependent depolarization causing the cells to separate from each other (Inaba et al. 2012). To investigate the effects of *kcnj13* mutations on iridophores, we induced labelled pigment cell clones in a *Tg(sox10:cre-ERT2)* line in the *kcnj13* mutant background and followed their behaviour during development. Tracing of the iridophore lineage revealed an ectopic acquisition of the dense form in the dark stripe areas, suggesting that melanophores and iridophores fail to interact properly in the mutants. Our results suggest that the lack of *kcnj13* function, which is autonomously required in the melanophores, prohibits homotypic and heterotypic interactions between all three pigment cell types for their correct acquisition of specific shapes dependent on their location. Mutant melanophores might only be partially recognized by the other two cell types, which could also cause indirect effects on interactions between xanthophores and iridophores (Frohnhofer et al. 2013, Patterson et al. 2013).

One-way interspecific complementation tests revealed the repeated and independent evolution of *kcnj13* function during pigment pattern diversification between *D. rerio* and *D. aesculapii*, *D. tinwini* and *D. choprae*. Reciprocal hemizyosity tests confirmed evolution in *kcnj13* between *D. rerio* and *D. aesculapii*. *D. aesculapii*, the closest sister species to *D. rerio* forms a bar pattern of variable width and number. Melanophores and pigmented xanthophores mix at the boundary between the melanophore bars and the light regions; they do not seem to mix within the melanophore bars. Melanophores at this boundary do not form long protrusions. These phenotypes observed in wild type *D. aesculapii* are reminiscent of the occasional mixing of melanophores and xanthophores as well as the unpolarized

melanophore protrusions in *kcnj13* mutant *D. rerio*. The melanophore protrusions presumably contact xanthophores directly (Hamada et al. 2014) and might represent a mechanism, which evolved to contribute to differences in the way the pigment cells interact during pattern formation and maintenance. It is unclear whether these differences, potentially caused by *kcnj13* evolution, result from heterochronic or heterotopic changes. In heterochronic terms, patterning differences might arise from changes in the timing or quantity of pigment cells, which affects differentiation, migration and interactions among them. However, there might be contributions from heterotopic changes, i.e. changes in how the pigment cells interact through species-specific intrinsic differences. In vitro studies have demonstrated a function of *kcnj13* for the separation of xanthophores from melanophores (Inaba et al. 2012), suggesting that evolution in *kcnj13* might primarily cause heterotopic change. The establishment and live imaging of reporter lines in *D. aesculapii* will uncover the shapes of all three pigment cells and whether they acquire distinct states depending on their location. Location-specific acquisition of pigment cell shapes might be a developmental mechanism, which evolved to contribute to patterning differences between species.

Cis-regulatory evolution in *kcnj13*

Finally, we tested two contrasting hypotheses on whether *kcnj13* evolution between *D. rerio* and *D. aesculapii* occurred via changes in the protein itself or through regulatory changes. The two species differ by only two amino acid changes, Q23L and D180G. We used Tol2-mediated transgenesis to express the coding regions of either species under the control of the melanophore-specific promoter *mitfa* in the *D. rerio* loss-of-function mutant. In both cases the transgenes were able to restore stripes to a similar degree in the mutant, indicating the protein from *D. aesculapii* can function in a similar way to the *D. rerio* protein. We observed differences between several independent transgenic lines for both of the transgenes. These differences could be possibly due to copy number variations and novel and/or variable patterns of gene expression caused by position effects of the randomly inserted transgenes into non-native genomic locations. These results suggest that coding regions from both species function similarly and the two amino acid changes are irrelevant for the functional evolution in the gene. We have not been able yet to achieve genomic allele exchanges, which would avoid the limitations of the transgenic assay we used.

The alternative to protein evolution is divergence in *kcnj13* function by cis-regulatory changes. We tested this scenario by generating hybrids between the species and performing transcriptome analysis via RNA-seq on the skin tissue. We found significantly higher levels of the *kcnj13* allele from *D. rerio* as compared to *D. aesculapii*, thereby confirming cis-regulatory evolution. We assume that these quantitative differences in *kcnj13* expression in the hybrids reflect similar expression differences between the parental species. Preliminary evidence comes from the analysis of transcriptomes obtained from different developmental stages of both species; metamorphic and adult *D. rerio* seem to express higher levels of *kcnj13* as compared to *D. aesculapii* (data not shown). Although we measured expression from bulk skin cells, it is likely that the relevant signals come from the pigment cells, which seem to be the only cell types in expressing *kcnj13* in the skin of our reporter line *Tg(kcnj13::venus)*. Species-specific levels of *kcnj13* expression might cause differences in pigment cell behaviour and shapes observed between *D. rerio* and *D. aesculapii*. Pleiotropic effects of differential gene regulation in the skin might be low compared to effects caused by protein changes, as *kcnj13* has important functions in the eyes^{127,128}. We hypothesize that cis-regulatory differences also underlie the repeated and independent evolution in *kcnj13* function in *D. tinwini* and *D. choprae*, which also form very different pigment patterns.

Closing remarks

As *kcnj13* is required only in one pigment cell type with functions in cell shape acquisition and direct interactions between all three pigment cell types in *D. rerio*. Regulatory changes in this potential “evolutionary hotspot gene” might permit heterotopic rather than heterochronic differences in pigment pattern evolution even in other teleosts. There are 30,000 teleost species, which evolved an amazing diversity of pigment patterns for about 260 million years. They partly develop homologous pigment cell types and patterning functions of genes might be selectively conserved or diverged to contribute to patterning differences between species. This “evo-devo” perspective does not yet account for the ecological context. This can be an influential factor as seen in the plastic pattern development in clownfish, which depends upon the presence of specific sea anemone species¹⁴. Animal pigmentation fascinates biologists at least since Darwin¹²⁹ and will continue to keep them on their toes.

GLOSSARY

bp, base pair

kbp, kilobase pair

Cas, CRISPR associated protein

CRISPR, clustered regularly interspaced short palindromic repeats

DNA, deoxyribonucleic acid

DRG, dorsal root ganglion

dpf, days post fertilization

e.g., from Latin *exempli gratia* or “for example”

EMT, epithelial-to-mesenchymal transition

ENU, N-ethyl-N-nitrosourea

GWAS, genome-wide association study

HDR, homology-directed repair

HM, horizontal myoseptum

HR, homologous recombination

i.e., from Latin *id est* or “that is”

MSC, melanophore stem cell

Mya, million years ago

NC, neural crest

NCSC, neural crest-derived stem cell

QTL, quantitative trait locus

RHT, reciprocal hemizyosity test

RNA, ribonucleic acid

scRNA-seq, single-cell RNA sequencing

SNP, single-nucleotide polymorphism

TU, Tuebingen

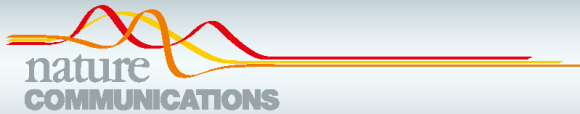
PNS, peripheral nervous system

WGD, whole-genome duplication

ACKNOWLEDGMENTS

I would like to thank my lab colleagues who have accompanied me and whom I have had the privilege of accompanying, especially Vincenzo Barone, Mateusz Blachnik, April Dinwiddie, Christopher Dooley, Anastasia Eskova, Andrei Fadeev, Hans Georg Frohnhöfer, Horst Geiger, Silke Geiger-Rudolph, Heike Heth, Uwe Irion, Gurpreet Kaur, Prateek Mahalwar, Christiane Nüsslein-Volhard, Roberta Occhinegro, Mario Pezzuti, Vera Schmidt, Ajeet Pratap Singh and Brigitte Walderich. I would also like to thank colleagues from other labs at the institute, especially Hadeer Elhabashy, Magdalena Firlej, Dorota Rousova, Veronika Altmannova, John Weir and Reinhard Albrecht. I would like to thank all the PhD students who voted for me during the elections of the Internal PhD Representative in 2020. My term lasted over two years, during which I had the privilege of working with the following colleagues: Michael Bell, Alejandra Duque, Hadeer Elhabashy, Liam Fitzstevens (with whom I had the great pleasure to complete the Via Alpina National Route 1 from 2019 to 2022), Saskia Funk, Anupam Gautam, Joe Joiner, Miriam Lucke, Anasuya Moitra and Minakshi Singh. We maintained a good cooperation with Andrei Lupas, the former Head of the PhD programs, and the Researcher Support Team (RST), especially Susan Jones, Jeanette Müller, Sybille Patheiger and Tina Peart. For help during the organization of three MiKo/DSSS events featuring Axel Meyer, Gilles Laurent and David Stern. I would like to thank Elisabeth Weir. I would also like to thank the IT team for their excellent service over the years, especially Harald Huss, Andre Noll, Joachim Sieler and Johannes Wörner. The only in-person symposium I joined during my PhD time was the Ringberg symposium in October 2022. I would like to thank Christiane Nüsslein-Volhard for the invitation to join together with Eric Wieschaus, Jörg Großhans, Martin Klingler, Peter Lawrence, Ruth Lehmann, Stefan Luschnig, Patrick Müller, Daniel StJohnston, Andreas Bergmann, Phil Ingham, Mahendra Sonawane, Tatjana Piotrowski, Frank Sprenger, Michael Granato, Robert Kelsh, Frank Schnorrer, Pat O'Farrell, Maria Leptin, Mark Fishman, Freek van Eeden, Francesca Peri, Matthias Hammerschmidt, Nicolas Rohner, Stefan Schulte-Merker, Jonathan Howard, Matthew Harris, Uwe Irion, Denis Duboule, Siegfried Roth, Dominic Ferrandon, Teresa Nicolson, David Ish-Horowicz, Anne Ephrussi, Gerd Jürgens, Judith Kimble, Trudi Schüpbach, Mary Mullins, Carl-Philip Heisenberg, Alessandro Mongera, Scott Holley, Bernard Moussian, Manfred Frasch and Florian Maderspacher.

THESIS APPENDIX I.I



ARTICLE



<https://doi.org/10.1038/s41467-020-20021-6>

OPEN

Evolution of the potassium channel gene *Kcnj13* underlies colour pattern diversification in *Danio* fish

Marco Podobnik¹, Hans Georg Frohnhöfer¹, Christopher M. Dooley^{1,2}, Anastasia Eskova^{1,3}, Christiane Nüsslein-Volhard¹ & Uwe Irion¹✉

The genetic basis of morphological variation provides a major topic in evolutionary developmental biology. Fish of the genus *Danio* display colour patterns ranging from horizontal stripes, to vertical bars or spots. Stripe formation in zebrafish, *Danio rerio*, is a self-organizing process based on cell–contact mediated interactions between three types of chromatophores with a leading role of iridophores. Here we investigate genes known to regulate chromatophore interactions in zebrafish that might have evolved to produce a pattern of vertical bars in its sibling species, *Danio aesculapii*. Mutant *D. aesculapii* indicate a lower complexity in chromatophore interactions and a minor role of iridophores in patterning. Reciprocal hemizyosity tests identify the potassium channel gene *obelix/Kcnj13* as evolved between the two species. Complementation tests suggest evolutionary change through divergence in *Kcnj13* function in two additional *Danio* species. Thus, our results point towards repeated and independent evolution of this gene during colour pattern diversification.

¹Max Planck Institute for Developmental Biology, Max-Planck-Ring 5, 72076 Tübingen, Germany. ²Present address: Max Planck Institute for Heart and Lung Research, Ludwigstrasse 43, 61231 Bad Nauheim, Germany. ³Present address: IBM Research and Development, Schönaicher Straße 220, 71032 Böblingen, Germany. ✉email: uwe.irion@tuebingen.mpg.de

Colour patterns are common features of animals and have important functions in camouflage, as signals for kin recognition, or in mate choice. As targets for natural and sexual selection, they are of high evolutionary significance^{1–4}. Colour patterns are highly variable and evolve rapidly leading to large diversities even within a single genus and to remarkable similarities in distant genera. The patterns frequently involve spots or stripes of different orientations. The identification of genes involved in colour patterning has become a major goal in evolutionary developmental biology^{5–9}. Colour pattern development and evolution is studied in many systems, from insects to vertebrates, that use fundamentally different mechanisms to form the patterns. In insects most colour patterns are generated in the two-dimensional sheets of epidermal cells that produce pigments or light-scattering structures, which are secreted into the cuticle. The patterns often are oriented along morphological landmarks, such as segment boundaries or wing veins. Patterning in butterfly wings is essentially controlled by well-known signalling systems such as *dpp* or *hedgehog* and guided by spatially expressed transcription factors serving as anatomical prepatterns¹⁰. Particularly well studied are the wing patterns of *Heliconius* butterflies where adaptive radiations in Central and South America led to many species with a large variety of patterns that are used in Müllerian mimicry and predator avoidance. It has been found that only few genes with large effects cause wing pattern adaptations in these species; cis-regulatory changes in the gene, *optix*, were identified as the basis for the convergent evolution of the patterns in a number of different species^{11,12}.

In contrast to insects, pigment patterns in vertebrates are not of epithelial origin, but are produced by specialised pigment cells (chromatophores) derived from the neural crest, a transient embryonic structure that develops at the boundary between neural tissue and epidermis. The neural crest cells delaminate from the invaginating neural tube, become migratory and distribute in the organism contributing to many different tissues and organs. The pigment cell precursors migrate into the skin where they distribute and produce pigments or structural colours. Whereas mammals and birds only possess one type of pigment cell, the melanocyte producing brown or black melanin pigments, several more pigment cell types are present in cold-blooded vertebrates such as fish, amphibia and reptiles; most widely distributed are orange to yellow xanthophores, red erythrophores and light reflecting white or silvery iridophores¹³. Differential distribution and superposition of pigment cells allows for the generation of a rich diversity of colour patterns in these basal vertebrates. Pattern formation by neural crest-derived pigment cells involves direct contact-based interactions among cells of the same type or between different types of pigment cells. These interactions control cell proliferation, shape changes and migration resulting in superimposed layers of differently coloured pigment cells under the skin generating a large variety of patterns, particularly rich in fishes.

The adult patterns of fish as targets for sexual selection and kin recognition are particularly well suited to study the evolution of colour patterns in vertebrates: In many genera a rich diversity of patterns in closely related species exist, and the development of the adult patterns in the juvenile fish can be followed directly as it takes place outside the maternal organism. A teleost-specific whole genome duplication followed by sub-functionalization of the paralogues resulted in many genes in fish that are specific for adult colour patterning without having other vital functions, thus reducing constraints for the evolution of these genes^{14,15}. Cichlids from the great African lakes are examples of recent adaptive radiations that led to the emergence of hundreds of new species and sub-species with many divergent patterns, frequently made up of bars or horizontal stripes of different colours. Genetic

mapping using hybrids between striped and non-striped cichlid species was recently used to show that the secreted signalling molecule Agouti-related peptide 2 (*Agrp2*) is a main driver in the suppression of horizontal stripes¹⁶. Further analysis revealed higher levels of expression of *Agrp2* in other non-striped species compared to striped species from two different lake systems, confirming a further example of convergent evolution of the same gene.

The zebrafish, *Danio rerio*, has emerged as an excellent system to study colour pattern development in a vertebrate^{7,8,13,17–19}. In this model organism a fair number of genes have been identified in mutant screens that are required for the formation of the pattern^{7,8}, which is composed of a series of horizontal light and dark stripes on the flank of the fish as well as in the anal and tail fins (Fig. 1a). The adult pattern is created by three different types of chromatophores in the skin, in the dark stripes black melanophores are overlaid by blue iridophores and lightly coloured stellate xanthophores. The light stripes are composed of dense, silvery iridophores underneath compact orange xanthophores^{20–23}. The chromatophores producing this pattern mainly originate from multipotent neural crest-derived stem cells located at the dorsal root ganglia of the peripheral nervous system^{24–28}. Several signalling pathways control proliferation and tiling of the different chromatophore types; Kit-signalling is required for most melanophores, Csf1-signalling for the development of xanthophores and Edn3-signalling for dense iridophores^{29–31}. During metamorphosis, the period when adult form and colour pattern are established, stripe formation is initiated by iridophores emerging along the horizontal myoseptum. Iridophores proliferate and spread in the skin to form a series of light stripes alternating with dark stripes of melanophores that emerge in between. Cell shape changes and assembly into the striped pattern are controlled by interactions among the three cell types^{23,32–34}. Several genes are autonomously required in the chromatophores for these heterotypic interactions^{32,33,35–40}. These genes typically encode integral membrane proteins such as adhesion molecules³⁶, channels³⁸, or components of cellular junctions, some of which mediate direct cell contacts^{40–42}. Stripe formation is also influenced by the local tissue environment^{43–45} and by global hormonal signals, such as galanin-regulated thyroid hormone^{46–48} and insulin⁴⁹. The correct orientation of the stripes in zebrafish depends on the horizontal myoseptum. In *Meox1* (*choker*) mutants, which lack this structure, the horizontal orientation of the stripes is lost, but they form of normal width and composition (Fig. 1b), indicating that stripe formation is a process of self-organisation of the pigment cells³².

To study the evolution of colour patterns we can now, based on the knowledge we have from the model organism *D. rerio*, examine other closely related *Danio* species. These show an amazing variety of colour patterns, which range from horizontal stripes in *D. rerio* (Fig. 1a), to vertical bars in *D. aesculapii*⁵⁰, *D. choprae* or *D. erythromicron* (Fig. 1c, g, m), spotted patterns in *D. tinwini*⁵¹ or *D. margaritatus* (Fig. 1d, h) or an almost complete lack of any pattern in *D. albolineatus*. The *Danio* species diversified for at least 13 million years in Southeast Asia and their spatial distributions only partially overlap today^{52,53}. Hybrids between *D. rerio* and other *Danio* species can be produced in the laboratory by natural matings or by in vitro fertilisation⁵⁴. They invariably display colour patterns similar to the stripes in *D. rerio*, thus, horizontal stripes appear to be dominant over divergent patterns (Fig. 1e, f, i, j)⁵⁴; whether this is due to a gain-of-function in striped species or losses in the other species is an open question^{7,8,18}. The hybrids are virtually sterile impeding further genetic experiments, like QTL mapping, but they allow inter-specific complementation tests⁵⁴.

Three *Danio* species, *D. aesculapii*, *D. choprae* and *D. erythromicron*, display vertical bars. Surprisingly, these species are

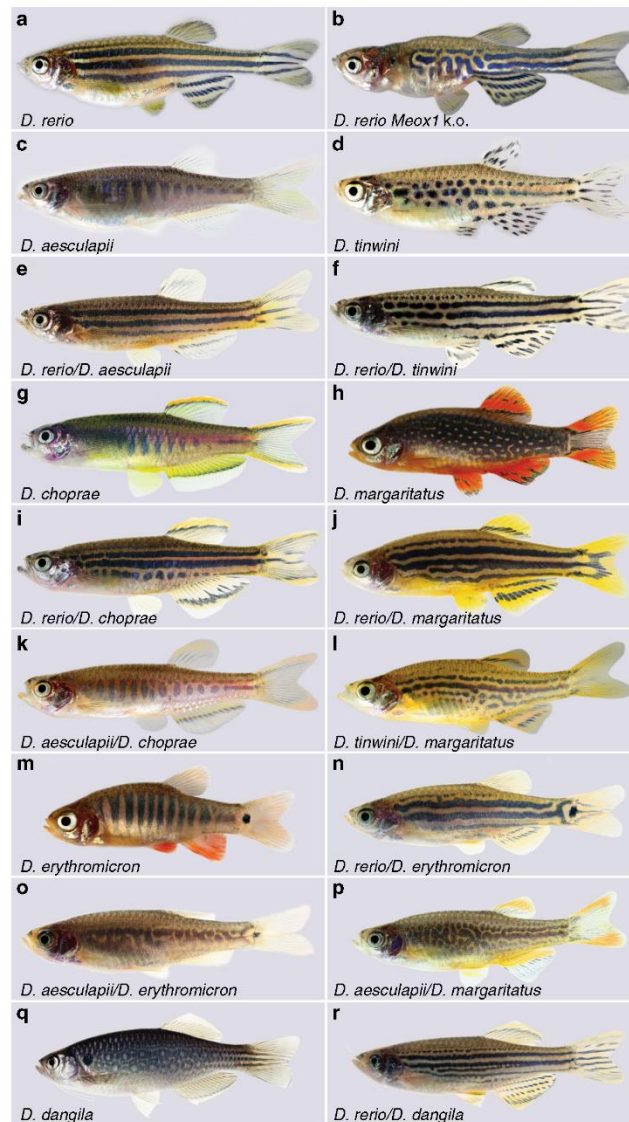


Fig. 1 Colour patterns in *Danio* fish and interspecific hybrids. **a** Colour pattern of zebrafish, *D. rerio*. **b** *D. rerio* *Meox1* (choker) mutants, which lack a horizontal myoseptum. **c** *D. aesculapii*. **d** *D. tinwini*. **e** Hybrid between *D. rerio* and *D. aesculapii* and **f** hybrid between *D. rerio* and *D. tinwini*. **g** *D. choprae*. **h** *D. margaritatus*. **i** Hybrid between *D. rerio* and *D. choprae*, **j** and hybrid between *D. rerio* and *D. margaritatus*. **k** Hybrid between *D. aesculapii* and *D. choprae*. **l** Hybrid between *D. tinwini* and *D. margaritatus*. **m** *D. erythromicron*. **n** Hybrid between *D. rerio* and *D. erythromicron*. **o** Hybrid between *D. aesculapii* and *D. erythromicron*. **p** Hybrid between *D. aesculapii* and *D. margaritatus*. **q** *D. dangila*. **r** Hybrid between *D. rerio* and *D. dangila*. All pictures are representative for the corresponding species or hybrids; for the variability of hybrid patterns see Supplementary Fig. 1. Please note that not all panels are shown to the same scale; the sizes of the fish are ~18 mm (*D. margaritatus* and *D. erythromicron*), 24 mm (*D. tinwini*), 30 mm (*D. choprae*), 35 mm (*D. rerio*, *D. aesculapii*) and 75 mm (*D. dangila*).

not monophyletically related within the genus *Danio*. In this paper we describe hybrids between these barred species, showing that all three of them lack the cues for a horizontal orientation of the pattern. However, we find that vertical bars develop in a different manner in *D. erythromicron* compared to *D. aesculapii* and *D. choprae*, showing that bar formation likely evolved convergently by two different modes.

Using the CRISPR/Cas9 system, we generated loss-of-function mutations in known regulators of chromatophore interactions from *D. rerio* in its closest sibling species, *D. aesculapii*. The phenotypes confirmed that these genes regulate patterning also in this species and demonstrate a lower complexity in the interactions among chromatophores. Further they suggest a minor role of iridophores in the patterning of this barred species compared to *D. rerio*^{32,33}. We then performed reciprocal hemizygosity tests³⁵ with null alleles of four known regulators of chromatophore interactions, the two connexin genes *Cx39.4* (*luchis*)⁴⁰ and *Cx41.8/Gja5b* (*leopard*)^{37,41}, the potassium channel gene *Kcnj13* (*obelix/jaguar*)^{37,38} and the cell adhesion gene *Igsf11* (*seurat*)³⁶. In the case of *Kcnj13*, we found that the reciprocal hybrids display qualitatively different phenotypes indicating that the function has diverged between *D. rerio* and *D. aesculapii*, whereas in the other three cases the function of the genes appears to be conserved. One-way complementation tests with eight more *Danio* species suggest that the *Kcnj13* gene has also evolved between *D. rerio* and two more species, *D. tinwini* and *D. choprae*. The separated phylogenetic positions of these species suggest that the evolution of *Kcnj13* contributing to the pattern diversity in *Danio* fish has occurred several times independently.

Results

Horizontal pattern orientation is lost in barred species. To reconstruct the history of colour pattern evolution we first investigated how pattern orientation is inherited in hybrids. The horizontal orientation of the stripes in *D. rerio* (Fig. 1a) depends on the horizontal myoseptum along which iridophores emerge to form the first light stripe. In *Meox1* mutants (*choker*), which lack the horizontal myoseptum, meandering stripes form without clear orientation (Fig. 1b)³². The closest sibling species to *D. rerio*, *D. aesculapii*, shows a very different pattern of vertically oriented dark bars (Fig. 1c)⁵⁰. Similar barred patterns are exhibited by the more distantly related *D. choprae* and *D. erythromicron* (Fig. 1g, m). These patterns clearly do not use the horizontal myoseptum, which is present in all species, for orientation. In all three cases, hybrids with *D. rerio* show a pattern that resembles the horizontal *D. rerio* stripes (Fig. 1e, i, n)⁸. Strikingly, hybrids between *D. aesculapii* and *D. choprae* display a barred pattern, similar to the species pattern (Fig. 1k). This indicates that in both species the cues for horizontal orientation are lacking and that the barred pattern develops in a similar manner. In contrast, hybrids between *D. aesculapii* and *D. erythromicron* develop highly variable patterns without any clear orientation (Fig. 1o and Supplementary Fig. 1). Therefore, the vertical bars must develop in a different manner in *D. erythromicron* compared to *D. aesculapii* and *D. choprae*.

Two *Danio* species display spotted patterns: *D. tinwini* has dark spots on a light background (Fig. 1d)⁵¹, whereas *D. margaritatus* shows light spots on a dark background (Fig. 1h). In both cases, hybrids with *D. rerio* show a stripe pattern similar to *D. rerio* (Fig. 1f, j)⁸. Hybrids between the two spotted species also develop a pattern of horizontal stripes, albeit with some interruptions and irregularities (Fig. 1l). These results indicate that the horizontal myoseptum functions to orient the pattern in the hybrids between *D. tinwini* and *D. margaritatus*, and therefore in at least one of the two parental species. It seems

likely that this is the case in *D. tinwini*, as the spots show some horizontal orientation reminiscent of interrupted stripes. Hybrids between *D. aesculapii* and *D. margaritatus* develop meandering patterns that do not resemble either of the parental species and lack a clear horizontal or vertical orientation (Fig. 1p). *D. dangila*, the most distantly related species to *D. rerio* that we examined in this study, show a pattern of rows of dark rings (Fig. 1q). Hybrids between *D. rerio* and *D. dangila* develop horizontal stripes, which often partially split (Fig. 1r)⁵⁴. Based on the most recent phylogeny⁵², we hypothesise an evolutionary history, in which the horizontal orientation of the pattern in the *D. rerio* group was gained from an ancestral ambiguous pattern and lost again in *D. aesculapii*. Two other species, *D. erythromicron* and *D. choprae*, independently might have acquired a vertical orientation from this ancestral pattern. The patterns of the hybrids between *D. aesculapii* and *D. erythromicron* or *D. margaritatus*, which are more variable than the species patterns (Supplementary Fig. 1) and without clear orientation, might resemble such an ancestral pattern. A variable ancestral pattern without well-defined orientation might not have functioned as recognition signal but rather provided camouflage.

A minor role of iridophores in cellular interactions forming bars. To investigate the developmental and genetic basis for the differences in pattern orientation, we focussed on the sibling species *D. rerio* and *D. aesculapii*, which display horizontal stripes and vertical bars, respectively (Fig. 1a, c). In *D. rerio*, during early metamorphosis, iridophores emerge along the horizontal myoseptum to form the first light stripe (Fig. 2a)^{20,32,33}. In contrast, in *D. aesculapii* iridophores appear only during later stages, are more scattered over the flank and fewer in number (Fig. 2b, d). This indicates that it is not the physical presence of the horizontal myoseptum, which exists in both species, but rather specific guidance signals, which are not present in *D. aesculapii*, that direct iridophores into the skin in *D. rerio*. Later, when iridophores, covered by compact xanthophores, have formed the first contiguous light stripe with adjacent melanophore stripes in *D. rerio* (Fig. 2c, e), in *D. aesculapii* melanophores and xanthophores intermix broadly (Fig. 2f); they sort out loosely into vertical bars of low contrast without coherent sheets of dense iridophores between the melanophore bars during later stages (Fig. 2h), when the *D. rerio* pattern is already fully formed (Fig. 2g). Our observations suggest that the different patterns in these sibling species are produced by the presence or absence of guidance signals for iridophores along the horizontal myoseptum as well as by cellular interactions that prevent mixing of melanophores and xanthophores in *D. rerio* but not in *D. aesculapii*.

To address the role of the different cell types, we used the CRISPR/Cas9 system to generate mutants lacking individual chromatophore types in *D. aesculapii*. Whereas in *D. rerio* vestiges of the striped pattern form in the absence of one chromatophore type (Fig. 3a, c, e)³², loss of either melanophores (Fig. 3b) or xanthophores (Fig. 3d) completely abolishes the patterning in *D. aesculapii*. This indicates that the repulsive interactions between melanophores or xanthophores and iridophores, which account for the residual patterns in *D. rerio*^{32,33}, are absent in *D. aesculapii*. In contrast, eliminating iridophores in *D. aesculapii* still permits some melanophore bar formation (Fig. 3f). This indicates that iridophores, which play a dominant role for stripe formation in *D. rerio*, are dispensable for the formation of vertical bars in *D. aesculapii*.

Weak heterotypic chromatophore interactions in bars. Next, we analysed genes with known functions in heterotypic interactions between chromatophores in *D. rerio*. Null alleles in the connexin

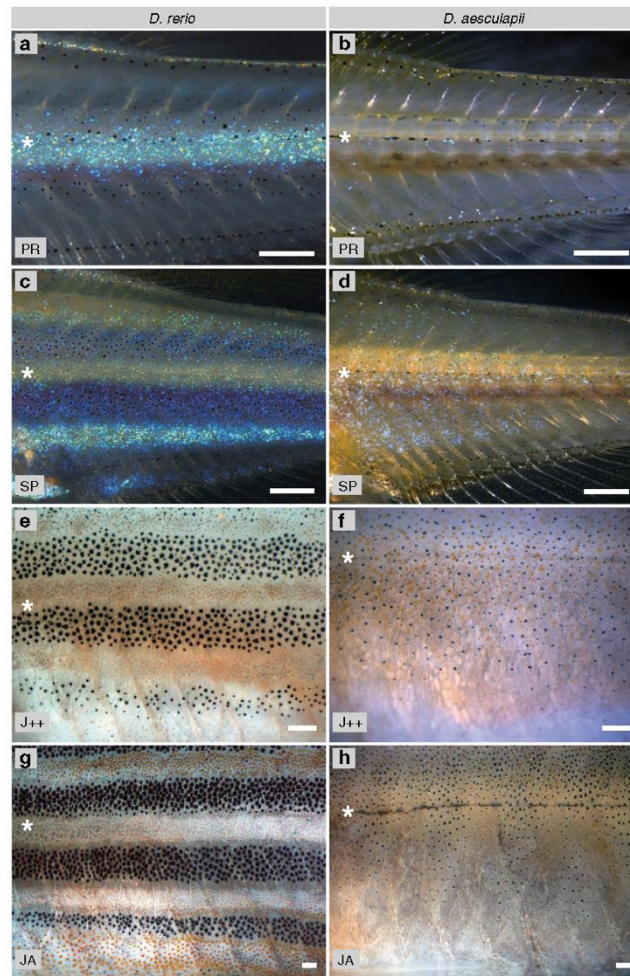


Fig. 2 Development of colour patterns in *D. rerio* and *D. aesculapii*. **a** *D. rerio* fish at stage PR, iridophores (arrowhead) emerge along the horizontal myoseptum (asterisk) to form the first light stripe. **b** *D. aesculapii* fish at stage PR. **c** *D. rerio* at stage SP, the first light stripe is flanked dorsally and ventrally by emerging dark stripes. **d** *D. aesculapii* at stage SP, iridophores emerge in a scattered fashion. **e** *D. rerio* at stage J++, light stripes are covered by compact xanthophores. **f** *D. aesculapii* at stage J++, melanophores and xanthophores broadly intermix. **g** *D. rerio* at stage JA, the stripes are fully formed. **h** *D. aesculapii* at stage JA, melanophores and xanthophores sort out loosely into vertical bars of low contrast; no dense iridophores are visible between the dark bars. **a–d** Incident light illumination to highlight iridophores, **e–h** bright field illumination to visualise xanthophores and melanophores. All pictures are representative for the corresponding species and stages ($n \geq 3$). Staging of animals according to Parichy et al.⁶³. PB (pectoral fin bud, 7.2 mm SL). SP (squamation posterior, 9.5 mm SL). J++ (juvenile posterior, 16 mm SL). JA (juvenile-adult, >16 mm SL). Scale bars correspond to 250 μm .

genes *Cx39.4* (*luchs*)⁴⁰ and *Cx41.8/Gja5b* (*leopard*)^{37,41} lead to melanophore spots (Fig. 4a, b). Both connexins are thought to form heteromeric gap junctions involved in the interaction between xanthophores and melanophores^{40,42}. Missense mutations in *Igsf11* (*seurat*)³⁶, which codes for a cell adhesion molecule, also cause a spotted pattern. We generated a frame-shift mutation in exon 3 of *Igsf11* in *D. rerio*. This mutation leads to a truncation of the protein at the end of the first Ig-domain and is, presumably, a functional null allele. Fish heterozygous for this mutation show no mutant phenotype, whereas homozygous fish

display slightly stronger pattern aberrations than those seen in the previously identified alleles (Fig. 4c)³⁶.

Mutations in *Kir7.1/Kcnj13* (*obelix/jaguar*), which codes for an inwardly rectifying potassium channel, result in fewer and wider stripes with some mixing of melanophores and xanthophores^{35,37,38}. So far, five *Kcnj13* alleles, all of which are dominant, have been identified in *D. rerio* in several independent genetic screens (Supplementary Figs. 4 and 5)^{37,38,40,56,57}. We used the CRISPR/Cas9 system to generate novel mutations in *Kcnj13* in *D. rerio*. A six-base pair in-frame deletion in exon 1,

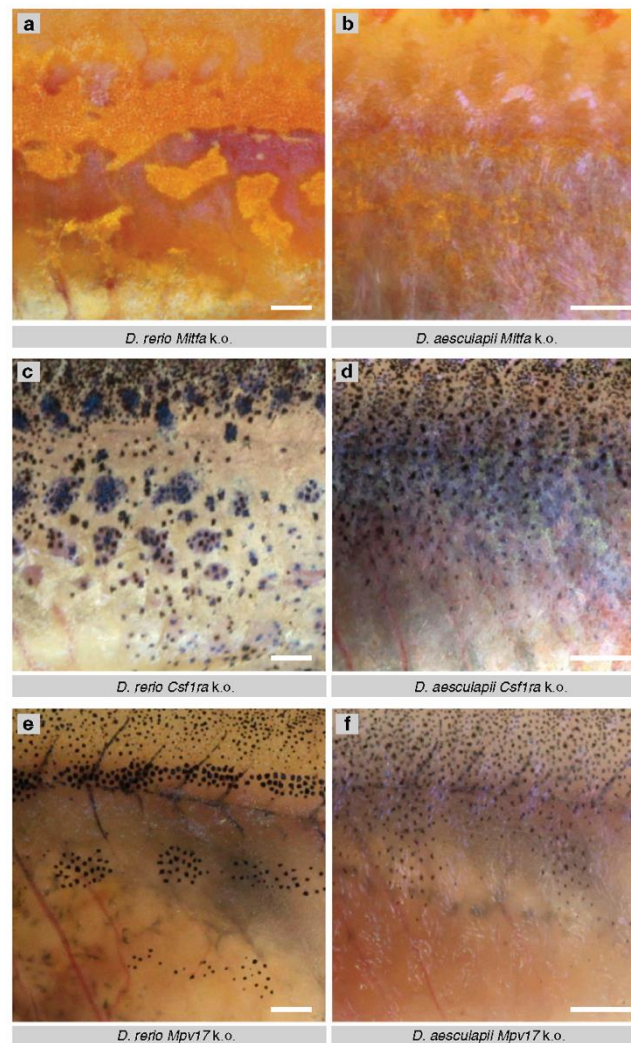


Fig. 3 Mutant phenotypes in *D. rerio* and *D. aesculapii* of genes required for individual pigment cell types. In *D. rerio* loss of one type of pigment cell type, **a** melanophores in *Mitfa* (*nacre*) mutants, **c** xanthophores in *Csf1ra* (*peffer*) mutants, or, **e** iridophores in *Mpv17* (*transparent*) mutants, still permits rudimentary aggregation of dense iridophores (**a**) or melanophores (**b**, **c**). In *D. aesculapii*, loss of melanophores, **b**, in *Mitfa* mutants ($n > 100$) or loss of xanthophores, **d**, in *Csf1ra* mutants ($n > 50$), abrogate any residual pattern formation. However, vertical melanophore bars still form in *Mpv17* mutants ($n = 8$), **f** despite the absence of iridophores. All images show representative examples of the corresponding genotypes. Scale bars correspond to 1 mm.

which leads to a loss of two amino acids in the protein (Supplementary Fig. 4), also gives rise to a dominant phenotype, similar to the already known alleles. However, using a second CRISPR target site we also recovered a frame-shift mutation. This 14-base pair insertion near the end of the first coding exon leads to an early truncation of the protein before the second transmembrane domain. This allele is recessive: heterozygous carriers have a complete wild-type pattern, homozygous mutants are indistinguishable from homozygous mutants for any of the

dominant alleles (Fig. 4d). We consider this new recessive allele to be a functional null allele.

To investigate the functions of all four genes in *D. aesculapii*, we generated presumptive null alleles in the orthologs. In all of the mutants, bar formation is abolished and we find an even distribution of melanophores (Fig. 4e–h) indicating that the interactions mediated by each of these genes are essential to generate the melanophore bars in *D. aesculapii*. The complete loss of a pattern in single mutants in *D. aesculapii* is different from *D.*

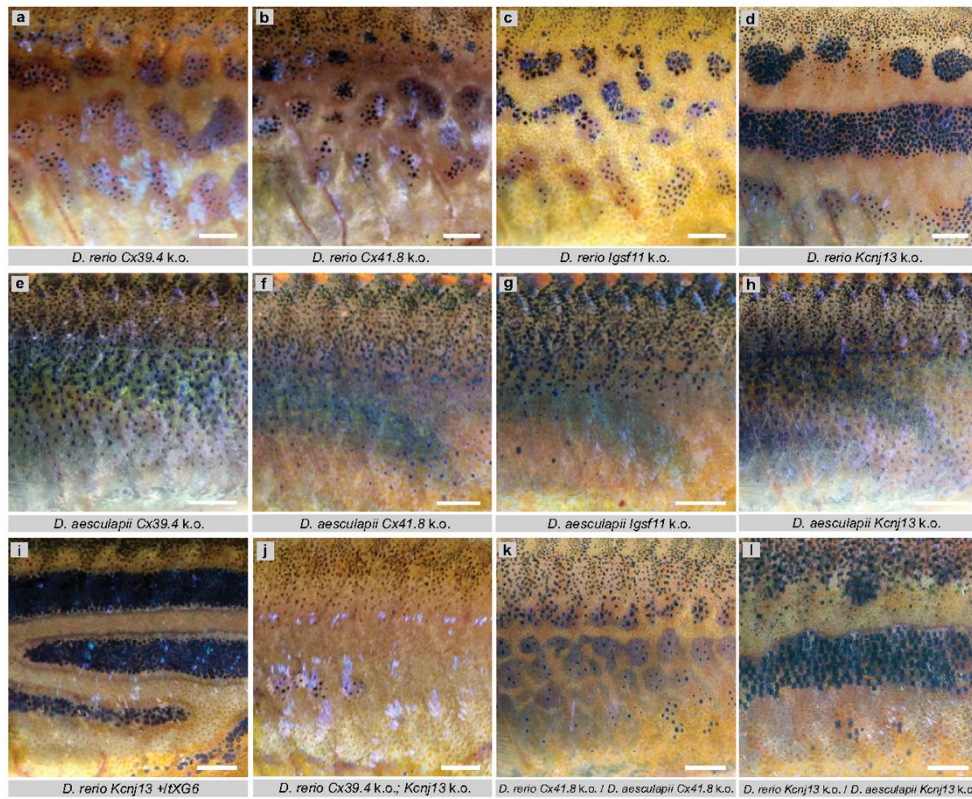


Fig. 4 Mutant phenotypes in *D. rerio*, *D. aesculapii* and their hybrids of genes required for heterotopic interactions. In *D. rerio* mutations in, **a**, *Cx39.4* (*luchs*), **b**, *Cx41.8* (*leopard*), and **c**, *Igsf11* (*seurat*) lead to spotted patterns, whereas, **d**, mutations in *Kcnj13* (*obelix*) result in fewer and wider stripes. In *D. aesculapii*, **e–h**, mutations in the orthologous genes lead to the complete loss of any pattern. In *D. rerio* dominant alleles of *Kcnj13*, **i**, cause broader stripes and irregularities when heterozygous. Double mutants, **j**, *Cx39.4* k.o.; *Kcnj13* k.o., loose almost all melanophores and pattern. Interspecific hybrids between *D. rerio* and *D. aesculapii*, which are both mutant, **k**, for *Cx41.8*, or, **l**, for *Kcnj13*, show patterns of spots or wider stripes similar to the corresponding *D. rerio* mutants (**b**, **d**; $n = 15$). All images show representative examples of the corresponding genotypes. Scale bars correspond to 1 mm.

rerio where this occurs only in double mutants (Fig. 4j)⁴⁰. In concert with predictions of agent-based models of patterning⁵⁸, this indicates that the robust formation of horizontal stripes in *D. rerio* is due to a gain in complexity based on partially redundant chromatophore interactions. These are dominated by iridophores and oriented by an as yet unidentified signal along the horizontal myoseptum. *D. aesculapii* might have secondarily lost the dominance of iridophores leading to a pattern based primarily on interactions between xanthophores and melanophores and thus of lower complexity.

We next investigated whether these genes function in the *D. rerio*/*D. aesculapii* hybrids in the same way they function in *D. rerio*. The ability to produce frame-shift mutations in both species allowed us to generate mutant hybrids that carry null alleles from both parental species. Wild-type hybrids form stripes similar to *D. rerio* (Fig. 1e)^{8,54}, hence we expect similar phenotypes comparing *D. rerio* mutants and mutant hybrids. The mutant hybrids show indeed patterning phenotypes very similar to the respective *D. rerio* mutants (Fig. 4k, l), confirming that stripe formation in the hybrids is very similar to the

process in *D. rerio* and showing that these genes have the same functions in *D. rerio* and in the hybrids.

Kcnj13 has evolved between *D. rerio* and *D. aesculapii*. Next, we generated reciprocal hemizygotes, i.e., interspecific hybrids carrying a null allele from each parental species in an otherwise identical genetic background⁵⁵. We expect similar patterns in these hybrids if the gene function has not evolved between species. A qualitatively altered hybrid pattern would reveal that one of the parental alleles cannot complement the induced loss-of-function of the other, therefore indicating functional changes in the gene during evolution. We found that hemizygous hybrids with the null allele of *Kcnj13* from *D. rerio* display a novel pattern of spots or interrupted stripes whereas a striped pattern forms with the null allele from *D. aesculapii* (Fig. 5a, b and Supplementary Fig. 2a, b). This indicates a functional diversification between the wild-type alleles from *D. rerio* and *D. aesculapii*. The phenotype of the hemizygous hybrid with a functional *D. aesculapii* allele (Fig. 5a) is qualitatively different from that of the



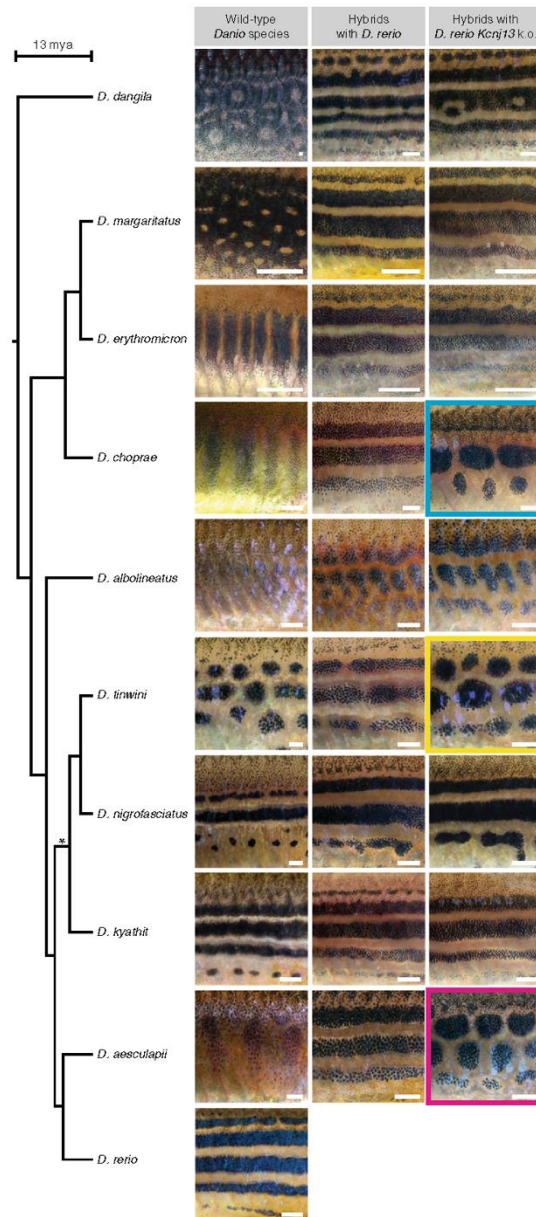
Fig. 5 A reciprocal hemizygosity test to identify *Kcnj13* evolution. Two hybrids between *D. rerio* and *D. aesculapii*, which are hemizygous for a *Kcnj13* loss-of-function mutation. **a** stripes are interrupted in hybrids carrying the mutant allele from *D. rerio* ($n > 60$, nick in the blue line representing the zebrafish genome). **b** hybrids carrying the mutant allele from *D. aesculapii* ($n = 6$, nick in the magenta line, representing the *D. aesculapii* genome) are indistinguishable from wild-type hybrids (Fig. 1e).

homozygous mutant hybrid (Fig. 4l), indicating that the *D. aesculapii* *Kcnj13* gene is functional in the hybrid. In contrast, in the case of hemizygous hybrids with *Cx39.4*, *Cx41.8* and *Igsf11* striped patterns indistinguishable from wild-type hybrids are formed regardless whether the null allele stems from *D. rerio* (Supplementary Fig. 2c, e, g) or *D. aesculapii* (Supplementary Fig. 2d, f, h). These reciprocal hemizygosity tests indicate that *Cx39.4*, *Cx41.8* and *Igsf11* provide similar functions in both species, whereas the function of *Kcnj13* has evolved between the two species.

***Kcnj13* may have evolved repeatedly in the *Danio* genus.** To investigate if *Kcnj13* underlies the pattern variation more broadly across the *Danio* genus, we crossed the *D. rerio* *Kcnj13* null allele to eight other *Danio* species (Fig. 6 and Supplementary Fig. 3). As mentioned above, wild-type hybrids between *D. rerio* and other *Danio* species display horizontal stripes, resembling the *D. rerio* pattern, with slight defects in *D. albolineatus* (Fig. 6). Strikingly, not only *D. rerio* *Kcnj13*/*D. aesculapii* hybrids (Fig. 6, highlighted in magenta, Supplementary Fig. 2a) but also *D. rerio* *Kcnj13*/*D. tinwini* hybrids (Fig. 6, highlighted in yellow, Supplementary Fig. 3c) and *D. rerio* *Kcnj13* k.o./*D. choprae* hybrids (Fig. 6, highlighted in cyan, Supplementary Fig. 3e) developed patterns of spots or interrupted stripes suggesting that the *Kcnj13* function has evolved compared to *D. rerio*. As we do not yet have the means to generate reciprocal hybrids with these additional two species, we cannot completely rule out that effects of the novel genetic background in these hybrids also contribute to the observed phenotypes. The spotted pattern in the hybrids carrying the *D. rerio* *Kcnj13* null allele, which is qualitatively different from all wild-type hybrids and also from the *D. rerio* *Kcnj13* mutant pattern, is similar to the parental pattern of *D. tinwini*, where dense iridophores interrupt the dark melanophore stripes (Figs. 1d and 6). No qualitative differences were detected between wild-type hybrids and hybrids hemizygous for *D. rerio* *Kcnj13* in the case of *D. kyathit*, *D. nigrofasciatus*, *D. albolineatus*, *D. erythromicron*, *D. margaritatus* and *D. dangila* (Fig. 6). This indicates that the alleles from these species complement the loss of the *D. rerio* *Kcnj13* allele and supports the notion that the barred pattern in *D. erythromicron* develops in a different manner from the other two barred species. Taken together, functional changes of *Kcnj13* occurred between *D. rerio* and *D. aesculapii*, possibly also between *D. rerio* and *D. tinwini* and *D. choprae*. However, we never observed pure *D. rerio* *Kcnj13* mutant patterns in

hemizygous hybrids, similar to mutant hybrids (Fig. 4l), indicating that the orthologs provide essential functions for patterning across all species tested and that a patterning function of *Kcnj13* might have predated the origin of the *Danio* genus. The separated positions of the three species with putative functional changes of *Kcnj13* in the phylogenetic tree (graph on the left of Fig. 6)⁵² suggest a repeated and independent evolution of an ancestral gene function.

The potassium channel gene *Kcnj13*. Potassium channels have important roles in tissue patterning⁵⁹, notably in the regulation of allometric growth of fins in *D. rerio*^{57,60–62}. *Kcnj13* encodes an inwardly rectifying potassium channel (Kir7.1) conserved in vertebrates (Supplementary Fig. 4). Mutations are known to cause defects in tracheal development in mice⁶³ and two rare diseases in humans leading to visual impairment^{64–70}. During colour pattern formation in *D. rerio*, *Kcnj13* function is autonomously required in melanophores³⁵, and in ex vivo studies it was shown that the channel is involved in the contact-dependent depolarisation of melanophores upon interactions with xanthophores leading to a repulsion between these cells³⁹. Evolution in *Kcnj13* in *D. aesculapii*, *D. tinwini* and *D. choprae* might therefore cause differences in heterotypic chromatophore interactions between species. The *Kcnj13* protein functions as a tetramer, where each subunit contributes two transmembrane helices (M1 and M2, Supplementary Figs. 4 and 5) to the formation of the channel pore, as well as a short extracellular loop that folds back to form the pore lining ion selectivity filter (P-loop or H5, Fig. 4). The N- and C-termini of all four subunits reside in the cytoplasm, where they also contribute to the ion pore, but are mainly involved in gating of the channel (reviewed in Hibino et al.⁷¹). In *D. rerio* dominant mutant alleles of *Kcnj13* show broad stripes with irregular interruptions when heterozygous (Fig. 4i) and stronger pattern aberrations with fewer, wider and interrupted dark stripes and some mixing of melanophores and xanthophores when homozygous or trans-heterozygous. Three of them carry point mutations affecting H5 or M2, one is the result of a C-terminal truncation (Supplementary Fig. 5). The point mutations lead to proteins that do not produce functional channels and it has been suggested that the dominant phenotype is caused by a dosage-dependent effect, i.e., haploinsufficiency³⁵. As the presumptive null allele we generated is recessive and shows a homozygous phenotype that is indistinguishable from the phenotype of the dominant alleles, these must in fact be dominant-negatives, where



the mutant proteins inhibit the function of the wild-type protein still present in heterozygotes.

Using transcriptome data from species across the genus in combination with published data from *D. rerio*⁷² we reconstructed the protein coding sequences of *Kcnj13* orthologs, which are highly conserved with only very few diverged sites in the cytoplasmic N- and C-terminal parts of the protein

(Supplementary Fig. 5). Whether these amino acid changes are the basis for the potentially repeated and independent evolution of *Kcnj13*, and if or how they might affect the function of the channel will require further experiments. The alleles in the three other species cannot simply be loss-of-function alleles, because the hybrid phenotypes differ from the homozygous mutant hybrids and also from *D. rerio Kcnj13* mutants. It is also possible

Fig. 6 One-way complementation tests suggest repeated *Kcnj13* evolution. On the left the phylogenetic tree depicts the relationship between the *Danio* species; the asterisk denotes a node with lower bootstrap support. The left column shows the patterns of the different species. In the middle column patterns of wild-type hybrids with *D. rerio* are shown (see also Supplementary Fig. 1). In the right column patterns of hybrids that carry a mutant *Kcnj13* allele from *D. rerio* are shown. Pattern defects are obvious in three cases: hybrids with *D. aesculapii* ($n > 60$, magenta), with *D. tinwini* ($n = 12$, yellow) and *D. choprae* ($n = 40$, cyan). In the other six cases the patterns in hemizygous hybrids do not differ from the striped patterns of wild-type hybrids (*D. rerio Kcnj13* k.o./*D. kyathit*, $n = 32$; *D. rerio Kcnj13* k.o./*D. nigrofasciatus*, $n = 16$; *D. rerio Kcnj13* k.o./*D. albolineatus*, $n = 4$; *D. rerio Kcnj13* k.o./*D. erythromicron*, $n = 38$; *D. rerio Kcnj13* k.o./*D. margaritatus*, $n = 12$; and *D. rerio Kcnj13* k.o./*D. dangila*, $n = 16$). All pictures show representative examples of the corresponding species/hybrids/genotypes; for variability of the hybrid patterns see also Supplementary Fig. 3. Scale bars correspond to 1 mm.

that qualitative or quantitative changes in gene expression might be the basis for the observed divergence in gene function.

Discussion

In contrast to mammals and birds, basal vertebrates retained several chromatophore types providing a substrate for the development of elaborate colour patterns. In zebrafish a relatively large number of genes regulating the formation of pigment patterns have already been identified by mutant screens. Due to the teleost-specific whole genome duplication and the following sub-functionalisation and retention of paralogs, many of these genes are specifically involved in adult colour patterning^{14,15} and mutations in them show few, if any, pleiotropic effects^{43,73}. Therefore, these genes are candidates for mediating pattern evolution^{5,9}.

In the *Danio* genus the pattern of *D. nigrofasciatus*, with fewer and interrupted dark stripes (Fig. 6), resembles the mutant phenotype of weak alleles involved in endothelin signalling in *D. rerio*. In zebrafish, endothelin signalling is directly required in iridophores for their development and proliferation; iridophores indirectly promote and sustain melanophore development³². Several paralogs exist for endothelin receptors and ligands⁷⁴, only one of each is specifically involved in patterning^{7,29,73,75}. Indeed, it has been shown that in *D. nigrofasciatus*, due to cis-regulatory changes, the expression of the secreted ligand Endothelin 3b (*Edn3b*) is lower than in *D. rerio*⁷³. Interspecific hybrids between the two species show lower expression of *Edn3b* from the *D. nigrofasciatus* allele compared to the *D. rerio* allele, confirming cis-regulatory changes in this gene between the two species.

We compared the development of the pattern in *D. rerio* with its closest sibling species, *D. aesculapii*, which has a completely different pattern of vertical bars. Whereas the orientation of the stripes in *D. rerio* depends on the presence of the horizontal myoseptum³², as a structure through which the first iridophores reach the skin during metamorphosis, this is not the case in *D. aesculapii*. Here iridophores appear more scattered and only during later developmental stages (Fig. 2). This result might mean that in zebrafish the iridophores follow an attractive signal that lines the horizontal myoseptum; this signal, or the ability to respond to it, could be lost in *D. aesculapii*. The signal would be present in all the interspecific hybrids that have *D. rerio* as one parent, explaining the dominance of the horizontal stripes.

However, additional differences must also exist, because the pattern in *D. aesculapii* is very dissimilar to *D. rerio* mutants that lack the horizontal myoseptum (Fig. 1b)³². To address this question, we generated mutations in *D. aesculapii* that lead to the absence of one class of pigment cells (Fig. 3). The phenotypic analysis of these mutants showed that, if melanophores or xanthophores are missing, the remaining two cell types completely intermingle. This indicates that the cellular interactions are less complex in *D. aesculapii*. In contrast, we find that in the absence of iridophores a residual pattern is formed, which shows that iridophores, which play a leading role in patterning in *D. rerio*^{20,32,33}, only have a minor influence on the pattern in *D. aesculapii*.

To start revealing the genetic basis for the evolution of colour patterns in *Danio* fish we focused on a group of genes regulating heterotypic interactions among chromatophores^{35–41}. These generally have strong recessive phenotypes and appear to have no obvious effects on other vital functions. Using reciprocal hemizygosity tests we identified the potassium channel gene *Kcnj13* as contributing to the patterning divergence between *D. rerio* and *D. aesculapii* (Fig. 5); one-way complementation tests suggest a broader role for *Kcnj13* in pattern diversification in the genus *Danio* including two more species, *D. tinwini* and *D. choprae* (Fig. 6). In *D. rerio* over 100 genes code for potassium channels of several different families, calcium-activated (K_{Ca}), two-pore (K_{2P}), voltage-gated (K_v) and inwardly rectifying (K_{IR}) channels. Potassium channels are expressed in many tissues and have diverse physiological roles, e.g., in the heart, kidney or nervous system. During development and regeneration potassium channels are involved in bioelectric signalling regulating allometric fin growth in *D. rerio*. Overgrowth of fins is caused by gain-of-function mutations in *Kcnh2a* (*longfin*)⁶² and *Kcnk5b* (*another longfin*)⁶⁰. In *schleier* mutants overgrowth is caused by a loss-of-function of the K^+ - Cl^- -cotransporter *Slc12a7a/Kcc4a*⁶¹. It has also been shown that ectopic expression in the myotome of *Kcnj13* leads to overgrowing fins, arguing in favour of the predicted general role of this class of channels in setting the resting membrane potential of cells⁵⁷. Zebrafish mutant for *Kcnj13*, including the newly generated null allele, are viable and show a phenotype specifically in pigment patterning; this might favour *Kcnj13* as a target for evolutionary change. The gene is expressed in other tissues besides chromatophores^{76–78} and the apparent lack of pleiotropy could be due to redundancies with other potassium channels. *Kcnj13* is cell-autonomously required in melanophores, which appear ectopically in light stripes, and form irregular enlarged dark stripes sometimes intermixed with ectopic xanthophores in the mutants^{35,37–39}. In *D. aesculapii*, mutations in *Kcnj13* cause a uniform distribution of melanophores, and no repulsive interactions with xanthophores are observed. The phenotype of hybrids with *D. aesculapii*, in which only the *D. aesculapii* allele is functional, is qualitatively different from the null allele of either species, and also from the dominant hypomorphic phenotype in *D. rerio*. This suggests that the change in *D. aesculapii* cannot simply be due to reduced expression levels, however spatial or temporal quantitative changes of gene expression might affect the function of the gene. Whether changes in the coding sequence are involved remains an open question. We do know, however, that *Kcnj13* from all tested species still has at least some residual function in patterning in the hybrids; none of them showed a complete mutant phenotype when only the *D. rerio* allele was non-functional. Therefore, we conclude that *Kcnj13* is active in colour pattern formation in all *Danio* species. Whereas the other patterning genes that we tested in *D. rerio/D. aesculapii* hybrids, *Cx39.4*, *Cx41.8* and *Igsf11*, show no divergence in function between these two species, it is likely that they are involved in pattern evolution in other species. The results of our study show that the genus *Danio* offers the opportunity to identify evolved genes and to reconstruct evolutionary history of biodiversity.

Methods

No statistical methods were used to predetermine sample size. The experiments were not randomised. The investigators were not blinded to allocation during experiments and outcome assessment.

Fish husbandry. Zebrafish, *D. rerio*, were maintained as described earlier⁷⁹. If not newly generated (Table 4 and Supplementary Information), the following genotypes were used: wild-type Tuebingen/TU, *nacre*^{em2}/Mittfa⁸⁰, *pfeffer*^{tm236}/Csflra⁸¹, *transparent*^{tm6}/Mpv1⁷⁸², *leopard*¹/Cx41.8^{37,41}, *luchis*^{ts7a}/Cx39.4⁴⁰ and *obelix*^{XG6}/Konj13⁴⁰.

D. aesculapii and *D. albolineatus* were maintained identical to *D. rerio*. For the other *Danio* species, *D. kyathit*, *D. tinwini*, *D. nigrofasciatus*, *D. choprae*, *D. margaritatus*, *D. erythromicron* and *D. dangila* individual pair matings were not successful. Therefore, the fish were kept in groups in tanks containing boxes lightly covered with Java moss (*Taxiphyllum barbieri*), which resulted in sporadic matings and allowed us to collect fertilised eggs.

Interspecific hybrids were either obtained by natural matings or by in vitro fertilisations⁵⁴. Hemizygous or homozygous mutant hybrids were identified by PCR and sequence analysis using specific primer pairs (Tables 1 and 3 and Supplementary Information).

All species were staged according to the normal table of *D. rerio* development⁸⁸. All animal experiments were performed in accordance with the rules of the State of Baden-Württemberg, Germany, and approved by the Regierungspräsidium Tübingen.

CRISPR/Cas9 gene editing. The CRISPR/Cas9 system was applied either as described in Irion et al.⁸⁹ or according to the guidelines for embryo microinjection of Integrated DNA Technologies (IDT). Briefly, oligonucleotides were cloned into pDR274 to generate the sgRNA vector (Supplementary Tables 1 and 2). sgRNAs were transcribed from the linearised vector using the MEGAscript T7 Transcription Kit (Invitrogen). Alternatively, target-specific crRNAs and universal tracrRNAs were purchased from IDT. sgRNAs or crRNA:tracrRNA duplexes were injected as ribonucleoprotein complexes with Cas9 proteins into one-cell stage embryos. The efficiency of indel generation was tested on eight larvae at 1 dpf by PCR using specific primer pairs and by sequence analysis as described previously (Supplementary Tables 1 and 3)⁸⁵. The remaining larvae were raised to adulthood. Mature F0 fish carrying indels were outcrossed. Loss-of-function alleles in heterozygous F1 fish were selected to establish homozygous or trans-heterozygous mutant lines (Supplementary Table 4).

Image acquisition. Anaesthesia of adult fish was performed as described previously⁸⁵. A Canon 5D Mk II camera was used to obtain images. Fish with different colour patterns vary considerably in contrast, thus requiring different settings for aperture and exposure time, which can result in slightly different colour representations in the pictures. Juvenile fish were either embedded in low melting point agarose or fixed in 4% formaldehyde/0.08% glutaraldehyde and then photographed under a Leica MZ1 stereo microscope (Fig. 2). Images were processed Adobe Photoshop and Adobe Illustrator CS6.

Transcriptomics and sequence analysis. Adult fish ($n = 5$ each for *D. rerio* (TU), *D. aesculapii*, *D. kyathit*, *D. nigrofasciatus*, *D. tinwini*, *D. albolineatus*, *D. choprae*, *D. erythromicron* and *D. margaritatus*) were euthanized by exposure to buffered 0.5 g/L MS-222 (Tricaine). Skin tissues were dissected in ice-cold PBS and collected using TRIzol (Life Technologies). RNA integrity and quantity were assessed by Agilent 2100 Bioanalyzer. Library preparation (TruSeq stranded mRNA, Illumina; 200 ng per sample) and sequencing (NovaSeq 6000, 2 × 100 bp) were performed by CeGaT GmbH (Tübingen, Germany). RNA-Seq analysis was carried out using the *Danio rerio* GRCz11 genome build for all *Danio* species and STAR aligner with default settings⁸⁶. We found SNPs in the coding region of *Konj13* and considered other resources⁸⁷, including the latest zebrafish reference genome assembly (GRCz11), the ENA deposition Zebrafish Genome Diversity (PRJEB20043, Wellcome Trust Sanger) and the Zebrafish Mutation Project⁷². The variant calling pipeline for all *Danio* species consisted of GATK 3.8 and 4 and picard⁸⁸ from STAR-aligned bam files based on GATK Best-Practices pipeline. The full commands used can be found here: <https://github.com/najasplus/STAR-deseq2> and https://github.com/najasplus/rnaseq_variant_calling. Variants were also called and checked using SAMtools, mpileup and bcftools⁸⁹. The protein sequence alignment was produced using T-coffee⁹⁰.

Reporting summary. Further information on research design is available in the Nature Research Reporting Summary linked to this article.

Data availability

The authors declare that all data supporting the findings of this study are available within the article and its supplementary information files or from the corresponding author upon reasonable request. The dataset generated during this study is available at The European Nucleotide Archive (ENA) accession number: PRJEB36366.

Received: 10 June 2020; Accepted: 6 November 2020;

Published online: 04 December 2020

References

- Darwin, C. *The Descent Of Man, And Selection In Relation To Sex* (John Murray, London, 1871).
- Protas, M. E. & Patel, N. H. Evolution of coloration patterns. *Annu. Rev. Cell Dev. Biol.* **24**, 425–446 (2008).
- Cuthill, I. C. et al. The biology of color. *Science* <https://doi.org/10.1126/science.aan0221> (2017).
- Nüsslein-Volhard, C., Grutzmacher, S. & Howard, J. *Animal Beauty: On The Evolution Of Biological Aesthetics* (The MIT Press, 2019).
- Stern, D. L. & Orgogozo, V. Is genetic evolution predictable? *Science* **323**, 746–751 (2009).
- Martin, A. & Orgogozo, V. The Loci of repeated evolution: a catalog of genetic hotspots of phenotypic variation. *Evolution* **67**, 1235–1250 (2013).
- Irion, U. & Nüsslein-Volhard, C. The identification of genes involved in the evolution of color patterns in fish. *Curr. Opin. Genet. Dev.* **57**, 31–38 (2019).
- Patterson, L. B. & Parichy, D. M. Zebrafish pigment pattern formation: insights into the development and evolution of adult form. *Annu. Rev. Genet.* **53**, 505–530 (2019).
- Orteu, A. & Jiggins, C. D. The genomics of coloration provides insights into adaptive evolution. *Nat. Rev. Genet.* <https://doi.org/10.1038/s41576-020-0234-z> (2020).
- Nijhout, H. F. Molecular and physiological basis of colour pattern formation. *Adv. Insect Physiol.* **38**, 219–265 (2010).
- Reed, R. D. et al. Optix drives the repeated convergent evolution of butterfly wing pattern mimicry. *Science* **333**, 1137–1141 (2011).
- Van Belleghem, S. M. et al. Complex modular architecture around a simple toolkit of wing pattern genes. *Nat. Ecol. Evol.* **1**, 52 (2017).
- Singh, A. P. & Nüsslein-Volhard, C. Zebrafish stripes as a model for vertebrate colour pattern formation. *Curr. Biol.* **25**, R81–R92 (2015).
- Braasch, I., Brunet, F., Volff, J. N. & Scharl, M. Pigmentation pathway evolution after whole-genome duplication in fish. *Genome Biol. Evol.* **1**, 479–493 (2009).
- Lorin, T., Brunet, F. G., Laudet, V. & Volff, J. N. Teleost fish-specific preferential retention of pigmentation gene-containing families after whole genome duplications in vertebrates. *G3* **8**, 1795–1806 (2018).
- Kratochwil, C. P. et al. Agouti-related peptide 2 facilitates convergent evolution of stripe patterns across cichlid fish radiations. *Science* **362**, 457–460 (2018).
- Irion, U., Singh, A. P. & Nüsslein-Volhard, C. In *Current Topics in Developmental Biology*. Ch. 8 (Elsevier Inc., 2016).
- Parichy, D. M. Evolution of danio pigment pattern development. *Heredity* **97**, 200–210 (2006).
- Kondo, S., Iwashita, M. & Yamaguchi, M. How animals get their skin patterns: fish pigment pattern as a live Turing wave. *Int. J. Dev. Biol.* **53**, 851–856 (2009).
- Singh, A. P., Schach, U. & Nüsslein-Volhard, C. Proliferation, dispersal and patterned aggregation of iridophores in the skin prefigure striped colouration of zebrafish. *Nat. Cell Biol.* **16**, 607–614 (2014).
- Hirata, M., Nakamura, K. & Kondo, S. Pigment cell distributions in different tissues of the zebrafish, with special reference to the striped pigment pattern. *Dev. Dyn.* **234**, 293–300 (2005).
- Hirata, M., Nakamura, K., Kanemaru, T., Shibata, Y. & Kondo, S. Pigment cell organization in the hypodermis of zebrafish. *Dev. Dyn.* **227**, 497–503 (2003).
- Mahalwar, P., Walderich, B., Singh, A. P. & Nüsslein-Volhard, C. Local reorganization of xanthophores fine-tunes and colors the striped pattern of zebrafish. *Science* **345**, 1362–1364 (2014).
- Budi, E. H., Patterson, L. B. & Parichy, D. M. Post-embryonic nerve-associated precursors to adult pigment cells: genetic requirements and dynamics of morphogenesis and differentiation. *PLoS Genet.* **7**, e1002044 (2011).
- Mongera, A. et al. Genetic lineage labeling in zebrafish uncovers novel neural crest contributions to the head, including gill pillar cells. *Development* **140**, 916–925 (2013).
- Dooley, C. M., Mongera, A., Walderich, B. & Nüsslein-Volhard, C. On the embryonic origin of adult melanophores: the role of ErbB and Kit signalling in establishing melanophore stem cells in zebrafish. *Development* **140**, 1003–1013 (2013).
- Patterson, L. B., Bain, E. J. & Parichy, D. M. Pigment cell interactions and differential xanthophore recruitment underlying zebrafish stripe reiteration and Danio pattern evolution. *Nat. Commun.* **5**, 5299 (2014).
- Singh, A. P. et al. Pigment cell progenitors in zebrafish remain multipotent through metamorphosis. *Dev. Cell* **38**, 316–330 (2016).

29. Parichy, D. M. et al. Mutational analysis of endothelin receptor b1 (rose) during neural crest and pigment pattern development in the zebrafish *Danio rerio*. *Dev. Biol.* **227**, 294–306 (2000).
30. Parichy, D. M. & Turner, J. M. Temporal and cellular requirements for Fms signaling during zebrafish adult pigment pattern development. *Development* **130**, 817–833 (2003).
31. Walderich, B., Singh, A. P., Mahalwar, P. & Nüsslein-Volhard, C. Homotypic cell competition regulates proliferation and tiling of zebrafish pigment cells during colour pattern formation. *Nat. Commun.* **7**, 11462 (2016).
32. Fröhnhofer, H. G., Krauss, J., Maischein, H. M. & Nüsslein-Volhard, C. Iridophores and their interactions with other chromatophores are required for stripe formation in zebrafish. *Development* **140**, 2997–3007 (2013).
33. Patterson, L. B. & Parichy, D. M. Interactions with iridophores and the tissue environment required for patterning melanophores and xanthophores during zebrafish adult pigment stripe formation. *PLoS Genet.* **9**, e1003561 (2013).
34. Mahalwar, P., Singh, A. P., Fadeev, A., Nüsslein-Volhard, C. & Irion, U. Heterotypic interactions regulate cell shape and density during color pattern formation in zebrafish. *Biol. Open* **5**, 1680–1690 (2016).
35. Maderspacher, P. & Nüsslein-Volhard, C. Formation of the adult pigment pattern in zebrafish requires leopard and obelix dependent cell interactions. *Development* **130**, 3447–3457 (2003).
36. Eom, D. S. et al. Melanophore migration and survival during zebrafish adult pigment stripe development require the immunoglobulin superfamily adhesion molecule Igsf11. *PLoS Genet.* **8**, e1002899 (2012).
37. Haffter, P. et al. Mutations affecting pigmentation and shape of the adult zebrafish. *Dev. Genes Evol.* **206**, 260–276 (1996).
38. Iwashita, M. et al. Pigment pattern in jaguar/obelix zebrafish is caused by a *Kir7.1* mutation: implications for the regulation of melanosome movement. *PLoS Genet.* **2**, e197 (2006).
39. Inaba, M., Yamana, H. & Kondo, S. Pigment pattern formation by contact-dependent depolarization. *Science* **335**, 677 (2012).
40. Irion, U. et al. Gap junctions composed of connexins 41.8 and 39.4 are essential for colour pattern formation in zebrafish. *Elife* **3**, e05125 (2014).
41. Watanabe, M. et al. Spot pattern of leopard *Danio* is caused by mutation in the zebrafish connexin41.8 gene. *EMBO Rep.* **7**, 893–897 (2006).
42. Watanabe, M., Sawada, R., Aramaki, T., Skerrett, I. M. & Kondo, S. The physiological characterization of Connexin41.8 and Connexin39.4, which are involved in the striped pattern formation of zebrafish. *J. Biol. Chem.* **291**, 1053–1063 (2016).
43. Lang, M. R., Patterson, L. B., Gordon, T. N., Johnson, S. L. & Parichy, D. M. *Basonuclin-2* requirements for zebrafish adult pigment pattern development and female fertility. *PLoS Genet.* **5**, e1000744 (2009).
44. Eom, D. S. & Parichy, D. M. A macrophage relay for long-distance signaling during postembryonic tissue remodeling. *Science* **355**, 1317–1320 (2017).
45. Eskova, A. et al. Gain-of-function mutations in *Aqp3a* influence zebrafish pigment pattern formation through the tissue environment. *Development* **144**, 2059–2069 (2017).
46. McMenamin, S. K. et al. Thyroid hormone-dependent adult pigment cell lineage and pattern in zebrafish. <https://doi.org/10.1126/science.1256251> (2014).
47. Eom, D. S., Bain, E. J., Patterson, L. B., Grout, M. E. & Parichy, D. M. Long-distance communication by specialized cellular projections during pigment pattern development and evolution. *Elife* <https://doi.org/10.7554/eLife.12401> (2015).
48. Eskova, A., Fröhnhofer, H. G., Nüsslein-Volhard, C. & Irion, U. Galanin signaling in the brain regulates color pattern formation in zebrafish. *Curr. Biol.* **30**, 298–303.e293 (2020).
49. Zhang, Y. M. et al. Distant insulin signaling regulates vertebrate pigmentation through the sheddase *Bace2*. *Dev. Cell* **45**, 580–594.e587 (2018).
50. Kullander, S. O. & Fang, P. *Danio aesculapii*, a new species of danio from south-western Myanmar (Teleostei: Cyprinidae). *Zootaxa* **2164**, 41–48 (2009).
51. Kullander, S. O. & Fang, P. *Danio tinwini*, a new species of spotted danio from northern Myanmar (Teleostei: Cyprinidae). *Ichthyol. Explor. Freshw.* **20**, 223–228 (2009).
52. McCluskey, B. M. & Postlethwait, J. H. Phylogeny of zebrafish, a “model species,” within *Danio*, a “model genus”. *Mol. Biol. Evol.* **32**, 635–652 (2015).
53. Parichy, D. M. Advancing biology through a deeper understanding of zebrafish ecology and evolution. *Elife* <https://doi.org/10.7554/eLife.05635> (2015).
54. Parichy, D. M. & Johnson, S. L. Zebrafish hybrids suggest genetic mechanisms for pigment pattern diversification in *Danio*. *Dev. Genes Evol.* **211**, 319–328 (2001).
55. Stern, D. L. Identification of loci that cause phenotypic variation in diverse species with the reciprocal hemizygosity test. *Trends Genet.* **30**, 547–554 (2014).
56. Henke, K. et al. Genetic screen for postembryonic development in the zebrafish (*Danio rerio*): dominant mutations affecting adult form. *Genetics* **207**, 609–623 (2017).
57. Silic, M. R. et al. Potassium channel-associated bioelectricity of the dermomyotome determines fin patterning in zebrafish. *Genetics* **215**, 1067–1084 (2020).
58. Volkening, A. & Sandstede, B. Iridophores as a source of robustness in zebrafish stripes and variability in *Danio* patterns. *Nat. Commun.* **9**, 3231 (2018).
59. Dahal, G. R. et al. An inwardly rectifying K⁺ channel is required for patterning. *Development* **139**, 3653–3664 (2012).
60. Perathoner, S. et al. Bioelectric signaling regulates size in zebrafish fins. *PLoS Genet.* **10**, e1004080 (2014).
61. Lanni, J. S. et al. Integrated K⁺ channel and K⁺Cl⁻ cotransporter functions are required for the coordination of size and proportion during development. *Dev. Biol.* **456**, 164–178 (2019).
62. Stewart, S. et al. longfin causes cis ectopic expression of the *kcnh2a* ether-a-go-go K⁺ channel to autonomously prolong fin outgrowth. *bioRxiv* <https://doi.org/10.1101/790329> (2019).
63. Yin, W. et al. The potassium channel KCNJ13 is essential for smooth muscle cytoskeletal organization during mouse tracheal tubulogenesis. *Nat. Commun.* **9**, 2815 (2018).
64. Lee, M. M., Ritter, R. 3rd, Hirose, T., Vu, C. D. & Edwards, A. O. Snowflake vitreoretinal degeneration: follow-up of the original family. *Ophthalmology* **110**, 2418–2426 (2003).
65. Hejtmančík, J. P. et al. Mutations in KCNJ13 cause autosomal-dominant snowflake vitreoretinal degeneration. *Am. J. Hum. Genet.* **82**, 174–180 (2008).
66. Sergouniotis, P. I. et al. Recessive mutations in KCNJ13, encoding an inwardly rectifying potassium channel subunit, cause leber congenital amaurosis. *Am. J. Hum. Genet.* **89**, 183–190 (2011).
67. Khan, A. O., Bergmann, C., Neuhaus, C. & Bolz, H. J. A distinct vitreo-retinal dystrophy with early-onset cataract from recessive KCNJ13 mutations. *Ophthalmic Genet.* **36**, 79–84 (2015).
68. Pattnaik, B. R. et al. A novel KCNJ13 nonsense mutation and loss of *Kir7.1* channel function causes leber congenital amaurosis (LCA16). *Hum. Mutat.* **36**, 720–727 (2015).
69. Perez-Roustit, S. et al. Leber congenital amaurosis with large retinal pigment clumps caused by compound heterozygous mutations in *Kcnj13*. *Retin. Cases Brief. Rep.* **11**, 221–226 (2017).
70. Toms, M. et al. Missense variants in the conserved transmembrane M2 protein domain of KCNJ13 associated with retinovascular changes in humans and zebrafish. *Exp. Eye Res.* **189**, 107852 (2019).
71. Hibino, H. et al. Inwardly rectifying potassium channels: their structure, function, and physiological roles. *Physiol. Rev.* **90**, 291–366 (2010).
72. Dooley, C. M. et al. Multi-allelic genotyping—a systematic approach for the simultaneous analysis of multiple induced mutations. *Methods* **62**, 197–206 (2013).
73. Spiewak, J. E. et al. Evolution of Endothelin signaling and diversification of adult pigment pattern in *Danio* fishes. *PLoS Genet.* **14**, e1007538 (2018).
74. Braasch, L., Volf, J. N. & Scharf, M. The endothelin system: evolution of vertebrate-specific ligand-receptor interactions by three rounds of genome duplication. *Mol. Biol. Evol.* **26**, 783–799 (2009).
75. Camargo-Sosa, K. et al. Endothelin receptor Aa regulates proliferation and differentiation of Erb-dependent pigment progenitors in zebrafish. *PLoS Genet.* **15**, e1007941 (2019).
76. Watanabe, M., Hiraide, K. & Okada, N. Functional diversification of *kir7.1* in cichlids accelerated by gene duplication. *Genes* **9**, 46–52 (2017).
77. White, R. J. et al. A high-resolution mRNA expression time course of embryonic development in zebrafish. *Elife* <https://doi.org/10.7554/eLife.30860> (2017).
78. Toms, M. et al. Phagosomal and mitochondrial alterations in RPE may contribute to KCNJ13 retinopathy. *Sci. Rep.* **9**, 3793 (2019).
79. Brand, M., Granato, M. & Nüsslein-Volhard, C. In *Zebrafish: A Practical Approach* (eds C. Nüsslein-Volhard & R. Dahm) (Oxford University Press, 2002).
80. Lister, J. A., Robertson, C. P., Lepage, T., Johnson, S. L. & Raible, D. W. *nacre* encodes a zebrafish microphthalmia-related protein that regulates neural-crest-derived pigment cell fate. *Development* **126**, 3757–3767 (1999).
81. Odenthal, J. et al. Mutations affecting xanthophore pigmentation in the zebrafish, *Danio rerio*. *Development* **123**, 391–398 (1996).
82. Krauss, J., Astrinidis, P., Fröhnhofer, H. G., Walderich, B. & Nüsslein-Volhard, C. transparent, a gene affecting stripe formation in Zebrafish, encodes the mitochondrial protein Mpv17 that is required for iridophore survival. *Biol. Open* **2**, 703–710 (2013).
83. Parichy, D. M., Elizondo, M. R., Mills, M. G., Gordon, T. N. & Engeszer, R. E. Normal table of postembryonic zebrafish development: staging by externally visible anatomy of the living fish. *Dev. Dyn.* **238**, 2975–3015 (2009).
84. Irion, U., Krauss, J. & Nüsslein-Volhard, C. Precise and efficient genome editing in zebrafish using the CRISPR/Cas9 system. *Development* **141**, 4827–4830 (2014).
85. Meeker, N. D., Hutchinson, S. A., Ho, L. & Trede, N. S. Method for isolation of PCR-ready genomic DNA from zebrafish tissues. *Biotechniques* **43**, 610, 612, 614 (2007).

86. Dobin, A. & Gingeras, T. R. Mapping RNA-seq Reads with STAR. *Curr. Protoc. Bioinform.* **51**, 11.14.11–11.14.19 (2015).
87. Bowen, M. E., Henke, K., Siegfried, K. R., Warman, M. L. & Harris, M. P. Efficient mapping and cloning of mutations in zebrafish by low-coverage whole-genome sequencing. *Genetics* **190**, 1017–1024 (2012).
88. Poplin, R. et al. Scaling accurate genetic variant discovery to tens of thousands of samples. *bioRxiv* <https://doi.org/10.1101/201178> (2018).
89. Li, H. et al. The Sequence Alignment/Map format and SAMtools. *Bioinformatics* **25**, 2078–2079 (2009).
90. Notredame, C., Higgins, D. G. & Heringa, J. T-Coffee: A novel method for fast and accurate multiple sequence alignment. *J. Mol. Biol.* **302**, 205–217 (2000).

Acknowledgements

We thank Silke Geiger-Rudolph, Horst Geiger and Roberta Occhinegro for excellent technical assistance and Patrick Müller for discussion. This work was supported by an ERC Advanced Grant "DanioPattern" (694289) and the Max Planck Society, Germany.

Author contributions

All authors were involved in the design of the experiments. M.P., U.I. and H.G.F. performed the experiments. U.I., C.N.V., M.P., H.G.F. and C.M.D. analysed the data with support of A.E.; M.P. made the figures with contributions from U.I. and C.N.V.; U.I., C.N.V. and M.P. wrote the manuscript. C.N.V. and U.I. acquired funding.

Funding

Open Access funding enabled and organized by Projekt DEAL.

Competing interests

The authors declare no competing interests.

Additional information

Supplementary information is available for this paper at <https://doi.org/10.1038/s41467-020-20021-6>.

Correspondence and requests for materials should be addressed to U.I.

Peer review information *Nature Communications* thanks Bjorn Sandstede and David Stern for their contribution to the peer review of this work. Peer reviewer reports are available.

Reprints and permission information is available at <http://www.nature.com/reprints>

Publisher's note Springer Nature remains neutral with regard to jurisdictional claims in published maps and institutional affiliations.



Open Access This article is licensed under a Creative Commons Attribution 4.0 International License, which permits use, sharing, adaptation, distribution and reproduction in any medium or format, as long as you give appropriate credit to the original author(s) and the source, provide a link to the Creative Commons license, and indicate if changes were made. The images or other third party material in this article are included in the article's Creative Commons license, unless indicated otherwise in a credit line to the material. If material is not included in the article's Creative Commons license and your intended use is not permitted by statutory regulation or exceeds the permitted use, you will need to obtain permission directly from the copyright holder. To view a copy of this license, visit <http://creativecommons.org/licenses/by/4.0/>.

© The Author(s) 2020, corrected publication 2021

Supplementary Information

Evolution of the potassium channel gene *Kcnj13* underlies colour pattern diversification in *Danio* fish

Marco Podobnik, Hans Georg Frohnhöfer, Christopher M. Dooley, Anastasia Eskova, Christiane Nüsslein-Volhard, Uwe Irion



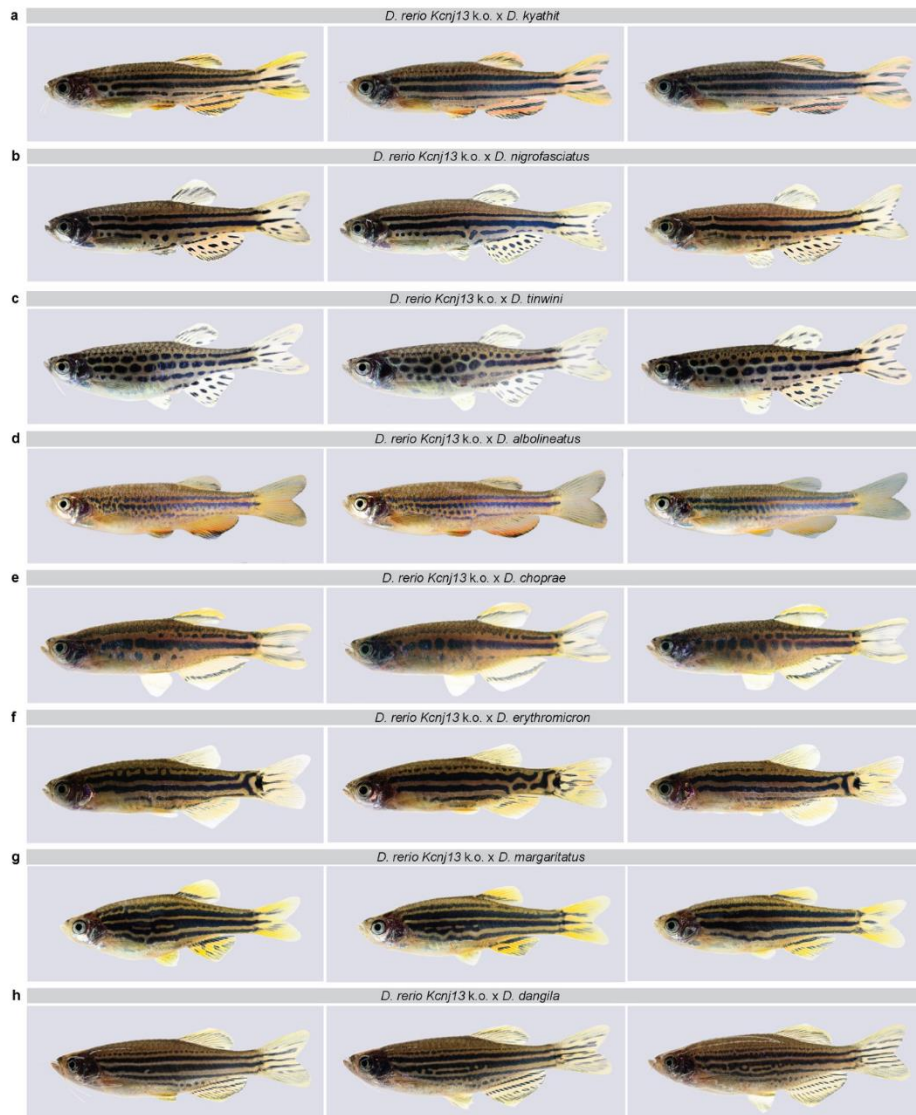
Supplementary Fig. 1: Examples of wild-type hybrids.

In each row three different individuals of wild-type hybrids are shown. **a**, Hybrids between *D. rerio* and *D. aesculapii*, **b**, *D. rerio* and *D. choprae* and **c**, *D. rerio* and *D. erythromicron* all develop horizontal stripes similar to the *D. rerio* pattern. **d**, Hybrids between *D. aesculapii* and *D. choprae* develop a barred pattern similar to the parental species. **e**, Hybrids between *D. aesculapii* and *D. erythromicron* and **f**, hybrids between *D. aesculapii* and *D. margaritatus* show variable patterns without clear horizontal or vertical orientation.



Supplementary Fig. 2: Examples of hemizygous hybrids.

In each row three different individuals of hemizygous hybrids between *D. rerio* and *D. aesculapii* are shown. **a**, Only the hybrids carrying a mutant *Kcnj13* allele from *D. rerio* show a spotted pattern, different from wild-type hybrids. **b**, Hybrids with the mutant *Kcnj13* allele from *D. aesculapii* and, **c/d**, all hemizygous hybrids for *Cx39.4*, **e/f**, *Cx41.8*, and, **g/h**, *Igsf11* develop horizontal stripes indistinguishable from wild-type hybrids.



Supplementary Fig. 3: Examples for *Danio* hybrids with mutant *Kcnj13* from *D. rerio*.

In each row three different individuals of hybrids carrying the mutant *Kcnj13* allele from *D. rerio* are shown. **a**, Hybrids with *D. kyathit*, **b**, *D. nigrofasciatus*, **d**, *D. albolineatus*, **f**, *D. erythromicron*, **g**, *D. margaritatus*, **h**, and *D. dangila* are indistinguishable from wild-type hybrids, whereas hybrids with, **c**, *D. tinwini* and, **e**, *D. choprae* show spotted patterns different from the corresponding wild-type hybrids.

Supplementary Fig. 4: Kcnj13 sequence alignment of vertebrate orthologues.

Sequence alignment of Kcnj13 orthologues from different vertebrate species. The two transmembrane domains (M1/M2) are shaded in light grey, the P-Loop (H5) in dark grey. Dominant (d) or recessive (r) mutations are indicated for zebrafish¹⁻⁵ (blue) and human⁶⁻¹² (purple). Positions that are different between *D. rerio* and *D. aesculapii* (magenta), *D. tinwini* (yellow), *D. choprae* (cyan) and polymorphic positions in *D. rerio* (dark grey) are highlighted. Kcnj13 sequences of *Danio rerio* (zebrafish, NP_001039014.1), *Lepisosteus oculatus* (spotted gar, XP_006638004.1), *Xenopus tropicalis* (tropical clawed frog, NP_001096437.1), *Anolis carolinensis* (green anole, XP_016847621.1), *Geospiza fortis* (medium ground finch, XP_005430275.1), *Gallus gallus* (chicken, XP_015132697.1), *Mus musculus* (house mouse, NP_001103697.1) and *Homo sapiens* (human, NP_002233.2).

Supplementary Fig. 5: Sequence alignment of Kcnj13 orthologues from *Danio* species.

Kcnj13 sequences from *D. rerio*, *D. aesculapii*, *D. kyathit*, *D. nigrofasciatus*, *D. tinwini*, *D. albolineatus*, *D. choprae*, *D. margaritatus*, *D. erythromicron*. Amino acids evolved between *D. rerio* and *D. aesculapii* (magenta), *D. tinwini* (yellow) and *D. choprae* (cyan). Dominant (d) or recessive (r) mutations in *D. rerio* Kcnj13¹⁻⁵ (blue). Amino acid polymorphisms in *D. rerio* (dark grey). Transmembrane domains (M1/M2) (light grey blocks) and the P-loop (H5) (dark grey block).

Supplementary Table 1 | List of targeted genes.

target	CRISPR target sequence (5'-3')	genotyping
<i>D. aesculapii csf1ra</i>	GGCCTTTAACCTGGTCGGTC	T2143, T2144
<i>D. aesculapii cx39.4</i>	GGACTCACAGCCGGGCTGTT	T2145, T2146
<i>D. aesculapii cx41.8</i>	GAACTTTCTAGAAGAAGTCC	MP92, MP318
<i>D. aesculapii igsf11</i>	GCTGAAAGTACAGGGCAAGA	MP330, MP 331
<i>D. aesculapii kcnj13</i>	TGCTGTATTATGGTACCTGC	T963, T964
<i>D. aesculapii mitfa</i>	GGAGCGCTGGCTCCGGGTCC	T2147, T2148
<i>D. aesculapii mpv17</i>	GGTGCTTTTCTGGGAATAAC	T2149, T2150
<i>D. rerio igsf11</i>	GGACGCAATATAGGAGTGAT	T1449, T1450
<i>D. rerio kcnj13</i> (1)	GGCAAGCAGCGGATGGCAG	T2139, T2140
<i>D. rerio kcnj13</i> (2)	GGCTGGCGCTACGGTGGCGG	T963, T964

Supplementary Table 2 | Primer pairs used for the generation of sgRNAs.

target	forward	reverse
<i>D. aesculapii csf1ra</i>	AAACGACCGACCAGGTTAAAGG	TAGGCCTTTAACCTGGTCGGTC
<i>D. aesculapii cx39.4</i>	AAACAACAGCCCGGCTGTGAGT	TAGGACTCACAGCCGGGCTGTT
<i>D. aesculapii mitfa</i>	AAACGGACCCGGAGCCAGCGCT	TAGGAGCGCTGGCTCCGGGTCC
<i>D. aesculapii mpv17</i>	AAACGTTATTCCCAGAAAAGCA	TAGGTGCTTTTCTGGGAATAAC
<i>D. rerio csf1ra</i>	AAACGACCGACCAGGTTAAAGG	TAGGCCTTTAACCTGGTCGGTC
<i>D. rerio igsf11</i>	AAACATCACTCCTATATTGCGT	TAGGACGCAATATAGGAGTGAT
<i>D. rerio kcnj13</i> (1)	AAACCCGCCACCGTAGCGCCAG	TAGGCTGGCGCTACGGTGGCGG
<i>D. rerio kcnj13</i> (2)	AAACCTGCCATCGCGCTGCTTG	TAGGCAAGCAGCGCGATGGCAG

Supplementary Table 3 | Primers used for genotyping.

primer name	sequence (5'-3')
MP318	AGCTGTGCCCGAACCAAGA
MP330	CCCCATGCATTTTATTGACCA
MP331	CTGAATTCAGAAAGGAGGAGGT
MP92	CTCCCTCCATTCACACTACC
T963	GAAACTATTCTTGCCGTGACTTG
T964	TCAAACAAACCTGGGTGTGGAC
T1449	TCATCTACCAGAGTGGTCAG
T1450	CCTAAACTTTTGCAGCACAG
T2139	TCAATGGAGACCTGGATGTC
T2140	TGGACCAAAGTGTGAAAGC
T2143	TGCCTGTGTTTATGTGTCG
T2144	AATGACCAAGAAGGATGAGC
T2145	GCCTCTAGGAACATGATTGG
T2146	GCTTCTCATTTCTAGCCCTC
T2147	GGCAACATTGGCGTTATCTC
T2148	TCTCACAGCATTCTGGCAC
T2149	CTGCCGTTTATATCTCCACAG
T2150	GGCTGAAAATTGGCTGATTG

Supplementary Table 4 | List of generated mutants.

mutant	mutation	description according to ¹³
<i>D. aesculapii</i> Csf1ra ^{t31ui}	4 bp deletion	recessive, c.1500_1503delGGTC p.Gly502LysfsX35
<i>D. aesculapii</i> Cx39.4 ^{t15ui}	8 bp deletion	recessive, c.175_182delAAACAGCC p.Lys59_ArgfsX2
<i>D. aesculapii</i> Cx39.4 ^{t59ui}	21 bp deletion	recessive, c.168_188delCAACACCAAACAGCCCGGCTG p.Asn57_Cys63del
<i>D. aesculapii</i> Cx41.8 ^{t18mp}	18 bp deletion	recessive, c.41_58delTCCAGGAGCATTCAACCT p.Val14AlaGlu15_Ser20del
<i>D. aesculapii</i> Igsf1 ^{t10mp}	1 bp insertion	recessive, c.130dupT p.Leu44PhefsX12
<i>D. aesculapii</i> Igsf1 ^{t19mp}	11 bp deletion	recessive, c.129_139delCTTGCCCTGTA p.Leu44PhefsX8
<i>D. aesculapii</i> Kcnj13 ^{t11mp}	4 bp deletion	recessive, c.260_263delACCT p.Tyr87CysfsX27
<i>D. aesculapii</i> Mitfa ^{t30ui}	7 bp deletion	recessive, c.194_200delGACCCGG p.Gly65GlufsX22

<i>D. aesculapii</i> <i>Mpv17</i> ^{132<i>ui</i>}	4 bp deletion	recessive, c.321_324delAATA p.Ile108LeufsX6
<i>D. rerio</i> <i>Igsf1</i> <i>1</i> ^{135<i>ui</i>}	17 bp deletion	recessive, c.412_428delGTGATCGGCCTGACGGT p.Ile138AlafsX19
<i>D. rerio</i> <i>Kcnj13</i> ^{dt158<i>ui</i>}	6 bp deletion	dominant, c.190_195delTGGCGG p.Trp64Arg65del
<i>D. rerio</i> <i>Kcnj13</i> ^{24<i>ui</i>}	14 bp insertion	recessive, c.436_437insGATGGAAGATGCTT p.Ala146GlyfsX28

Supplementary References

- 1 Haffter, P. *et al.* Mutations affecting pigmentation and shape of the adult zebrafish. *Development genes and evolution* **206**, 260-276, doi:DOI 10.1007/s004270050051 (1996).
- 2 Iwashita, M. *et al.* Pigment pattern in jaguar/obelix zebrafish is caused by a Kir7.1 mutation: implications for the regulation of melanosome movement. *PLoS genetics* **2**, e197, doi:10.1371/journal.pgen.0020197 (2006).
- 3 Irion, U. *et al.* Gap junctions composed of connexins 41.8 and 39.4 are essential for colour pattern formation in zebrafish. *Elife* **3**, e05125, doi:10.7554/eLife.05125 (2014).
- 4 Henke, K. *et al.* Genetic Screen for Postembryonic Development in the Zebrafish (*Danio rerio*): Dominant Mutations Affecting Adult Form. *Genetics* **207**, 609-623, doi:10.1534/genetics.117.300187 (2017).
- 5 Silic, M. R. *et al.* Potassium Channel-Associated Bioelectricity of the Dermomyotome Determines Fin Patterning in Zebrafish. *Genetics* **215**, 1067-1084, doi:10.1534/genetics.120.303390 (2020).
- 6 Lee, M. M., Ritter, R., 3rd, Hirose, T., Vu, C. D. & Edwards, A. O. Snowflake vitreoretinal degeneration: follow-up of the original family. *Ophthalmology* **110**, 2418-2426, doi:10.1016/S0161-6420(03)00828-5 (2003).
- 7 Hejtmancik, J. F. *et al.* Mutations in KCNJ13 cause autosomal-dominant snowflake vitreoretinal degeneration. *Am J Hum Genet* **82**, 174-180, doi:10.1016/j.ajhg.2007.08.002 (2008).
- 8 Sergouniotis, P. I. *et al.* Recessive mutations in KCNJ13, encoding an inwardly rectifying potassium channel subunit, cause leber congenital amaurosis. *Am J Hum Genet* **89**, 183-190, doi:10.1016/j.ajhg.2011.06.002 (2011).
- 9 Khan, A. O., Bergmann, C., Neuhaus, C. & Bolz, H. J. A distinct vitreo-retinal dystrophy with early-onset cataract from recessive KCNJ13 mutations. *Ophthalmic Genet* **36**, 79-84, doi:10.3109/13816810.2014.985846 (2015).
- 10 Pattnaik, B. R. *et al.* A Novel KCNJ13 Nonsense Mutation and Loss of Kir7.1 Channel Function Causes Leber Congenital Amaurosis (LCA16). *Hum Mutat* **36**, 720-727, doi:10.1002/humu.22807 (2015).

- 11 Perez-Roustit, S. *et al.* Leber Congenital Amaurosis with Large Retinal Pigment Clumps Caused by Compound Heterozygous Mutations in Kcnj13. *Retin Cases Brief Rep* **11**, 221-226, doi:10.1097/ICB.0000000000000326 (2017).
- 12 Toms, M. *et al.* Missense variants in the conserved transmembrane M2 protein domain of KCNJ13 associated with retinovascular changes in humans and zebrafish. *Exp Eye Res* **189**, 107852, doi:10.1016/j.exer.2019.107852 (2019).
- 13 Ogino, S. *et al.* Standard mutation nomenclature in molecular diagnostics: practical and educational challenges. *J Mol Diagn* **9**, 1-6, doi:10.2353/jmoldx.2007.060081 (2007).

THESIS APPENDIX I.II

1 **Title**

2 Interspecific complementation tests for pigment pattern diversification in *Danio* fish

3

4 **Authors**

5 Podobnik, M., Nüsslein-Volhard, C. & Irion U.

6 Max Planck Institute for Biology, Tübingen, Germany

7

8 **Abstract**

9 The genetic basis of pigment pattern variation in vertebrates is an important topic in
10 evolutionary biology. Fish of the genus *Danio*, containing the model species zebrafish,
11 *Danio rerio*, develop amazingly different pigment patterns. Here we show results from
12 genus-wide interspecific complementation tests between *D. rerio* mutants of three
13 pigment patterning genes and eight *Danio* species to identify potentially evolved genes
14 in the hybrids. Among all 24 comparisons between wild-type and hemizygous hybrids,
15 we identify two clear functional differences in the gap junction gene *gja5b* and the
16 adhesion molecule gene *igsf11* between *D. rerio* and *D. margaritatus*. This
17 comprehensive analysis provides an invitation to investigate the consequences of
18 evolution in the identified genes for pigment cell behaviour during the divergent pattern
19 development in different species. Our results highlight the genetic complexity
20 underlying the diversification of pigment patterning in *Danio* fish.

21

22 **Introduction**

23 Teleosts are the most species-rich group in the class Actinopterygii, the ray-finned
24 fishes, and also form the largest group of vertebrates. Cyprinid fish of the genus *Danio*,
25 belonging to the subfamily of the *Danioninae*, develop very different pigment patterns
26 (Fig. 1a). Horizontal stripes form in zebrafish, *D. rerio*, but also in *D. kyathit* and
27 partially in *D. nigrofasciatus*. *D. aesculapii*, *D. choprae* and *D. erythromicron* display
28 vertical bars and *D. tinwini* and *D. margaritatus* develop spots. Meandering patterns
29 of stripes and spots form in *D. dangila*, whereas *D. albolineatus* lack almost any

|

1

30 pattern. The phylogenetic relationships between these species have been recently
31 resolved, indicating a complex genetic basis for their speciation and morphological
32 diversification¹. Given the advantages of the model species *D. rerio*, the *Danio* genus
33 is an excellent system to study the genetic basis of pigment pattern diversification in
34 vertebrates²⁻⁷.

35 The very precise and stereotypic horizontal dark stripes in *D. rerio* are composed of
36 black melanophores, faint and stellate-shaped xanthophores and silvery-blue
37 iridophores, as opposed to compact, orange xanthophores and shiny, dense
38 iridophores in the light stripes. The specific superposition and localisation of the
39 pigment cells to different layers in the skin creates the colour and contrast of the
40 pattern⁸⁻¹¹. Interactions among the pigment cells control their cell shape acquisition
41 and assembly into the stripe pattern in a largely self-organizing process^{12,13}. These
42 cellular interactions require the functions of genes, which typically encode integral
43 membrane proteins such as ion channels or co-transporters^{14,15}, adhesion
44 molecules^{16,17} or connexins, which are components of gap junctions that mediate
45 direct cell contacts¹⁸⁻²¹. Local interactions within the tissue environment²²⁻²⁴ as well
46 as global signals such as thyroid hormone, regulated by galanin signalling in the
47 brain^{25,26}, and insulin²⁷ influence stripe formation. The orientation of the pattern is
48 provided by the horizontal myoseptum, which serves as an anatomical pre-pattern¹².

49 In this study, we focus on four genes known to play roles during stripe formation in *D.*
50 *rerio*. *kcnj13* encodes an inwardly rectifying potassium channel and is required in
51 melanophores for heterotypic interactions with xanthophores during patterning;
52 mutations lead to a pattern with fewer and wider stripes and occasional
53 interruptions^{14,28}. The two connexins Gja4 and Gja5b are both required in
54 melanophores and xanthophores for homotypic and heterotypic interactions during
55 stripe formation^{18-20,29}, whereas the cell adhesion molecule Igsf11 functions
56 autonomously in melanophores regulating their migration and survival through
57 adhesive properties¹⁶. In all three latter cases mutations lead to a spotted pattern
58 instead of the normal stripes. So far, involvement of the four genes in pattern formation
59 has been shown by the generation of loss-of-function mutations in only one additional
60 *Danio* species, *D. aesculapii*. For one of these genes, *kcnj13*, evolutionary divergence
61 within the *Danio* genus was demonstrated³⁰. Hybrids between *D. rerio* and other *Danio*
62 species develop patterns of horizontal stripes similar to the ones in *D. rerio*. Thus, the

63 striped pattern of *D. rerio* appears to be largely dominant over the divergent patterns
64 from other *Danio* species. Almost all F1 *Danio* hybrids are sterile thus not allowing
65 further genetic tests such as QTL mapping. One-way interspecific complementation
66 tests have been used to investigate whether genes known from zebrafish have
67 evolved to cause differences in pigment patterning in other *Danio* species³⁰⁻³³. This
68 test is based on the comparison of interspecific hybrids either carrying a wild-type or
69 a loss-of-function allele from *D. rerio* and the corresponding wild-type allele from
70 another *Danio* species. Non-complementation in this test, i.e. if the pattern of the
71 hemizygous hybrids is significantly different from the pattern found in the wild-type
72 hybrids, indicates evolutionary divergence because it shows that the gene functions
73 are no longer equivalent in both species.

74 This test has been used to identify evolution in cell differentiation pathways such as
75 xanthophore-specific *Csf1* signalling in *D. albolineatus*³² and iridophore-specific *Edn3*
76 signalling in *D. nigrofasciatus*³³. We used this test systematically across the genus and
77 found evidence for repeated and independent evolution of the potassium channel gene
78 *kcnj13* in three species, *D. aesculapii*, *D. tinwini* and *D. choprae*³⁰. Using a reciprocal
79 hemizygosity test³⁴, as an extension of the interspecific complementation test, which
80 allows to rule out effects of the novel genetic background in the hybrids, the functional
81 divergence of *kcnj13* between *D. rerio* and *D. aesculapii* was demonstrated. In
82 contrast, the reciprocal hemizygosity tests ruled out roles for *gja4*, *gja5b* and *igsf11* in
83 mediating patterning differences between these two species³⁰.

84 Here, we extend the previous one-way interspecific complementation tests with the
85 three genes, *gja4*, *gja5b* and *igsf11* to the genus level. The three *D. rerio* mutants were
86 crossed to *D. kyathit*, *D. nigrofasciatus*, *D. tinwini*, *D. albolineatus*, *D. choprae*, *D.*
87 *erythromicron*, *D. margaritatus* and *D. dangila*. Our results suggest that in most cases
88 gene function during pattern formation is conserved. However, we find cases where
89 the hybrids indicate potential differences in the gene functions. In a few of them
90 phenotypic variability precludes firm conclusions without further experiments. In two
91 cases, however, in hybrids between *D. rerio* and *D. margaritatus* hemizygous for *gja5b*
92 or *igsf11* the phenotypes are less variable and significantly different from wild-type
93 hybrids. Our results suggest that evolution in these two genes contributed to patterning
94 differences between the species.

95 **Results and Discussion**

96 We have previously shown that *kcnj13* has probably evolved independently several
97 times in the *Danio* genus. Reciprocal hemizyosity tests between *D. rerio* and *D.*
98 *aesculapii* showed functional divergence and thereby verified evolution of the gene³⁰.
99 To investigate the role of three additional genes, *gja4*, *gja5b* and *igsf11*, for pigment
100 pattern variation across the genus, we crossed zebrafish carrying CRISPR/Cas9-
101 generated loss-of-function alleles with eight additional *Danio* species, *D. kyathit*, *D.*
102 *nigrofasciatus*, *D. tinwini*, *D. albolineatus*, *D. choprae*, *D. erythromicron*, *D.*
103 *margaritatus* and *D. dangila*. Wild-type hybrids between *D. rerio* and other *Danio*
104 species generally display a pattern of horizontal stripes, similar to the *D. rerio* pattern,
105 with slight aberrations in *D. albolineatus* and *D. tinwini* hybrids (Fig.1a). In combination
106 with previously published results, we compared altogether nine wild-type hybrids with
107 36 hemizygous hybrids carrying loss-of-function alleles in four genes, *kcnj13*, *gja4*,
108 *gja5b* and *igsf11*. In most of the cases (25 out of 36, 69.4%) we observed no
109 differences between the hybrids, suggesting that the majority of the tested genes are
110 functionally conserved between *D. rerio* and the nine other species. In six cases (16.7
111 %) hemizygous hybrids showed some defects in the stripe pattern, *D. rerio gja4* and
112 *D. choprae* or *D. erythromicron*, *D. rerio gja5b* and *D. tinwini*, *D. choprae* or *D.*
113 *erythromicron*, and *D. rerio igsf11* and *D. erythromicron*. However, the pattern defects
114 in these hybrids were variable and we found substantial overlap with patterns of wild-
115 type hybrids thus precluding clear distinctions. We assume that the genetic
116 background influenced the outcome of the tests in these six cases. In five cases (13.9
117 %) the hemizygous hybrids developed meandering patterns and broken stripes clearly
118 distinct from the horizontal stripes in wild-type hybrids. These cases were hybrids
119 between *D. rerio gja5b* or *igsf11* mutants and *D. margaritatus* (Fig. 1b,c) as well as
120 hybrids between *D. rerio kcnj13* and *D. aesculapii*, *D. tinwini* and *D. choprae*³⁰. This
121 suggests that the wild-type allele from these other *Danio* species cannot complement
122 the loss of function of the *D. rerio* allele in the hybrids.

123 We never observed complete non-complementation phenotypes in the hemizygous
124 hybrids, which would resemble those of homozygous *D. rerio* mutants, suggesting that
125 there is still some patterning function provided by the genes from the other *Danio*
126 species. We tested if we could establish complete non-complementation in hybrids by
127 crossing *kcnj13* and *gja5b* mutants of *D. rerio* and *D. aesculapii*. These mutant hybrids

128 resembled the *D. rerio* mutants, showing that the genetic background in the hybrids
129 between *D. rerio* and *D. aesculapii* is similar to the one in *D. rerio*³⁰. Comparing
130 phenotypes in reciprocal hemizygous hybrids accounts for effects caused by a novel
131 genetic background in hybrids³⁴. In the case of *kcnj13* the significant difference
132 between phenotypes of wild-type and hemizygous hybrids between *D. rerio kcnj13*
133 mutants and *D. aesculapii* might be therefore not caused by effects of the genetic
134 background. We further explored these findings by generating reciprocal hybrids.
135 Hemizygous hybrids between *D. rerio* and the four *D. aesculapii* mutants all developed
136 patterns indistinguishable from wild-type hybrids, indicating that the *D. rerio* alleles
137 complemented the loss of functions from the *D. aesculapii* alleles. Thus, these tests
138 ruled out evolution in *gja4*, *gja5b* and *igsf11*, but confirmed functional divergence in
139 *kcnj13* between the two species. Similar to previous conclusions³⁰, our results suggest
140 that all four genes are likely required for pigment pattern formation in all *Danio* species
141 tested and that their function in pigment patterning predate the origin of the *Danio*
142 genus.

143 The phenotypic variability observed between hybrids of different genotypes could be
144 caused by the influence of novel genetic backgrounds from specific species pairs
145 rather than by a functional divergence of the tested genes. Initially, we used the
146 established *D. rerio* strain *leo^{tl}*, carrying a nonsense mutation in *gja5b*^{18,35}, for the
147 complementation tests. However, we frequently observed variable phenotypes
148 unrelated to the genotypes of the resulting hybrids. Therefore, we repeated these
149 experiments with a new CRISPR/Cas9-generated loss-of-function allele, *gja5b^{tl21mp}*,
150 induced in the same genetic wild-type background as our other mutants. This allele
151 reduced the observed phenotypic variability in hybrids. Consequently, we used
152 CRISPR alleles for all other interspecific complementation tests.

153 Our one-way complementation tests suggest an apparent functional divergence in
154 *gja5b* and *igsf11* between *D. rerio* and *D. margaritatus*, but less clearly between *D.*
155 *rerio* and *D. erythromicron* or *D. choprae*, which are the closest relatives to *D.*
156 *margaritatus*. It seems possible that both genes are involved in the divergence of
157 pigment patterns in this clade, however this effect might be rather subtle and, in
158 addition, partially obscured by background effects. We have not yet generated loss-
159 of-function mutants in *D. tinwini*, *D. choprae*, *D. erythromicron* or *D. margaritatus*,
160 which will be necessary to demonstrate a requirement of the genes tested for pattern

161 formation in these species. Such mutants are also needed to perform reciprocal
162 interspecific crosses. The analysis of reciprocal hemizygous hybrids derived from the
163 same parents can largely exclude phenotypic effects of the genetic background and
164 therefore provide more robust results.

165 It was anticipated that similarities between *D. rerio* mutants and wild types of *Danio*
166 species, so-called *natural mutants*, could be due to a common genetic basis^{36,37} We
167 found that *gja5b* but likely not *gja4* is involved in the patterning differences between
168 *D. rerio* and *D. tinwini* and *D. margaritatus*; *igsf11* only between *D. rerio* and *D.*
169 *margaritatus*. Evolution in these genes might be either sufficient to induce spotted
170 phenotypes or, more likely, further, as yet unknown, genes with patterning functions
171 could exist. Some of them might be homozygous-lethal or function redundantly with
172 paralogues, which stem from a teleost-specific whole-genome duplication after the
173 split from the holosteian group of ray-finned fish³⁸⁻⁴⁰. Our study highlights the power of
174 the *Danio* genus to investigate the complex genetic basis of pigment pattern variation
175 in a vertebrate system.



177

178 **Fig. 1: Genus-wide one-way complementation tests suggest evolution in *gja5b***
 179 **and *igsf11* between *D. rerio* and *D. margaritatus*.** a On the left the phylogenetic tree
 180 depicts the relationship (partially unpublished) between the eight *Danio* species
 181 tested¹; pigment patterns of each species are shown in square boxes in the first
 182 column. In addition to pattern defects observed in hybrids between *D. rerio kcnj13*
 183 mutants and *D. aesculapii*, *D. tinwini* and *D. choprae* wild types³⁰, we find pattern
 184 defects in two more cases: hybrids between *D. margaritatus* and b *D. rerio gja5b* (n =
 185 7) c and *igsf11* mutants (n = 14), respectively. In six cases the patterns in the
 186 hemizygous hybrids differed less clearly from wild-type hybrid patterns (*D. rerio gja4*
 187 k.o./*D. choprae*, n = 6; *D. rerio gja4* k.o./*D. erythromicron*, n = 14; *D. rerio gja5b* k.o./*D.*
 188 *tinwini*, n = 15; *D. rerio gja5b* k.o./*D. choprae*, n = 5; *D. rerio gja5b* k.o./*D.*
 189 *erythromicron*, n = 11; *D. rerio igsf11* k.o./*D. erythromicron*, n = 7). In all other 16 cases
 190 the patterns of the hemizygous hybrids did not differ from wild-type patterns (*D. rerio*
 191 *gja4* k.o./*D. kyathit*, n = 5; *D. rerio gja4* k.o./*D. nigrofasciatus*, n = 7; *D. rerio gja4* k.o./*D.*
 192 *tinwini*, n = 12; *D. rerio gja4* k.o./*D. albolineatus*, n = 13; *D. rerio gja4* k.o./*D.*
 193 *margaritatus*, n = 6; *D. rerio gja4* k.o./*D. dangila*, n=5, *D. rerio gja5b* k.o./*D. kyathit*, n
 194 = 4; *D. rerio gja5b* k.o./*D. nigrofasciatus*, n = 28; *D. rerio gja5b* k.o./*D. albolineatus*, n
 195 = 15; *D. rerio gja5b* k.o./*D. dangila*, n = 3; *D. rerio igsf11* k.o./*D. kyathit*, n = 21; *D. rerio*

196 *igsf11* k.o./*D. nigrofasciatus*, n = 21; *D. rerio igsf11* k.o./*D. tinwini*, n = 21; *D. rerio*
 197 *igsf11* k.o./*D. albolineatus*, n = 3; *D. rerio igsf11* k.o./*D. choprae*, n = 24; *D. rerio igsf11*
 198 k.o./*D. dangila*, n = 6). Hybrids between the three *D. rerio* mutants and *D. aesculapii*
 199 were tested in³⁰. All pictures show representative examples of the corresponding
 200 species/hybrids/genotypes. Scale bars correspond to 1 mm.

201

202 **Methods**

203 Fish husbandry

204 *D. rerio* were maintained as described in Brand & Nüsslein-Volhard⁴¹. If not newly
 205 generated, the following lines were used for experiments: Wild-type *D. rerio*
 206 Tuebingen/TU, *gja4*^{137ui19} and *igsf11*^{135ui30}. Wild-type Tuebingen strains of *D.*
 207 *aesculapii*, *D. nigrofasciatus* and *D. albolineatus* were maintained identical to *D. rerio*.
 208 For the other *Danio* species, *D. kyathit*, *D. tinwini*, *D. choprae*, *D. margaritatus*, *D.*
 209 *erythromicron* and *D. dangila*, individual pair matings were not successful. Therefore,
 210 the fish were kept in groups in tanks containing boxes lightly covered with Java moss
 211 (*Taxiphyllum barbieri*), which resulted in sporadic matings and allowed us to collect
 212 fertilized eggs. Interspecific hybrids were either obtained by natural matings or by in
 213 vitro fertilisations. Wild-type or hemizygous hybrids were identified by PCR and
 214 sequence analysis using specific primer pairs (for *gja4*: TÜ838 and TÜ975, for *igsf11*:
 215 TÜ1449 and TÜ1450, Supplementary Table 1). All species were staged according to
 216 the normal table of *D. rerio* development. All animal experiments were performed in
 217 accordance with the rules of the State of Baden-Württemberg, Germany, and
 218 approved by the Regierungspräsidium Tübingen.

219

220 **Supplementary Table 1:** Primers used in this study.

Name	Sequence 5'-3'
TÜ838_for	TGCCTCTAGGAACATGATTGGG
TÜ975_rev	GGTCATCTTCGTCTCAACTCCG
TÜ1449_for	TCATCTACCAGAGTGGTCAG
TÜ1450_rev	CCTAAACTTTTGCAGCACAG

|

8

TÜ1037_for	TAGGCTGCTGAATCCTCGTGGG
TÜ1038_rev	AAACCCCACGAGGATTCAGCAG
MP335_for	CAGGCTCCTCTGAATAGGCA
MP336_rev	GTGTAGACACGAACACGATCTG

221

222

223 **CRISPR/Cas9-mediated knock-out**

224 The CRISPR/Cas9 system was applied to generate loss-of-function mutations in *gja5b*
 225 as described in⁴². Briefly, oligonucleotides TÜ1037 and TÜ1038 (Supplementary
 226 Table 1) were cloned into pDR274 to generate the sgRNA vector. sgRNAs were
 227 transcribed from the linearised vector using the MEGAscript T7 Transcription Kit
 228 (Invitrogen). sgRNAs were injected as ribonucleoprotein complexes with Cas9
 229 proteins into one-cell stage embryos. The efficiency of indel generation was tested on
 230 eight larvae at 1 dpf by PCR using specific primer pairs for *gja5b*, MP335 and MP336
 231 (Supplementary Table 1), and by sequence analysis as described previously⁴³. The
 232 remaining larvae were raised to adulthood. Mature F0 fish carrying indels were
 233 outcrossed. Loss-of-function alleles in heterozygous F1 fish were selected to establish
 234 the homozygous mutant line *gja5b*^{l21mp}.

235

236 **Image acquisition and processing**

237 Anesthesia of postembryonic and adult fish was performed as described previously¹⁰.
 238 Bright field images of adult fish were obtained using a Canon 5D Mk II camera. Fish
 239 with different pigment patterns vary considerably in contrast, thus requiring different
 240 settings for aperture and exposure time, which can result in slightly different color
 241 representations in the pictures. Images were processed using Adobe Photoshop and
 242 Adobe Illustrator CS6.

243 **References**

- 244 1 McCluskey, B. M. & Postlethwait, J. H. Phylogeny of zebrafish, a "model
245 species," within Danio, a "model genus". *Mol Biol Evol* **32**, 635-652,
246 doi:10.1093/molbev/msu325 (2015).
- 247 2 Singh, A. P. & Nusslein-Volhard, C. Zebrafish stripes as a model for vertebrate
248 colour pattern formation. *Curr Biol* **25**, R81-R92, doi:10.1016/j.cub.2014.11.013
249 (2015).
- 250 3 Parichy, D. M. Advancing biology through a deeper understanding of zebrafish
251 ecology and evolution. *Elife* **4**, doi:10.7554/eLife.05635 (2015).
- 252 4 Patterson, L. B. & Parichy, D. M. Zebrafish Pigment Pattern Formation: Insights
253 into the Development and Evolution of Adult Form. *Annu Rev Genet* **53**, 505-
254 530, doi:10.1146/annurev-genet-112618-043741 (2019).
- 255 5 Irion, U. & Nusslein-Volhard, C. The identification of genes involved in the
256 evolution of color patterns in fish. *Curr Opin Genet Dev* **57**, 31-38,
257 doi:10.1016/j.gde.2019.07.002 (2019).
- 258 6 Parichy, D. M. Evolution of pigment cells and patterns: recent insights from
259 teleost fishes. *Curr Opin Genet Dev* **69**, 88-96, doi:10.1016/j.gde.2021.02.006
260 (2021).
- 261 7 Irion, U. & Nusslein-Volhard, C. Developmental genetics with model organisms.
262 *Proceedings of the National Academy of Sciences* **119**, e2122148119,
263 doi:doi:10.1073/pnas.2122148119 (2022).
- 264 8 Hirata, M., Nakamura, K. & Kondo, S. Pigment cell distributions in different
265 tissues of the zebrafish, with special reference to the striped pigment pattern.
266 *Dev Dyn* **234**, 293-300, doi:10.1002/dvdy.20513 (2005).
- 267 9 Hirata, M., Nakamura, K., Kanemaru, T., Shibata, Y. & Kondo, S. Pigment cell
268 organization in the hypodermis of zebrafish. *Dev Dyn* **227**, 497-503,
269 doi:10.1002/dvdy.10334 (2003).
- 270 10 Singh, A. P., Schach, U. & Nusslein-Volhard, C. Proliferation, dispersal and
271 patterned aggregation of iridophores in the skin prefigure striped colouration of
272 zebrafish. *Nat Cell Biol* **16**, 607-614, doi:10.1038/ncb2955 (2014).
- 273 11 Mahalwar, P., Walderich, B., Singh, A. P. & Nusslein-Volhard, C. Local
274 reorganization of xanthophores fine-tunes and colors the striped pattern of
275 zebrafish. *Science* **345**, 1362-1364, doi:10.1126/science.1254837 (2014).
- 276 12 Frohnhof, H. G., Krauss, J., Maischein, H. M. & Nusslein-Volhard, C.
277 Iridophores and their interactions with other chromatophores are required for
278 stripe formation in zebrafish. *Development* **140**, 2997-3007,
279 doi:10.1242/dev.096719 (2013).
- 280 13 Patterson, L. B. & Parichy, D. M. Interactions with iridophores and the tissue
281 environment required for patterning melanophores and xanthophores during
282 zebrafish adult pigment stripe formation. *PLoS Genet* **9**, e1003561,
283 doi:10.1371/journal.pgen.1003561 (2013).
- 284 14 Iwashita, M. *et al.* Pigment pattern in jaguar/obelix zebrafish is caused by a
285 Kir7.1 mutation: implications for the regulation of melanosome movement.
286 *PLoS Genet* **2**, e197, doi:10.1371/journal.pgen.0020197 (2006).
- 287 15 Lanni, J. S. *et al.* Integrated K⁺ channel and K⁺Cl⁻ cotransporter functions are
288 required for the coordination of size and proportion during development. *Dev*
289 *Biol* **456**, 164-178, doi:10.1016/j.ydbio.2019.08.016 (2019).
- 290 16 Eom, D. S. *et al.* Melanophore migration and survival during zebrafish adult
291 pigment stripe development require the immunoglobulin superfamily adhesion

- 292 molecule Igsf11. *PLoS Genet* **8**, e1002899, doi:10.1371/journal.pgen.1002899
 293 (2012).
- 294 17 Eom, D. S., Patterson, L. B., Bostic, R. R. & Parichy, D. M. Immunoglobulin
 295 superfamily receptor Junctional adhesion molecule 3 (Jam3) requirement for
 296 melanophore survival and patterning during formation of zebrafish stripes. *Dev*
 297 *Biol* **476**, 314-327, doi:10.1016/j.ydbio.2021.04.007 (2021).
- 298 18 Watanabe, M. *et al.* Spot pattern of leopard Danio is caused by mutation in the
 299 zebrafish connexin41.8 gene. *EMBO Rep* **7**, 893-897,
 300 doi:10.1038/sj.embor.7400757 (2006).
- 301 19 Irion, U. *et al.* Gap junctions composed of connexins 41.8 and 39.4 are essential
 302 for colour pattern formation in zebrafish. *Elife* **3**, e05125,
 303 doi:10.7554/eLife.05125 (2014).
- 304 20 Watanabe, M., Sawada, R., Aramaki, T., Skerrett, I. M. & Kondo, S. The
 305 Physiological Characterization of Connexin41.8 and Connexin39.4, Which Are
 306 Involved in the Striped Pattern Formation of Zebrafish. *J Biol Chem* **291**, 1053-
 307 1063, doi:10.1074/jbc.M115.673129 (2016).
- 308 21 Usui, Y., Aramaki, T., Kondo, S. & Watanabe, M. The minimal gap-junction
 309 network among melanophores and xanthophores required for stripe pattern
 310 formation in zebrafish. *Development* **146**, doi:10.1242/dev.181065 (2019).
- 311 22 Lang, M. R., Patterson, L. B., Gordon, T. N., Johnson, S. L. & Parichy, D. M.
 312 Basonuclin-2 requirements for zebrafish adult pigment pattern development
 313 and female fertility. *PLoS Genet* **5**, e1000744,
 314 doi:10.1371/journal.pgen.1000744 (2009).
- 315 23 Eom, D. S. & Parichy, D. M. A macrophage relay for long-distance signaling
 316 during postembryonic tissue remodeling. *Science* **355**, 1317-1320,
 317 doi:10.1126/science.aal2745 (2017).
- 318 24 Eskova, A. *et al.* Gain-of-function mutations in Aqp3a influence zebrafish
 319 pigment pattern formation through the tissue environment. *Development* **144**,
 320 2059-2069, doi:10.1242/dev.143495 (2017).
- 321 25 McMenamain, S. K. *et al.* Thyroid hormone-dependent adult pigment cell lineage
 322 and pattern in zebrafish. *Science* **345**, 1358-1361,
 323 doi:10.1126/science.1256251 (2014).
- 324 26 Eskova, A., Frohnhof, H. G., Nusslein-Volhard, C. & Irion, U. Galanin
 325 Signaling in the Brain Regulates Color Pattern Formation in Zebrafish. *Curr Biol*
 326 **30**, 298-303 e293, doi:10.1016/j.cub.2019.11.033 (2020).
- 327 27 Zhang, Y. M. *et al.* Distant Insulin Signaling Regulates Vertebrate Pigmentation
 328 through the Sheddase Bace2. *Dev Cell* **45**, 580-594 e587,
 329 doi:10.1016/j.devcel.2018.04.025 (2018).
- 330 28 Inaba, M., Yamanaka, H. & Kondo, S. Pigment pattern formation by contact-
 331 dependent depolarization. *Science* **335**, 677, doi:10.1126/science.1212821
 332 (2012).
- 333 29 Mahalwar, P., Singh, A. P., Fadeev, A., Nusslein-Volhard, C. & Irion, U.
 334 Heterotypic interactions regulate cell shape and density during color pattern
 335 formation in zebrafish. *Biol Open* **5**, 1680-1690, doi:10.1242/bio.022251 (2016).
- 336 30 Podobnik, M. *et al.* Evolution of the potassium channel gene Kcnj13 underlies
 337 colour pattern diversification in Danio fish. *Nat Commun* **11**, 6230,
 338 doi:10.1038/s41467-020-20021-6 (2020).
- 339 31 Parichy, D. M. & Johnson, S. L. Zebrafish hybrids suggest genetic mechanisms
 340 for pigment pattern diversification in Danio. *Dev Genes Evol* **211**, 319-328,
 341 doi:10.1007/s004270100155 (2001).

- 342 32 Patterson, L. B., Bain, E. J. & Parichy, D. M. Pigment cell interactions and
343 differential xanthophore recruitment underlying zebrafish stripe reiteration and
344 Danio pattern evolution. *Nat Commun* **5**, 5299, doi:10.1038/ncomms6299
345 (2014).
- 346 33 Spiewak, J. E. *et al.* Evolution of Endothelin signaling and diversification of adult
347 pigment pattern in Danio fishes. *PLoS Genet* **14**, e1007538,
348 doi:10.1371/journal.pgen.1007538 (2018).
- 349 34 Stern, D. L. Identification of loci that cause phenotypic variation in diverse
350 species with the reciprocal hemizyosity test. *Trends Genet* **30**, 547-554,
351 doi:10.1016/j.tig.2014.09.006 (2014).
- 352 35 Haffter, P. *et al.* Mutations affecting pigmentation and shape of the adult
353 zebrafish. *Dev Genes Evol* **206**, 260-276, doi:10.1007/s004270050051 (1996).
- 354 36 Meyer, A., Biermann, C. H. & Orti, G. The phylogenetic position of the zebrafish
355 (*Danio rerio*), a model system in developmental biology: an invitation to the
356 comparative method. *Proc Biol Sci* **252**, 231-236, doi:10.1098/rspb.1993.0070
357 (1993).
- 358 37 Meyer, A., Ritchie P. A., Witte, K.-E. Predicting developmental processes from
359 evolutionary patterns: a molecular phylogeny of the zebrafish (*Danio rerio*) and
360 its relatives. *Phil. Trans. R. Soc. Lond. B* **349**, 103-111,
361 doi:<https://doi.org/10.1098/rstb.1995.0096> (1995).
- 362 38 Braasch, I., Brunet, F., Volff, J. N. & Schartl, M. Pigmentation pathway evolution
363 after whole-genome duplication in fish. *Genome Biol Evol* **1**, 479-493,
364 doi:10.1093/gbe/evp050 (2009).
- 365 39 Braasch, I. *et al.* The spotted gar genome illuminates vertebrate evolution and
366 facilitates human-teleost comparisons. *Nat Genet* **48**, 427-437,
367 doi:10.1038/ng.3526 (2016).
- 368 40 Lorin, T., Brunet, F. G., Laudet, V. & Volff, J. N. Teleost Fish-Specific
369 Preferential Retention of Pigmentation Gene-Containing Families After Whole
370 Genome Duplications in Vertebrates. *G3 (Bethesda)* **8**, 1795-1806,
371 doi:10.1534/g3.118.200201 (2018).
- 372 41 Brand, M., Granato, M. & Nüsslein-Volhard, C. in *Zebrafish: A practical*
373 *approach* Vol. 7 (eds C Nüsslein-Volhard & R Dahm) 7-37 (2002).
- 374 42 Irion, U., Krauss, J. & Nusslein-Volhard, C. Precise and efficient genome editing
375 in zebrafish using the CRISPR/Cas9 system. *Development* **141**, 4827-4830,
376 doi:10.1242/dev.115584 (2014).
- 377 43 Meeker, N. D., Hutchinson, S. A., Ho, L. & Trede, N. S. Method for isolation of
378 PCR-ready genomic DNA from zebrafish tissues. *Biotechniques* **43**, 610, 612,
379 614, doi:10.2144/000112619 (2007).
- 380

1 **Title**

2 Cis-regulatory evolution of the potassium channel gene *kcnj13* during pigment
3 pattern diversification in *Danio* fish

4

5 **Authors**

6 ¹Marco Podobnik (<https://orcid.org/0000-0001-5480-7086>)

7 ²Ajeet P. Singh (<https://orcid.org/0000-0002-3819-5136>)

8 ³Zhenqiang Fu (<https://orcid.org/0000-0003-3766-1083>)

9 ⁴Christopher M. Dooley (<https://orcid.org/0000-0002-4941-9019>)

10 ¹Hans Georg Frohnhöfer (<https://orcid.org/0000-0003-4038-7089>)

11 ⁵Magdalena Firlej (<https://orcid.org/0000-0001-6156-9493>)

12 ^{6,7,8}Hadeer Elhabashy (<https://orcid.org/0000-0002-4677-7064>)

13 ⁹Simone Weyand (<https://orcid.org/0000-0002-7965-0895>)

14 ⁵John R. Weir (<https://orcid.org/0000-0002-6904-0284>)

15 ³Jianguo Lu (<https://orcid.org/0000-0002-3966-8812>)

16 ¹Christiane Nüsslein-Volhard (<https://orcid.org/0000-0002-7688-1401>)

17 ^{1,10}Uwe Irion (<https://orcid.org/0000-0003-2823-5840>)

18 ¹Max Planck Institute for Biology, Tübingen, Germany. ²Chemical Biology and
19 Therapeutics, Novartis Institutes for BioMedical Research, Cambridge, USA. ³School
20 of Marine Sciences, Sun Yat-sen University, Zhuhai 519082, China. ⁴Department of
21 Genetics, Max Planck Institute for Heart and Lung Research, Bad Nauheim,
22 Germany. ⁵Friedrich Miescher Laboratory of the Max Planck Society, Tübingen,
23 Germany. ⁶Department of Protein Evolution, Max Planck Institute for Biology,
24 Tübingen, Germany. ⁷Institute for Bioinformatics and Medical Informatics, University
25 of Tübingen, Tübingen, Germany. ⁸Department of Computer Science, University of
26 Tübingen, Tübingen, Germany. ⁹Department of Biochemistry, University of
27 Cambridge, Cambridge, United Kingdom. ¹⁰Corresponding author: Uwe Irion,
28 uwe.irion@tuebingen.mpg.de.

29

30 Abstract

31 Teleost fish of the genus *Danio* are excellent models to study the genetic and cellular
32 bases of pigment pattern variation in vertebrates. The two sister species *Danio rerio*
33 and *Danio aesculapii* show divergent patterns of horizontal stripes and vertical bars
34 that are partly caused by the evolution of the potassium channel gene *kcnj13*. In *D.*
35 *rerio*, *kcnj13* is required in melanophores for interactions with xanthophores and
36 iridophores, which cause location-specific pigment cell shapes and thereby influence
37 colour pattern and contrast. Here, we show that cis-regulatory rather than protein
38 coding changes underlie *kcnj13* evolution between the two species. *D. aesculapii*
39 express lower *kcnj13* levels and exhibit low-contrast patterns similar to *D. rerio*
40 mutants. Our results suggest that homotypic and heterotypic interactions between
41 the pigment cells and their shapes diverged between species by quantitative
42 changes in *kcnj13* expression during pigment pattern diversification.

43

44 Introduction

45 Teleost fish produce some of the most diverse pigment patterns in nature, which are
46 of great evolutionary importance as direct targets of natural and sexual selection.
47 Closely related species of the genus *Danio*, including the widely used model
48 organism zebrafish, *Danio rerio*, develop amazingly different patterns and are
49 therefore excellent models to investigate the evolution of pigment pattern
50 diversification in vertebrates¹⁻⁵. Recently, the phylogenetic relationships in the *Danio*
51 genus have been resolved, which led to the insight that a complex evolutionary
52 history underlies their speciation and morphological diversification⁶.

53 The horizontally striped pattern in *D. rerio* emerges during metamorphosis when
54 multipotent pigment cell progenitors derived from stem cells located at the dorsal
55 root ganglia (DRGs) migrate into the skin⁷⁻⁹. Here they differentiate and form the
56 pattern, presumably by a self-organizing process dependent on multiple cell-cell
57 interactions^{10,11}. These interactions lead to the acquisition of location-dependent cell
58 shapes, compact/yellow xanthophores and dense/reflective iridophores in the light
59 stripes, and stellate xanthophores and loose/blue iridophores in the dark
60 stripes^{7,12,13}. Melanophores are restricted to the dark stripes. Precise superimposition
61 of the differentially shaped pigment cells is required for colour and contrast of the
62 pattern. The cellular interactions are, at least partially, mediated by direct cell-cell
63 contacts through gap junctions, adhesion molecules and ion channels. Gap junctions
64 are formed by two connexins (Gja4 and Gja5b)¹⁴⁻¹⁶, Igsf11 and Jam3b regulate
65 adhesion^{17,18} and Kcnj13 is an inwardly rectifying potassium channel¹⁹. The diverse
66 patterns in other *Danio* fish are produced by the same three types of pigment cells;
67 however, the genetic and cell biological basis of the pattern variation is still largely
68 unexplored. So far, the evolution in two separate cell differentiation pathways,
69 xanthophore-specific Csf1 signalling in *D. albolineatus* and iridophore-specific Edn

2

70 signalling in *D. nigrofasciatus*, has been linked to patterning differences²⁰⁻²². This
71 mode of evolution might partly cause changes in the timing and strength of the
72 interactions between pigment cells, with cascading effects on their final distribution
73 within the skin.

74 In this study, we focus on the diversification of pigment patterns between the two
75 sister species *D. rerio* and *D. aesculapii*. Whereas *D. rerio* develop a very stereotypic
76 pattern of sharp horizontal dark and light stripes on the flanks and in the anal and tail
77 fins (Fig. 1a), in *D. aesculapii* a more variable pattern of vertical bars with lower
78 contrast is formed anteriorly on the flank that dissolves into irregular spots
79 posteriorly; the fins are not patterned, except for one dark stripe in the anal fin (Fig.
80 1b). We have shown that the potassium channel gene *kcnj13* evolved to contribute
81 to these patterning differences between the two species²³.

82 In *D. rerio* *kcnj13* mutants fewer, wider and interrupted stripes develop, and
83 melanophores and compact xanthophores fail to separate completely (Fig.
84 1c,e,f,g)^{14,19,23-28}. A CRISPR/Cas9-mediated loss-of-function allele of *kcnj13* in *D.*
85 *aesculapii* showed that the gene is also required for the formation of vertical bars in
86 this species. This null allele leads to a complete loss of any pattern with uniform
87 distribution of mixed pigment cells in the skin (Fig. 1d)²³. Hybrids between the two
88 species display stripes similar to the pattern in *D. rerio*. The evolutionary divergence
89 of *kcnj13* between *D. rerio* and *D. aesculapii* was demonstrated by reciprocal hybrids
90 between wild-type and mutant fish²³. This genetic test is used to identify evolved
91 genes by comparing the phenotypes of reciprocal hemizygotes; that is hybrids, which
92 carry a null allele from either one of the parental species in an otherwise identical
93 genetic background²⁹. It depends on the ability to generate null alleles in a given
94 species pair, which is possible in several *Danio* species since the introduction of the
95 CRISPR/Cas9 system. Hemizygous hybrids between *D. rerio* *kcnj13* mutant and *D.*
96 *aesculapii* wild type display a spotted phenotype indicating that *D. aesculapii* allele
97 fails to complement the *D. rerio* null-allele, whereas the reciprocal hybrid in which the
98 *D. aesculapii* allele was mutant displayed the striped phenotype of hybrids between
99 the wild-type species. The different phenotypes demonstrated that the wild-type
100 alleles from the two species are functionally no longer equivalent. Mutations in *gja4*,
101 *gja5b* and *igsf11* in *D. aesculapii* revealed functions for all these genes in the
102 formation of the bar pattern. However, all hemizygous hybrids showed patterns
103 indistinguishable from patterns of wild-type hybrids, ruling out functional evolution of
104 these loci. Hybrids between *D. rerio* *kcnj13* mutants and seven additional *Danio*
105 species suggest that *kcnj13* evolved independently several times in the genus, as
106 the wild-type alleles from three different species, *Danio aesculapii*, *Danio tinwini* and
107 *Danio choprae*, do not complement a *D. rerio* *kcnj13* loss-of-function allele in
108 hemizygous fish²³.

109 In chimeras produced by blastula transplantations, we corroborate previous
110 studies^{19,25} showing that *kcnj13* function is cell-autonomously required in

111 melanophores but not in xanthophores for normal stripe formation. In addition, we
112 show that the gene function is also not required in iridophores, the third pigment cell
113 type. In vitro experiments have shown that the function of *kcnj13* is required for the
114 depolarization of melanophore membranes upon contact with xanthophores²⁶. This
115 form of contact-dependent depolarisation might underlie the repulsive interactions
116 between melanophores and xanthophores during the establishment of the striped
117 pattern. To test the effects of *kcnj13* loss-of-function on the shapes of pigment cells
118 in vivo we performed further blastula transplantations, fluorescence imaging of
119 labelled pigment cells and cell-lineage tracing of marked clones. We find that the
120 shapes of all three types of pigment cells are altered in the mutants, suggesting that
121 cell-cell interactions responsible for the location-dependent acquisition of cell shapes
122 are dependent on *kcnj13* function and defective in the mutants. Using a newly
123 generated CRISPR/Cas9-mediated knock-in reporter line we detect *kcnj13*
124 expression in only very few differentiated melanophores in the skin, suggesting that
125 *kcnj13* function might be required only during a short period or in a subset of cells for
126 a longer time during pattern formation.

127 The coding sequence for *kcnj13* is highly conserved within the *Danio* genus with very
128 few non-synonymous changes between the species. However, it was not clear
129 whether these changes between *D. rerio* and *D. aesculapii* are functionally relevant,
130 or whether cis-regulatory evolution underlies *kcnj13* divergence²³. We show that
131 transgenic rescue of the *kcnj13* mutant phenotype is possible with the wild-type
132 coding sequences of both, *D. rerio* and *D. aesculapii*, suggesting that both proteins
133 are functionally equivalent. Strikingly, we observe a much higher expression of the
134 *D. rerio* allele compared to the *D. aesculapii* allele in the skin of wild-type hybrids.
135 We conclude that regulatory rather than protein changes underlie the evolution of the
136 gene between *D. rerio* and *D. aesculapii*. The differences in the two patterns might
137 result in part from the lower expression of *kcnj13* in *D. aesculapii* leading to variation
138 in pigment cell distribution and shapes reminiscent of those in *D. rerio* mutants
139 deprived of *kcnj13* activity.

140

141 **Results**

142 Development of the *kcnj13* phenotype in *D. rerio*

143 To understand the function of *kcnj13* during pattern formation, we focused on its role
144 during stripe formation in *D. rerio*. Multiple dominant alleles of *kcnj13* have been
145 found in several independent genetic screens^{14,19,23-28}. Fish homozygous for two
146 dominant alleles (Fig. 1e,f) and homozygotes for a recessive loss-of-function allele
147 (Fig. 1c) develop similar but variable phenotypes with fewer, wider and interrupted
148 stripes. To test whether this variability in our stocks is attributable to the nature of the
149 allele (dominant or recessive) or the genetic background, we compared different
150 allelic combinations in F2 fish with the same genetic background and found that all of

4

151 them lead to indistinguishable phenotypes. This indicates that dominant and
152 recessive alleles cause the same developmental effects in homozygous mutants
153 (Fig. 1g,h) showing that the dominant alleles are dominant-negative in
154 heterozygotes.

155 We followed the development of the mutant pattern during metamorphosis. As
156 previously described²⁵, and comparable to wild type, melanophores in the mutants
157 are cleared from the region of the first light stripe, where compact iridophores and
158 xanthophores develop (Fig. 1i-m). However, unlike in wild-type fish, iridophores later
159 fail to initiate the consecutive light stripes, which leads to a phenotype of fewer and
160 broader stripes in the mutants with occasional interruptions (Fig. 1n,o).

161

162 Cell-autonomy of the *kcnj13* function in *D. rerio*

163 Melanophores but not xanthophores require *kcnj13* function for stripe formation as
164 shown in chimeras created by blastula transplantations²⁵. We confirmed these
165 findings and also tested the requirement of *kcnj13* in iridophores. In these
166 experiments the donor embryos were mutant for *kcnj13* and genetically able to
167 provide only one of the three pigment cell types. Hosts were wild-type for *kcnj13* but
168 lacking this pigment cell type. Thus, in three sets of transplantations, the resulting
169 chimeras had one mutant pigment cell type placed adjacent to the respective other
170 two wild-type cell types. In contrast to mutant xanthophores and iridophores, only
171 mutant melanophores could not contribute to wild-type patterns in chimeras (Fig. 2a-
172 c) leading to the conclusion that *kcnj13* is cell-autonomously required in
173 melanophores but not in xanthophores or iridophores. By transplanting *kcnj13*
174 mutant cells into *albino/slc45a2* hosts we further tested whether mutant
175 melanophores can integrate into a normal pattern with wild-type melanophores in the
176 chimeric animals. We observed disruptions in the striped pattern wherever mutant
177 (pigmented) melanophores were present (Fig. 2d). Similar severe pattern defects
178 were never observed in chimeras that had not received mutant melanophores
179 suggesting the absence of any functional requirement in non-pigment cells (Fig. 2d).
180 These results indicate that stripe formation requires *kcnj13* function autonomously
181 only in melanophores or their progenitors.

182

183 Endogenous *kcnj13* expression during metamorphosis in *D. rerio*

184 To investigate when *kcnj13* functions in the melanophore lineage, we used
185 CRISPR/Cas9-mediated homology-directed repair to produce a *KalTA4::Venus*
186 knock-in line (for details see methods) as a reporter for endogenous *kcnj13*
187 expression in *D. rerio*. In early larvae we observed expression in the pronephros,
188 hindbrain and melanophores, a pattern very similar to previously published results

189 obtained by in situ hybridization²⁸, suggesting that our reporter line faithfully
190 recapitulates endogenous *kcnj13* expression (Fig. 3a). During later stages, at the
191 onset of metamorphosis, expression is detected in patches of cells in the spinal cord
192 along the entire anterior posterior axis of the fish (Fig. 3b). These positions do not
193 overlap with the DRGs, where the neural-crest derived stem cells for the pigment
194 cells are located⁷⁻⁹ (Fig. 3c). We conclude that *kcnj13* does not provide a function for
195 stripe formation in these cells as our transplantation experiments indicate no
196 functional requirement in non-pigment cells (Fig. 2d). While the signals in the kidney
197 and spinal cord persist throughout metamorphosis, we do not find expression of the
198 reporter in pigment cell progenitors, but in a few xanthophores and melanized
199 melanophores in the skin during the time of pattern formation (Fig. 3d-f). These
200 results show that *kcnj13* is expressed at detectable levels only in a small subset of
201 melanophores at any given time during pattern formation.

202

203 Effects of *kcnj13* mutations on pigment cell shape in *D. rerio*

204 A key aspect of pigment pattern formation in *D. rerio* is the location-specific
205 acquisition of different pigment cell shapes. In the dark stripes of wild-type *D. rerio*,
206 melanophores are densely packed and compact, only cells located at the boundaries
207 to the light stripes form long protrusions, possibly interacting directly with
208 xanthophores and iridophores^{10,30}. To investigate cell shapes in *kcnj13* mutants we
209 observed fish carrying *Tg(kita::mcherry)*, which labels both xanthophores and
210 melanophores. Some cells are unlabelled due to the variegation of the transgene,
211 which allows to visualize the shapes of the tightly packed melanophores. Similar to
212 previous findings¹⁹ we observed that in the dark regions in the mutants
213 melanophores are less compact and less tightly packed compared to wild-type cells.
214 We also find that the melanophores bordering the light stripes lack the very long
215 protrusions present in the wild type (Fig. 4a,b). This suggests that *kcnj13* mutant
216 melanophores do not interact with one another and with xanthophores and
217 iridophores in the same way wild-type melanophores do.

218 Next, we investigated the effect of *kcnj13* mutations on xanthophore behaviour
219 during stripe formation. Upon transplanting wild-type xanthophores, labelled with
220 *Tg(sox10::mrfp)*, into *kcnj13* mutants these cells acquire compact shapes in the dark
221 stripe regions, where they normally appear stellate (Fig. 4c,d). Similar to findings
222 from in vitro studies²⁶, these results suggest that wild-type xanthophores are not
223 always able to interact with mutant melanophores, which causes patterning defects
224 in vivo.

225 To assess the effects of mutations in *kcnj13* on iridophores, we induced fluorescently
226 labelled clones in the mutants using a *Tg(sox10::cre-ERT2)* line⁷ and followed labelled
227 iridophores during metamorphosis. We found clones of dense iridophores, which are
228 characteristic for light stripes, in the dark stripe area (Fig. 4e,f). This result suggests

6

229 that iridophores require the presence of and interaction with melanophores to
230 acquire the loose form; and that this interaction depends on *kcnj13* function. Thus,
231 iridophores might not be able to recognise mutant melanophores and therefore
232 develop ectopically in the dense form in the dark stripe regions. We conclude that
233 *kcnj13* function, required in melanophores, is important for homotypic and
234 heterotypic pigment cell interactions, which control the location-dependent cell shape
235 acquisition of all three pigment cell types during pattern formation. These cumulative
236 effects might inhibit the reiteration of dark and light stripes in the mutant fish.

237

238 Evolution of pigment cell shapes between *D. rerio* and *D. aesculapii*

239 Melanophores in *D. rerio* produce pronounced polarized protrusions towards
240 compact xanthophores and both cell types are strictly separated between the light
241 and dark stripes. The polarity of the protrusions is lost in *kcnj13* mutants, where both
242 cell types also mix occasionally (Fig. 4a,b,g,h). This mutant phenotype is similar to
243 the situation in wild-type *D. aesculapii*, where we found a mixing of cells and no
244 pronounced polarity of melanophores towards xanthophores (Fig. 4i). The contrast of
245 the bar pattern is therefore reduced; there is no contrast in *D. aesculapii kcnj13*
246 mutants, where all pigment cells mix and no bars are formed²³. Our observations
247 suggest that the divergence of the pigment patterns between *D. rerio* and *D.*
248 *aesculapii* could partially be due to evolutionary changes in the interactions between
249 all three pigment cell types, which influence the cell shapes.

250

251 Molecular basis of *kcnj13* evolution between species

252 To investigate the channel structure of Kcnj13 (Kir7.1), we expressed the *D. rerio*
253 protein fused to mCherry using a Multibac-derived baculovirus/insect cell expression
254 system^{31,32}, purified the recombinant protein by affinity and size-exclusion
255 chromatography, and measured the molecular mass with mass photometry³³
256 (Supplementary Fig. 1). The results suggest that Kcnj13 exists as a homo-tetramer,
257 which can explain the dominant-negative effects observed in alleles carrying point
258 mutations affecting the selectivity filter or the second transmembrane helix (Fig.
259 1a,b) as caused by mutant proteins negatively interfering with wild-type copies in the
260 complex in heterozygous fish^{14,19,23,24,27,28}. We constructed homology-based and
261 AlphaFold-multimer models of the homo-tetrameric Kcnj13 channel (Supplementary
262 Files). These models agree with published structures of similar potassium channels.
263 The protein sequences of *D. rerio* and *D. aesculapii* differ only by two amino acid
264 residues (Q23L and D180G in magenta) in the cytoplasmic domain²³; structure
265 modelling of the two alleles is insensitive to these differences.

266 Reciprocal hemizygoty tests showed that the divergence of *kcnj13* must reside
267 within the locus, either in the protein-coding region or in cis-regulatory elements, but
268 cannot be due to trans-acting factors²³. To test whether the amino acid changes
269 identified between the two species contribute to the evolution of *kcnj13*, we used
270 Tol2 transgenesis to express the coding regions from *D. rerio* or *D. aesculapii* under
271 the control of the melanophore-specific *mitfa* promoter in *kcnj13* null-mutant *D. rerio*
272 (Fig. 5b,d). In both cases the transgenes were able to restore the striped pattern in
273 the trunk of the fish, indicating that the protein from *D. aesculapii* can function in a
274 similar manner to the *D. rerio* protein (Fig. 5e). We observed some differences in the
275 rescue capabilities of the transgenes among the lines we established, possibly due
276 to copy number variations and expression differences of the randomly inserted
277 transgenes. The striped pattern of the caudal fin was never restored in the
278 transgenic lines, most likely due to the inactivity of the promoter at the appropriate
279 time points in this tissue, corroborating the finding of fundamental mechanistic
280 differences in pigment pattern formation between the trunk and fin (Frohnhofer et al.
281 2013). Our results suggest that the coding regions from both species function
282 similarly and that the protein-coding changes are irrelevant for *kcnj13* divergence.

283 Therefore cis-regulatory changes likely underlie *kcnj13* evolution and patterning
284 differences between the two species. To test this prediction, we produced hybrids
285 between the two species and performed allele-specific expression analysis in the
286 skin and posterior trunk of adult fish. We found significantly higher levels of the *D.*
287 *rerio* allele compared to the *D. aesculapii* allele (Fig. 5f, Supplementary Fig. 2),
288 indicating species-specific regulation of the locus and thereby confirming cis-
289 regulatory evolution. Quantitative differences in expression levels might cause
290 differences in pigment cell interactions and shapes observed between *D. rerio* and
291 *D. aesculapii*. Based on the repeated and independent evolution of the ancestral
292 *kcnj13* function in the *Danio* genus²³ we speculate that similar cis-regulatory changes
293 might also have occurred in *D. tinwini* and *D. choprae*. Our results highlight the
294 *Danio* genus as an excellent model system to study the molecular, genetic and
295 cellular basis of pigment pattern diversification in vertebrates.

296

297 Discussion

298 Teleost fish produce some of the most intricate pigmentation patterns in nature.
299 However, only in a few species the pattern forming mechanisms are studied in detail.
300 *D. rerio*, an excellent vertebrate model organism widely used in research, shows a
301 conspicuous pattern of horizontal stripes on the flank and in the anal and tail fins.
302 This pattern is produced by three types of pigment cells interacting in complex ways
303 to self-organize into dark and light stripes. During pattern formation the horizontal
304 myoseptum serves as an anatomical pre-pattern for the orientation of the stripes.
305 The stripes in the anal and tail fins are contiguous with the stripes in the body.
306 However, the fin pattern is formed by a different, possibly somewhat simpler

307 mechanism that involves only two cell types, melanophores and xanthophores.
308 Cellular interactions mediated by direct cell-cell contacts depending on gap junctions
309 and adhesion molecules are essential for stripe formation as demonstrated by the
310 spotted phenotypes of *gja4*, *gja5b*, *igsf11* and *jam3b* mutants^{14,15,17,18}. In addition,
311 mutations in *kcnj13* lead to defects in the pattern with fewer, wider and interrupted
312 stripes and occasional mixing of compact xanthophores with
313 melanophores^{14,19,23,24,26-28}. *Kcnj13* regulates the membrane potential of
314 melanophores²⁶, which might be important for the repulsion between xanthophores
315 and melanophores. By interspecies complementation tests in *Danio* hybrids it was
316 previously shown that of these four genes only the function of *kcnj13* diverged within
317 the *Danio* genus, probably several times independently²³.

318 To better understand the role of *kcnj13* in pattern formation and diversification, we
319 examined its function in *D. rerio* in more detail. All *kcnj13* alleles isolated in genetic
320 screens are dominant with a relatively weak heterozygous and considerably stronger
321 homozygous phenotype. We previously produced a loss-of-function allele, which is
322 completely recessive²³. The phenotypes of homozygous fish for a dominant or the
323 recessive allele in the same genetic background are indistinguishable (Fig. 1g,h).
324 This demonstrates that the dominant alleles are in fact dominant-negatives and not
325 neomorphs. The variability we observe in our mutant strains is dependent on the
326 genetic background.

327 Phenotypic analysis of chimeras obtained by blastula transplantations had already
328 demonstrated the autonomous requirement of *kcnj13* function in melanophores but
329 not in xanthophores²⁵. We repeated these transplantation experiments including the
330 third pigment cell type, iridophores. Our results show that *kcnj13* function is required
331 only in melanophores for stripe formation in *D. rerio*, but not in any other cell type
332 (Fig. 2a-c). In addition, we find that mutant melanophores lead to strong patterning
333 defects when transplanted into wild-type fish (Fig. 2d). This shows that the mutant
334 cells are not guided by their wild-type neighbours but influence the patterning
335 process cell-autonomously, possibly failing to instruct neighbouring xanthophores
336 and iridophores.

337 Our results support the prior observation that a *kcnj13* transgene expressed under
338 the control of the *mitfa* promoter, which is known to be active in melanophores and
339 their stem cells⁹, can rescue the mutant phenotype in the trunk²⁶. As these
340 experiments were conducted in the presence of a dominant-negative *kcnj13* allele,
341 which impedes the wild-type channel function, a complete rescue could not be
342 expected. In our transgenic rescue experiments, using the recessive mutant,
343 expression of *kcnj13* using the *mitfa* promoter restores the stripes on the flank of the
344 fish to a pattern very similar to the one observed in wild types (Fig. 5b), which further
345 supports the notion that *kcnj13* is required in melanophores. The striped pattern in
346 the anal and tail fins is not restored by the transgenes suggesting that expression
347 under the melanophore-specific *mitfa* promoter does not recapitulate all aspects of

348 the endogenous expression pattern of *kcnj13*, and mechanisms that form stripes in
349 the fins are fundamentally different from those that form stripes in the trunk¹⁰.

350 To visualize the expression pattern of *kcnj13* in *D. rerio* we made a reporter line by
351 homology directed knock-in of an optimized GAL4 coding sequence (KalTA4) into
352 the endogenous locus. In combination with a UAS:Venus transgene this reporter line
353 shows expression in early larvae in the pronephros and melanophores (Fig. 3a,b),
354 very similar to published data from in situ hybridizations²⁸, indicating that our line
355 faithfully recapitulates *kcnj13* expression. Later, during metamorphosis when the
356 pigment pattern is formed and also in adult fish, we detected expression in neurons
357 of the spinal cord (Fig. 4c). During these stages in situ hybridizations are difficult in
358 *D. rerio* and we rely on the reporter to indicate expression of the gene. As our
359 transplantation experiments clearly show a cell-autonomous requirement of *kcnj13* in
360 melanophores or their precursors (Fig. 2d) we can rule out a function of the gene for
361 pattern formation in these neuronal cells. We also found expression of the reporter
362 line during later stages in few xanthophores and, unexpectedly, only in a small
363 subset of melanophores (Fig. 4d). Expression of the reporter in xanthophores might
364 reflect earlier activation in a common precursor for melanophores and xanthophores
365 and the long persistence of the proteins (KalTA4 and Venus). Alternatively, *kcnj13*
366 could genuinely be expressed in xanthophores but without any obvious function in
367 stripe formation. Our observation that we cannot detect *kcnj13* expression in all
368 melanophores at any given time point suggests that it is either required only very
369 transiently or that only a few cells depend on *kcnj13* function and then influence the
370 behaviours of all the pigment cells. Alternatively, our reporter might not be sensitive
371 enough to allow the detection of very low expression levels, which could
372 nevertheless be relevant for pattern formation. A different possibility is that the
373 channel protein might be very stable and present in the cell membrane for prolonged
374 times even after transcription has ceased and also the reporter is no longer
375 detectable. In any case, our data is consistent with published data from single-cell
376 RNA sequencing³⁴, which also show expression of *kcnj13* to be low and limited to a
377 very minor fraction of pigment cell progenitors as well as differentiated melanophores
378 and xanthophores.

379 We conclude that *kcnj13* is only required in melanophores during pattern
380 development. Mutant melanophores are less compact and less tightly packed
381 affecting the tiling within the dark stripe. Mutant melanophores at the stripe
382 boundaries also do not form polarized protrusions towards the light stripes (Fig.
383 4a,b). The significance of these protrusions is unclear, they could be used for direct
384 repulsive interactions with xanthophores or iridophores to delineate the boundary
385 between light and dark stripe^{10,30}. In *kcnj13* mutants homotypic and heterotypic
386 interactions, among melanophores and between melanophores and the other two
387 pigment cell types, are affected, as seen, for example, by the mixing of the cells. We
388 find that the shapes of both cell types are affected in *kcnj13* mutants, with dense
389 iridophores and compact xanthophores, which are limited to the light stripes in wild

390 type, also appearing in dark stripe regions. Therefore, we conclude that
391 melanophores play a critical *kcnj13*-dependent role in directing dark stripe-specific
392 cell shape transitions in both, iridophores and xanthophores. In the absence of
393 Kcnj13 all three types of pigment cells may lose their dark stripe-specific shapes,
394 which might indicate that the default shapes for xanthophores and iridophores are
395 the ones these cells acquire in the light stripe region.

396 The same types of pigment cells that are found in *D. rerio* form a range of very
397 different patterns in closely related *Danio* species. The specification and
398 differentiation of pigment cells are similar in *D. rerio* and *D. aesculapii*. They both
399 require Mitfa- and Kit signalling in melanophores and Csf1 and Ltk signalling in
400 xanthophores and iridophores, respectively^{23,35}. Mutants indicate that iridophores do
401 not emerge along the horizontal myoseptum, are lower in number and dispensable
402 for bar formation in *D. aesculapii* whereas they guide stripe formation in *D. rerio*²³.
403 Whether genes required for iridophore development have evolved between these
404 two species is not known. However, for another species, *D. nigrofasciatus*, it was
405 shown that reduced iridophore proliferation contributes to a reduction in stripe
406 number and integrity²². In addition, species-specific differences in the developmental
407 timing of pigment cell proliferation and differentiation can lead to patterning
408 differences as observed for xanthophores, which differentiate precociously in *D.*
409 *albolineatus* resulting in a loss of the striped pattern²¹. We find that melanophores in
410 *D. aesculapii* do not form long protrusions towards the light regions (Fig. 4g-i), which
411 is similar to *kcnj13* mutants in *D. rerio* (Fig. 4a,b). In *D. rerio* these protrusions might
412 partly regulate melanophore survival³⁰ and the overall stability of the boundary
413 between dark and light stripes. Similar to the *D. rerio* mutant, the lack of such
414 protrusions in *D. aesculapii* might indicate a less robust mechanism for the
415 consolidation of the boundary between dark bars and light regions (Fig. 4i), where
416 melanophores and xanthophores frequently mix.

417 When tested in *D. aesculapii* the four genes (*kcnj13*, *gja4*, *gja5b* and *igsf11*), known
418 to function in cell-cell interactions during stripe formation in *D. rerio*, were found to be
419 also required to form the bar pattern²³. Whereas residual patterns of spots or wider
420 and interrupted stripes still form in *D. rerio* mutants, the bar pattern is completely lost
421 in *D. aesculapii* mutants and all pigment cells intermingle and distribute evenly in the
422 skin, a phenotype only seen in double mutants in *D. rerio*. This indicates that cellular
423 interactions in both species occur but are more complex in *D. rerio*, which could lead
424 to a higher robustness of the patterning mechanism in this species. Reciprocal
425 hemizyosity tests for all four genes lead to the conclusion that there is functional
426 conservation in three cases, *gja4*, *gja5b* and *igsf11*, while only *kcnj13* diverged
427 between the two species²³. Thus, the formation of the very different patterns of
428 horizontal stripes and vertical bars involves the same players. Three of these, Kcnj13
429 and the two gap junction proteins, might be involved in an electric coupling of
430 pigment cells, which could allow coordinated tissue-scale patterning³⁶. Evolution in

431 *kcnj13* between the two species might influence the conditions for these interactions,
432 with the consequence of evolutionary change in patterning.

433 In our rescue experiments the coding sequences from both species, *D. rerio* and *D.*
434 *aesculapii*, were equally able to restore stripe formation in *D. rerio kcnj13* mutants
435 indicating functional equivalency. However, the use of a non-native promoter and
436 possible position effects due to random integration of the transgenes might obscure
437 subtle functional differences between the two proteins. This question could be
438 addressed in the future by precise exchanges in the coding sequence of the
439 endogenous locus in *D. rerio*. However, we found allele-specific differences of *kcnj13*
440 expression in hybrids with much higher levels of expression from the *D. rerio* allele
441 (Fig. 5f) clearly indicating regulatory differences between the loci from the two
442 species. Therefore, the functional divergence of *kcnj13* between *D. rerio* and *D.*
443 *aesculapii* is most likely caused by evolution of cis-regulatory elements affecting the
444 levels of expression of the gene. Cis-regulatory evolution has been implicated in
445 other cases of pattern diversification of *Danio* fish. In *D. albolineatus* the increased
446 expression of *Csf1* causes early differentiation of xanthophores leading to a loss of
447 the striped pattern and the mixing of pigment cells²¹. In *D. nigrofasciatus* iridophore
448 development is reduced due to cis-regulatory changes in the *Edn3* gene leading to
449 an attenuated pattern with fewer melanophores and stripes, similar to hypomorphic
450 *D. rerio* mutants²². In the rare case of *D. kyathit* and *D. quagga* hybrids between the
451 two species are fertile, which allows for quantitative trait locus (QTL) mapping. QTL
452 analysis for differences between the spotted *D. kyathit* and the striped *D. quagga* led
453 to the identification of a complex genetic basis for the pattern differences with
454 multiple candidate loci, probably involving changes in a number of regulatory
455 regions³⁷. In the more distantly related cichlids bars and stripes evolved repeatedly in
456 species endemic to the Great African Lakes. Here, QTL mapping identified
457 regulatory changes in the gene *agouti-related peptide 2 (agrp2)* that underly these
458 patterning differences³⁸.

459 In three-spine sticklebacks genome-wide association studies identified loci
460 underlying repeated ecological adaptations in independent pairs of fresh- and
461 saltwater populations³⁹. These adaptive loci are predominantly affected by cis-
462 regulatory changes leading to differences in gene expression in the gills⁴⁰. In
463 contrast, trans-acting factors independently evolved to affect gene expression in the
464 pharyngeal tooth plate in sticklebacks⁴¹. It was speculated that the genetic
465 architecture of teeth formation is less complex than the adaptations to salt handling;
466 evolution of trans-acting factors might therefore be less pleiotropic in dental tissue
467 compared to multifunctional gills.

468 Dominant mutations in *kcnj13* in *D. rerio* cause pigment pattern defects but also late-
469 onset retinal degeneration^{42,43}, similar to mutations in the human ortholog that are
470 known to cause two rare retinal diseases^{44,45}. Mutations in mice lead to lethal defects
471 in tracheal development⁴⁶. Due to this observed pleiotropy protein evolution might be

472 highly constrained, favouring regulatory evolution. In general pigment patterns seem
473 to evolve often by regulatory mutations, whereas pigmentation frequently diverges by
474 protein changes⁴⁷. However, constraints on regulatory evolution also exist; ectopic
475 expression of *kcnj13* in the dermomyotome leads to a long-finned phenotype²⁸. Cis-
476 regulatory evolution in *kcnj13* specifically affecting expression in the skin is
477 presumably non-pleiotropic and might therefore be more permissive for evolutionary
478 change influencing pigment cell behaviour.

479 A basic colour-forming unit in cold-blooded vertebrates, fish, amphibians and
480 reptiles, consists of xanthophores in the top layer, iridophores in the middle layer and
481 melanophores in the bottom layer. Melanophores appear black in the absence of
482 shiny iridophores and yellow-orange xanthophores on top, as in *D. rerio shadyltk* or
483 *pfeffer/csf1ra* mutants. Modifications of this basic arrangement of pigment cells can
484 yield diverse colourations. By varying the mechanisms that regulate pigment cell
485 shape and layering, differences in colour, brightness and contrast can be achieved.
486 In this regard our study points towards *kcnj13* as a key node for evolutionary
487 tinkering that underlies colour pattern diversification in teleosts. *D. rerio kcnj13*
488 mutants develop light and dark stripe regions low in contrast due to pigment cells
489 that lack location-specific shapes and colouration. Regulation of colouration by cell
490 shape transition may point to an important mechanism employed across evolution,
491 where layer-specific and location-specific arrangement of diverse pigment cell types
492 leads to species-specific colouration.

493

494

495

496

497

498

499

500

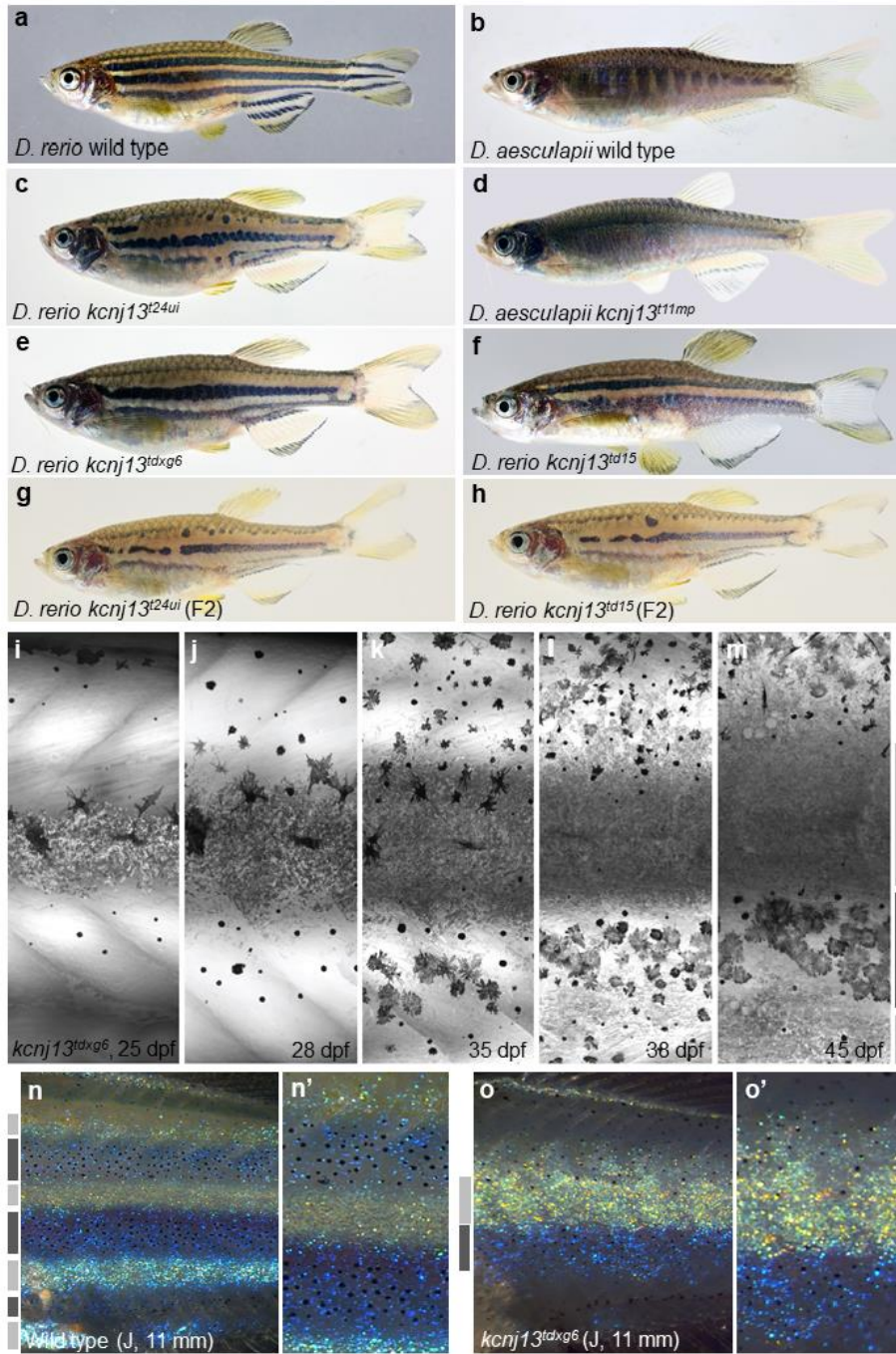
501

502

503

504

505 **Figures**



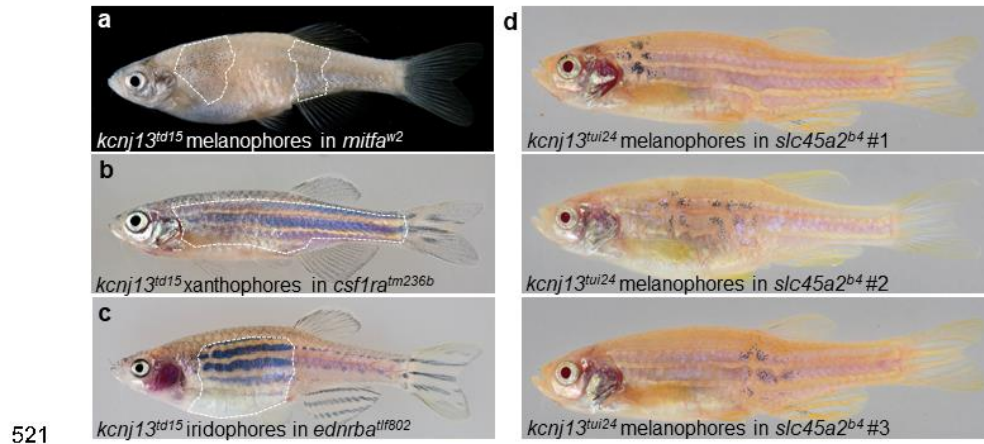
506

14

507 **Fig. 1: Pigment patterns in wild type and *kcnj13* mutant *D. rerio* and *D.***
508 ***aesculapii*.**

509 Pigment patterns in **a** *D. rerio* wild type, **b** *D. aesculapii* wild type, **c** *D. rerio*
510 *kcnj13^{l24ui}*, **d** *D. aesculapii kcnj13^{l11mp}*, **e** *D. rerio kcnj13^{lsg6}* and **f** *D. rerio kcnj13^{ld15}*.
511 *kcnj13^{l24ui}* and *kcnj13^{ld15}* were crossed to produce trans-heterozygous *kcnj13^{l24ui/ld15}*
512 F1 fish (not shown), which were then incrossed to generate F2 fish with the
513 genotypes **g** *kcnj13^{l24ui}* (n=8) and **h** *kcnj13^{ld15}* (n=12). **i-m** Melanophore clearance in
514 *kcnj13^{lsg6}* is similar to wild type during the development of the first light stripe
515 between 25 and 45 dpf. **n, n'** *D. rerio* wild-type and **o, o'** *kcnj13^{lsg6}* patterns at J
516 stage (11 mm). In the mutants, iridophores fail to reiterate the consecutive light
517 stripes, which ultimately leads to fewer and broader stripes with occasional
518 interruptions. Light and dark grey bars represent light and dark stripe areas,
519 respectively.

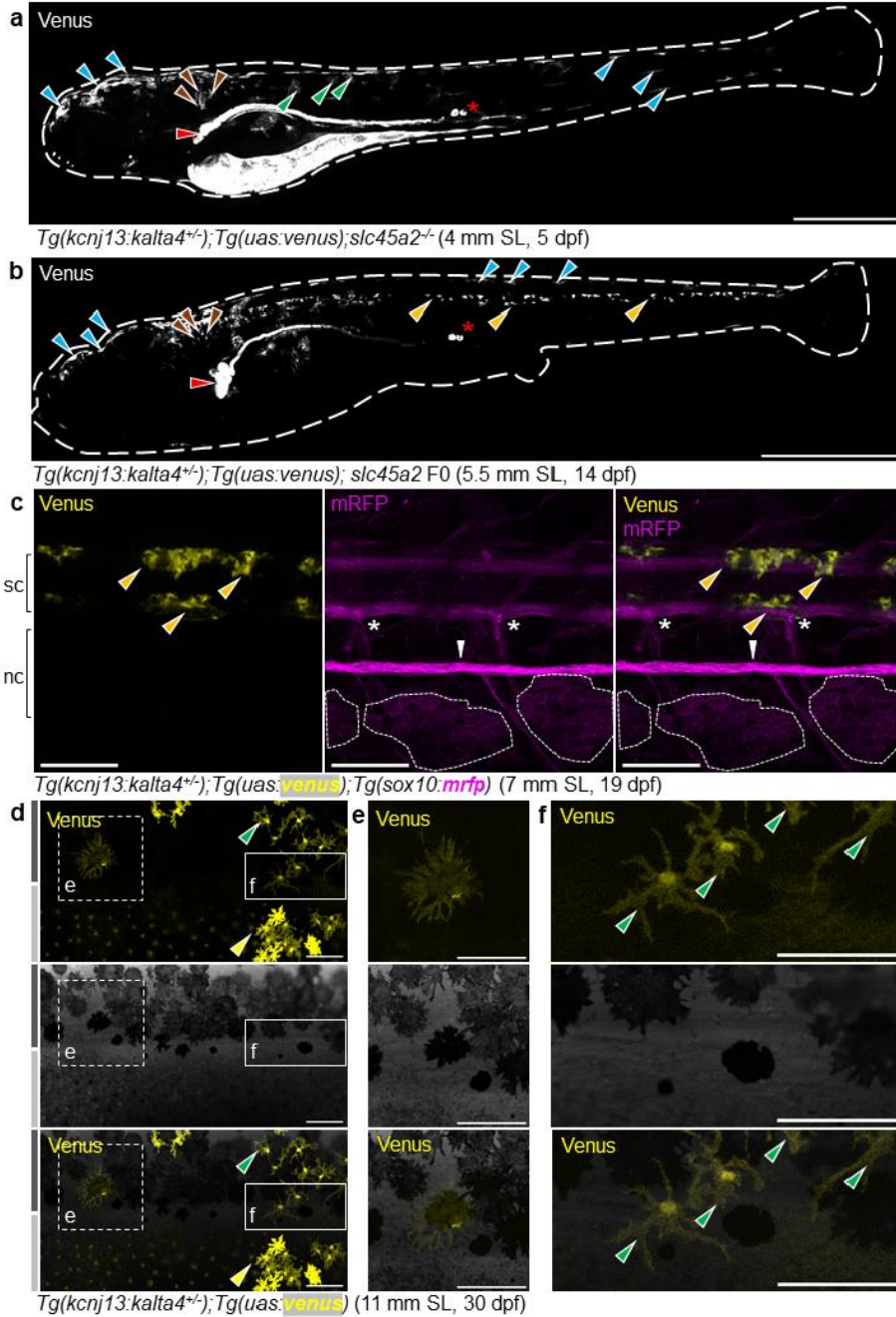
520



522 **Fig. 2: Melanophores require *kcnj13* autonomously during stripe formation.**

523 **a** Testing cell-autonomy of *kcnj13* by blastula transplantations reveals a genetic
524 requirement in melanophores (*kcnj13^{td15};ednrba^{tf802};csf1ra^{tm236b}* into *mitfa^{w2}*), but not
525 in **b** xanthophores (*kcnj13^{td15};kita^{b134};ednrba^{tf802}* into *csf1ra^{tm236b}*) or **c** iridophores
526 (*kcnj13^{td15};mitfa^{w2};csf1ra^{tm236b}* into *ednrba^{tf802}*). **d** Transplantation experiments
527 (*kcnj13^{tui24}* into *slc45a2^{b4}*) provide further evidence of a cell-autonomous function of
528 *kcnj13* in melanophores during stripe formation. Transplanted mutant melanophores
529 (pigmented) are associated with stripe perturbations in *albino* hosts (n=3). Strong
530 pattern deformations are never observed in chimeras without pigmented trunk
531 melanophores (n=41).

532



533

534

535 **Fig. 3: Endogenous *kcnj13* expression during *D. rerio* development.**

536 **a** Heterozygous *KalTA4::Venus* reporter larva showing signals in melanophores in
537 the head and tail regions (cyan arrowheads), xanthophores (green arrowheads),
538 hindbrain (brown arrowheads), along the entire pronephros (red arrowhead),
539 including corpuscles of Stannius (red asterisk), and the yolk. 4 mm SL, 5 dpf, sagittal
540 view, images of four positions along the AP axis combined into one composite; scale
541 bar=500 μ m. **b** Similar expression patterns can be observed in larva week older, with
542 additional signals in the spinal cord (orange arrowheads). These signals persist
543 throughout further development. 5.5 mm SL, 14 dpf, sagittal view, images of five
544 combined into one composite; scale bar=1 mm. **c** Venus expression does not
545 overlap with locations of the pigment cell stem cells at the DRGs (marked by white
546 asterisks). Iridophore patches in the skin indicated with white dashed circles, lateral
547 line nerve marked with a white arrowhead. nc: notochord, sc: spinal cord; 7 mm SL,
548 19 dpf; scale bar=100 μ m. **d** During and after the consolidation of the stripes in wild
549 types (see Fig. 1i-o), Venus expression can be detected in only a minority of **e**
550 melanophores and **f** xanthophores in the skin at any given time point. Green
551 arrowheads indicate stellate and Venus-positive xanthophores in the dark stripe,
552 while yellow arrowheads indicate compact, pigmented and Venus-positive
553 xanthophores in the light stripe. 11 mm SL, 30 dpf, scale bar=100 μ m.

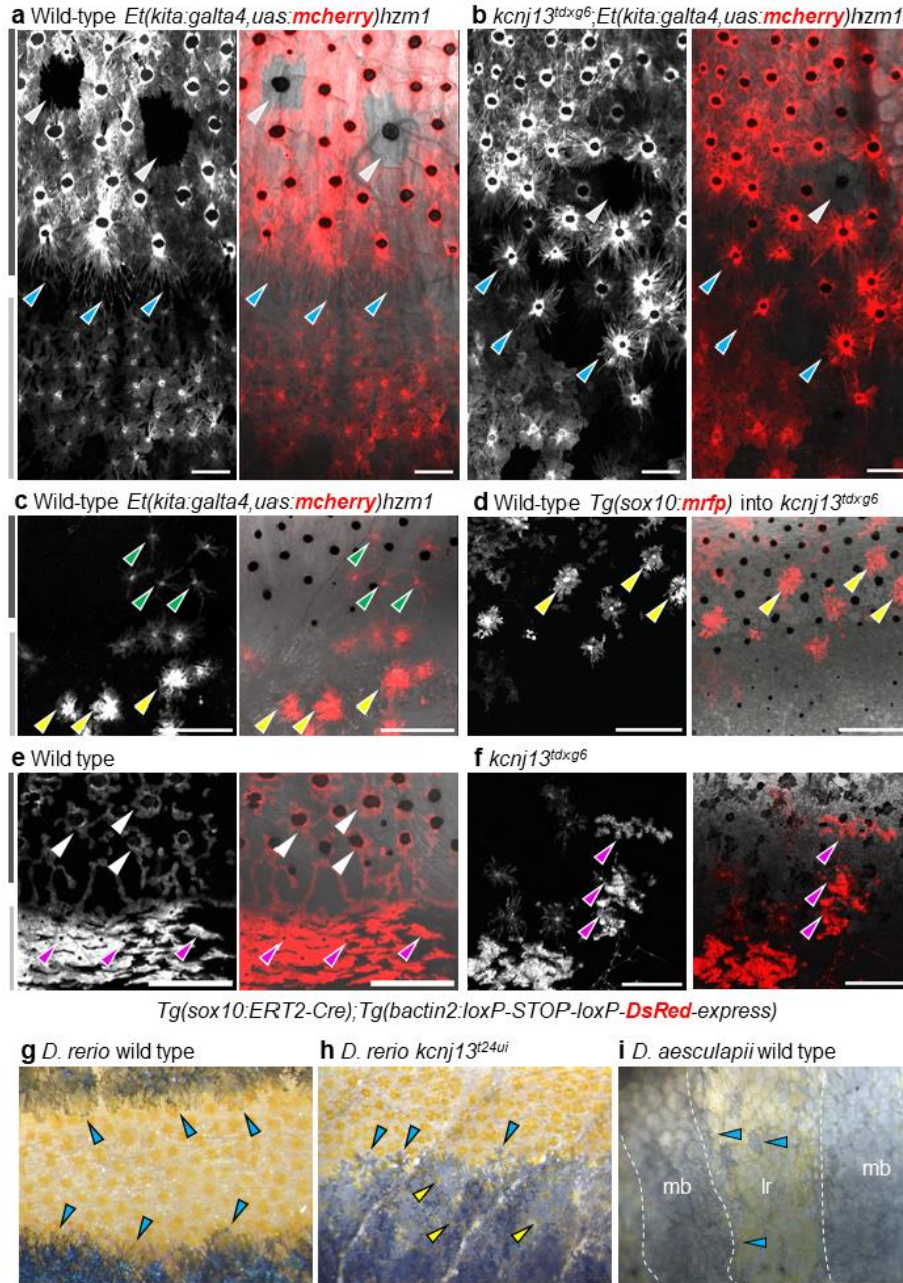
554

555

556

557

558



559

560

561 **Fig. 4: Pigment cell organization and shapes in *D. rerio* wild types and *kcnj13***
562 **mutants, and *D. aesculapii* wild types.**

563 **a** In adult wild-type *D. rerio*, melanophores in the stripe are densely packed (note
564 variegation of the transgene in a few cells indicated with light-grey arrowheads) and
565 cells at the boundary form long protrusions towards the light stripe (cyan
566 arrowheads). **b** In *kcnj13^{tdxg6}* mutants, cells are less tightly packed in the dark stripe
567 and short protrusions form without clear polarity (cyan arrowheads). **c** Wild-type
568 xanthophores acquire stellate shapes in the dark stripes (green arrowheads) and
569 compact shapes in the light stripes (yellow arrowheads). **d** Transplanted mRFP-
570 positive wild-type xanthophores acquire inappropriate compact shapes (yellow
571 arrowheads) in a dark stripe in *kcnj13^{tdxg6}* mutants (donor: *Tg(sox10:mrfp)*, host:
572 *kcnj13^{tdxg6}*). **e** Wild-type iridophores acquire loose shapes (white arrowheads) in the
573 dark stripes and dense shapes (magenta arrowheads) in the light stripes. **f**
574 Iridophores acquire ectopic compact shapes (magenta arrowheads) in the dark
575 stripes in *kcnj13^{tdxg6}* mutants, visualized by tracing labelled clones. Light and dark
576 grey bars represent light and dark stripes in *D. rerio*, respectively. **g** Wild-type *D.*
577 *rerio* form long melanophore protrusions towards the light stripe regions (cyan
578 arrowheads, see a). **h** Melanophore protrusions are not polarized in *D. rerio kcnj13*
579 mutants (cyan arrowheads, see b) and pigmented xanthophores are visible in the
580 dark stripe region (yellow arrowheads). **i** *D. aesculapii* wild types lack polarized
581 melanophores (cyan arrowheads), melanophores and xanthophores mix
582 occasionally, and the boundary between bars and light regions is of very low
583 contrast. mb=melanophore bar region, lr=light region.

584

585

586

587

588

589

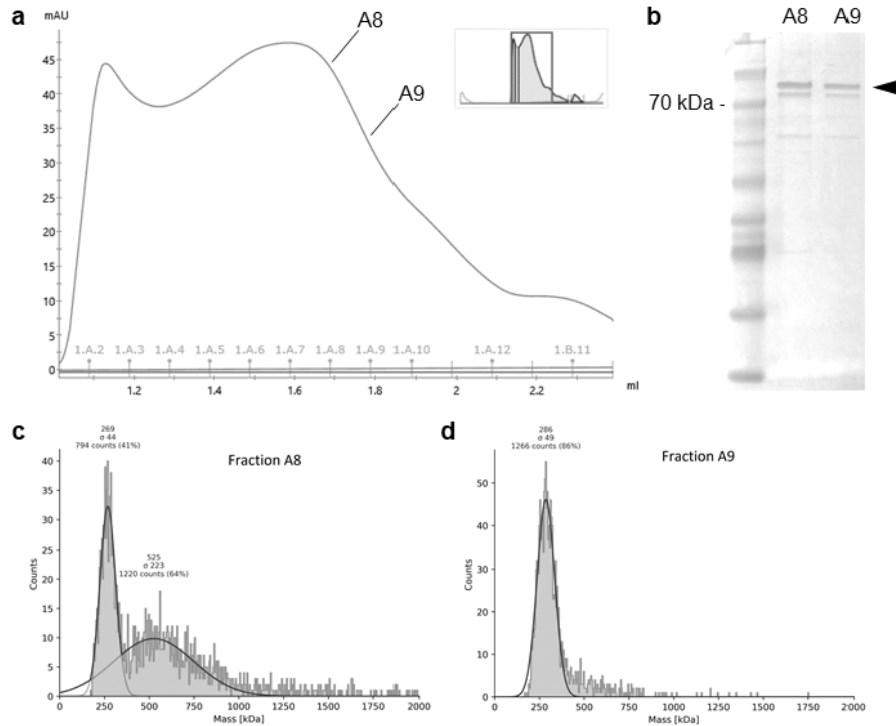
590

591

592

593

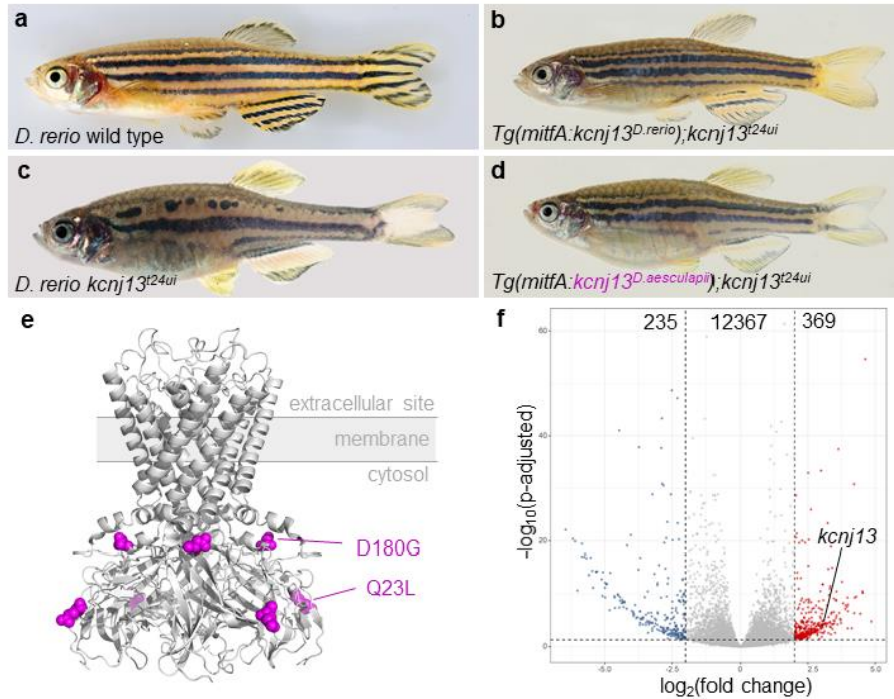
594



595

596 **Supplementary Fig. 1: Protein purification and analysis.** **a** Size-exclusion
597 chromatogram, fractions A8 and A9 are indicated. **b** Coomassie staining shows
598 bands corresponding to the expected size of about 70 kDa, with double bands
599 presumably due to glycosylation. **c** and **d** show mass-photometry peaks from
600 fractions A8 and A9, corresponding to a molecular mass of about 280 kDa, as
601 expected for a tetrameric complex. In **c** higher oligomeric states might be present.

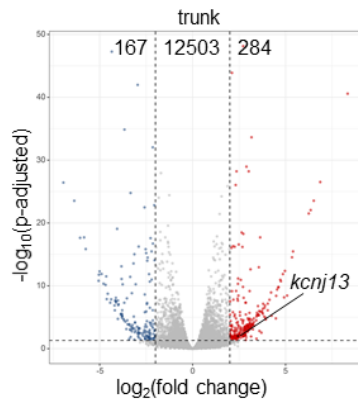
602



603

604 **Fig. 5: Molecular basis of *kcnj13* evolution between *D. rerio* and *D. aesculapii*.**
 605 **a** *D. rerio* wild type. **b** *D. rerio* *kcnj13^{tui24}*, in which either **c** the *D. rerio* allele of *kcnj13*
 606 (*Tg(mitfA:kcnj13^{D.rerio});kcnj13^{tui24}*) or **d** the *D. aesculapii* *kcnj13* allele
 607 (*Tg(mitfA:kcnj13^{D.aesculapii});kcnj13^{tui24}*) was expressed under the control of the *mitfA*
 608 promoter from *D. rerio*. In both cases, stripes were restored in the trunk of the fish.
 609 R224K was found to be polymorphic in *D. aesculapii* (Podobnik et al. 2020). **e**
 610 SWISS-MODEL derived homology model of the Kcnj13 tetramer (Q23L and D180G
 611 diverged between species in magenta). **f** Allele-specific expression analysis in
 612 interspecific hybrids shows higher *kcnj13* expression of the *D. rerio* allele in the skin
 613 ($n=12$; $p\text{-adjust} < 0.0001$), confirming cis-regulatory evolution. Overall, we found no
 614 differences in expression levels in 12,367 genes. 369 and 235 genes were
 615 significantly higher expressed from the *D. rerio* (red) or *D. aesculapii* allele (blue),
 616 respectively.

617



618

619 **Supplementary Fig. 2: Allele-specific expression analysis in hybrids between**
620 ***D. rerio* and *D. aesculapii*.** In the trunk, 284 and 167 genes were significantly higher
621 expressed from either the *D. rerio* (red) or *D. aesculapii* allele (blue). For most
622 transcripts (12,503) we observed no differences in expression levels. We found
623 significantly higher expression of *kcnj13* from the *D. rerio* allele ($p\text{-adjust} < 0.05$).

624

625 **Material and Methods**

626 No statistical methods were used to predetermine sample size. The experiments
627 were not randomized. The investigators were not blinded to allocation during
628 experiments and outcome assessment.

629

630 **Fish husbandry**

631 *D. rerio* and *D. aesculapii* were maintained as described in Brand & Nüsslein-
632 Volhard⁴⁸. If not newly generated (Supplementary Table 1), the following lines were
633 used for experiments: *D. rerio* wild-type Tuebingen (TU), *kcnj13*^{t24ui23}, *kcnj13*^{td1519},
634 *kcnj13*^{dxg614}, *nacre/mitfa*^{w249}, *pfeffer/csf1ra*^{tm236b50.51}, *rose/ednrba*^{tff80252},
635 *albino/slc45a2*^{b453}, *sparse/kita*^{b13454}, *Tg(sox10:mrfp)*⁷,
636 *Et(kita:galta4, uas:mcherry)hzm1*⁵⁵, *Tg(sox10:ERT2-Cre);Tg(bactin2:loxP-STOP-*
637 *loxP-DsRed-express)*^{56,57} and *D. aesculapii kcnj13*^{tmp1123}. Interspecific hybrids
638 between *D. rerio* and *D. aesculapii* were obtained by in vitro fertilizations²⁰. All
639 species were staged according to the normal table of *D. rerio* development⁵⁸. All
640 animal experiments were performed in accordance with the rules of the State of
641 Baden-Württemberg, Germany, and approved by the Regierungspräsidium
642 Tübingen.

643

644 **Supplementary Table 1: New transgenic lines used in this study**

Number	Line
1	<i>Tg(mitfa:kcnj13^{D.rerio});kcnj13^{t24ui}</i>
2	<i>Tg(mitfa:kcnj13^{D.aesculapii});kcnj13^{t24ui}</i>
3	<i>Tg(uas:venus)</i>
4	<i>Tg(kcnj13:kalta4);Tg(uas:venus)</i>
5	<i>Tg(kcnj13:kalta4);Tg(uas:venus);slc45a2^{l22mp}</i>

645

646 **Tol2-mediated transgenesis**

647 To generate the transgenic rescue lines plasmids with the *mitfa* promoter sequence
648 from *D. rerio*⁴⁹, the coding sequences of *kcnj13* from *D. rerio* or *D. aesculapii*, and
649 the coding sequence of sfGFP was constructed. The construct was subcloned into
650 the Tol2 vector *pGEM-T pminiTol2* carrying SV40 elements, a green heart marker
651 *cmlc2:venus* and Tol2 restriction sites^{59,60}. The resulting plasmids were designated
652 as *pTol2gh-mitfa-kcnj13^{D.rerio}-sfGFP* (GenBank accession number: OP326275) and

24

653 *pTol2gh-mitfa-kcnj13^{D.aesculapii}-sfGFP* (GenBank accession number: OP326276). Tol2
654 transgenesis was performed as previously described⁶⁰; briefly, a solution (12.5 ng/μL
655 Tol2 mRNA, 50 ng/μL plasmid DNA, and 5 % Phenol Red) was injected into fertilised
656 eggs of *D. rerio kcnj13^{t24ui}* at the one-cell-stage. 100 F0 embryos were selected for
657 marker gene expression at around 2 dpf and raised to adulthood. Mature F0 founder
658 fish were outcrossed to *D. rerio kcnj13^{t24ui}* and F1 larvae positive for marker gene
659 expression were selected to obtain stable transgenic lines. In both cases, lines were
660 identified in which the mutant phenotype was partially rescued. These lines were
661 designated as *Tg(mitfa:knj13^{D.rerio});knj13^{t24ui}* and
662 *Tg(mitfa:knj13^{D.aesculapii});knj13^{t24ui}*, outcrossed to *D. rerio kcnj13^{t24ui}*, and selected
663 for marker gene expression in embryos and intact stripe patterns in adults for at least
664 three generations (Supplementary Table 1).

665 To generate a *D. rerio* UAS:Venus line a plasmid with the coding sequence for the
666 Venus-variant of YFP under the control of the yeast transcription factor GAL4 (6
667 UAS-sites) was constructed (pminiTol2_UAS:Venus, GenBank accession:
668 OP243708); mRNA for the Tol2 transposase was transcribed in vitro from the
669 plasmid pCS2FA-transposase⁶¹ using the mMessageMachine and Poly-A tailing Kits
670 (Invitrogen). TU embryos at the one-cell stage were injected with approximately 2-4
671 nL of injection mix containing 250 ng/μL of in vitro transcribed mRNA and 25 ng/μL of
672 plasmid DNA in PBS with Phenol Red as a tracer dye. The adult F0 fish were
673 crossed to TU and the F1 larvae were screened for expression of the mCherry
674 marker in the heart. From the positive F1 fish a stable line was established by
675 another outcross to TU followed by sibling matings of the F2 fish (Supplementary
676 Table 1).

677

678 **CRISPR/Cas9-mediated knock-out and knock-in**

679 For gene knock-outs the CRISPR/Cas9 system was applied either as described in
680 Irion et al.⁶² or according to the guidelines for embryo microinjection of Integrated
681 DNA Technologies (IDT). Briefly, oligonucleotides were cloned into pDR274 to
682 generate the sgRNA vector. sgRNAs were transcribed from the linearised vector
683 using the MEGAscript T7 Transcription Kit (Invitrogen). Alternatively, target-specific
684 crRNAs and universal tracrRNAs were purchased from IDT. Cas9 was expressed as
685 a fusion protein with mCherry in *E. coli* (BL21(DE)3pLysS) from the plasmid pOPT-
686 Kan_Cas9-mCherry (GenBank accession: OP243709) and purified via double affinity
687 chromatography (His-Tag and Twin-StrepTag) using standard procedures. Before
688 use, the purified protein was dialyzed into PBS containing additionally 300 mM NaCl
689 and 150 mM KCl, aliquoted and stored at -70°C. sgRNAs or crRNA:tracrRNA
690 duplexes were injected as ribonucleoprotein complexes with Cas9 proteins into one-
691 cell stage embryos. The efficiency of indel generation was tested on eight larvae at 1
692 dpf by PCR using specific primer pairs and by sequence analysis as described
693 previously⁶³. The remaining larvae were raised to adulthood. Mature F0 fish carrying

25

694 indels were outcrossed. Loss-of-function alleles in heterozygous F1 fish were
695 selected to establish homozygous or trans-heterozygous mutant lines
696 (Supplementary Table 1).

697 To generate a reporter line for the expression of *kcnj13* the CRISPR/Cas9-system
698 was used. For the sgRNA template two oligonucleotides (5'-
699 TAGGCCGTCTTTGCTGACCAGG-3' and 5'-AAACCCTGGTCAGCAAAGACGG-3')
700 were annealed and cloned into pDR274; the RNA was transcribed in vitro with the
701 MegaScript Kit from Invitrogen. A donor plasmid was constructed containing the
702 KaITA4 variant⁵⁵ of the GAL4 coding sequence flanked by homology arms and
703 CRISPR target sites (GenBank accession: OP243710). This plasmid (25 ng/ μ L) was
704 co-injected with Cas9 protein (500 ng/ μ L) and sgRNA (35 ng/ μ L) into one-cell stage
705 embryos from the UAS:Venus line. The resulting F0 fish were backcrossed to
706 UAS:Venus and the F1 larvae were screened for expression of Venus. One founder
707 fish was identified with offspring showing a very strong early signal in the yolk and
708 later also in the pronephros and melanophores, consistent with published expression
709 data (Supplementary Table 1). To achieve good imaging conditions in this line we
710 generated an *albino* loss-of-function allele, *slc45a2*^{22mp}, as previously described⁶²
711 (Supplementary Table 1).
712

713 **Blastula transplantations**

714 Chimeric animals in Fig. 2a-d and Fig. 4d were generated by transplantations of cells
715 during blastula stage as described in⁶⁴.

716

717 **Cre induction and clonal analyses**

718 Cre induction was carried out as described in⁷. Labelled clones in Fig. 4e,f were from
719 fish followed over pattern development.

720

721 **Image acquisition and processing**

722 Anesthesia of postembryonic and adult fish was performed as described previously⁷.
723 Bright-field images of adult fish in Fig. 1a-h and Fig. 2a-d were obtained using a
724 Canon 5D Mk II camera. To visualize melanophore protrusions via dispersion of
725 melanosomes using bright-field imaging (Fig. 4g-i), fish were kept in the dark with a
726 final concentration of 100 μ M yohimbine (CAS: 65-19-0, Sigma-Aldrich) for 30
727 minutes before imaging as described in³⁰. Fish with different pigment patterns vary
728 considerably in contrast, thus requiring different settings for aperture and exposure
729 time, which can result in slightly different colour representations in the pictures.
730 Fluorescence images of postembryonic and adult fish were acquired on a Zeiss LSM

731 780 NLO confocal (BioOptics Facility, Max Planck Institute for Biology Tübingen) and
732 a Leica M205 FA stereo-microscope. Repeated imaging of pigment cell clones in
733 metamorphic *D. rerio* was performed as described in⁷. Maximum intensity projections
734 of confocal scans were uniformly adjusted for brightness and contrast. Images were
735 processed using Adobe Photoshop, Adobe Illustrator CS6 and Fiji⁶⁵.

736

737 Protein expression and purification

738 We expressed Kcnj13-mCherry with N-terminal His-tags in Sf9-insect cells using a
739 baculovirus/insect cell expression system^{31,32}. Pink pellets were washed with PBS,
740 stored at -70 °C, and later purified at 4 °C at all stages. We selected n-Dodecyl-B-D-
741 Maltoside (DDM, Serva Elec.) detergents at around 2x critical micelle concentration
742 (CMC) and supplied Cholesteryl Hemisuccinate (CHS, Serva Elec.) lipids for
743 solubilization of the membrane protein. Cell pellets were resuspended in lysis buffer
744 A, treated with a high-pressure homogeniser (Avestin EmulsiFlex-C3) and samples
745 were centrifuged at 40,000 rpm for one hr. The supernatant was incubated with Ni-
746 NTA beads for four hrs and applied to a polypropylene column (BioRad) equilibrated
747 in lysis buffer A. The column was washed with buffers B and C, and protein was
748 eluted with buffer D. Fractions were isolated based on pink-marker colouration and
749 concentrated using an AMICON ULTRA-15 filter (100 kDa cut-off). The concentrated
750 sample was spun for one hr on a table-top centrifuge at full speed and supernatant
751 was applied onto a Superose 6 Increase 5/150 GL column for gel filtration using
752 buffer E. Buffer compositions are provided in Supplementary Table 2.

753

754 Supplementary Table 2: Buffers used for protein purification.

Buffer	Composition
Lysis buffer A	50 mM HEPES pH 7.5, 100 mM NaCl, 20 mM imidazole, 1 % w/v DDM, 0.5 % w/v CHS, 1 % protease inhibitor (cOmplete Protease Inhibitor Cocktail EDTA-free, Sigma-Aldrich)
Wash buffer B	50 mM HEPES pH 7.5, 100 mM NaCl, 20 mM imidazole, 0.01 % w/v DDM, 0.005 % CHS, 1 % protease inhibitor
Wash buffer C	50 mM HEPES pH 7.5, 100 mM NaCl, 50 mM imidazole, 0.01 % w/v DDM, 0.005 % CHS, 1 % protease inhibitor
Elution buffer D	50 mM HEPES pH 7.5, 100 mM NaCl, 350 mM imidazole, 0.01 % w/v DDM, 0.005 % CHS, 1 % protease inhibitor
Gel filtration buffer E	50 mM HEPES pH 7.5, 100 mM NaCl, 0.01 % w/v DDM, 0.005 % CHS

755

756

757 **Mass photometry**

758 Measurements were performed in buffer E (see above) using an One^{MP} mass
759 photometer (Refeyn Ltd, Oxford, UK)³³. Immediately before analysis, the sample was
760 diluted 1:10 with the aforementioned buffer. Molecular mass was determined in the
761 analysis software provided by the manufacturer using a NativeMark- (Invitrogen).

762

763 **Structure modelling**

764 The homology model of the tetrameric Kcnj13 channel (Fig. 5e) was built using
765 SWISS-MODEL⁶⁶⁻⁷⁰ based on the crystal structure template (2.6-Å resolution) of the
766 potassium channel Kir2.2 from *Gallus gallus* (PDB ID: 3spg), sharing a sequence
767 similarity of 37 % with the target protein Kcnj13 from *D. rerio*. Similar models with a
768 pTM-based confidence score of ~ 60 % were generated using AlphaFold-
769 Mutlimer^{71,72}.

770

771 **Genome and transcriptome sequencing**

772 Reciprocal crosses between species (male *D. aesculapii* x female *D. rerio* (pair 1),
773 and male *D. rerio* x female *D. aesculapii* (pair 2)) were performed via in vitro
774 fertilization to produce F1 hybrids. Adult parental fish (n=4) and F1 hybrids (n=12; 7
775 hybrids from cross 1, 5 hybrids from cross 2) were euthanized by exposure to
776 buffered 0.5 g/L MS-222 (Tricaine). Tissues were dissected in ice-cold PBS and
777 collected using TRIzol (Life Technologies). DNA from the parental individuals was
778 isolated from posterior trunk tissue including the fins. RNA was obtained from skin
779 and posterior trunk tissue of F1 hybrids. RNA integrity and quantity were assessed
780 by Agilent 2100 Bioanalyzer. Metadata is provided in Supplementary Table 3. Library
781 preparation (DNA/RNA: TruSeq DNA Nano Kit (Illumina); 100 ng per sample) and
782 sequencing (NovaSeq 6000 (Illumina), for DNA: 2x 250 bp, for RNA: 2x 100 bp) were
783 performed by CeGaT GmbH (Tübingen, Germany). Data are available in:
784 PRJEB53585.

785 All subsequent analyzes were based on high-quality clean reads. Quality of the
786 sequencing data was checked using FastQC (version 0.11.9) and adapter
787 sequences were trimmed using fastp (version 0.23.2)⁷³. Genome resequencing
788 reads were aligned to the *D. rerio* reference genome (GRCz11) using BWA-MEM
789 (version 0.7.17-r1188)⁷⁴. The aligned SAM files were sorted and converted into BAM
790 files using SAMtools (version 1.11)⁷⁵. Then the sorted BAM files were de-realigned
791 and indexed again using Picard (version 2.18.29,
792 <https://broadinstitute.github.io/picard/>). Transcriptomes were aligned to GRCz11
793 using STAR aligner (version 2.7.10a)⁷⁶. The BAM files directly output by STAR in
794 two-pass mode are deduplicated and indexed by Picard.

28

795 Variant calling and filtration

796 To identify species-specific alleles, variant calling was performed according to the
 797 best practice pipeline of the Genome Analysis Toolkit (GATK4)^{77,78}. Specifically,
 798 Haplotypecaller was used to detect variants based on genome and transcriptome
 799 data. The called variants were joint-genotyped using GentypeGVCFs into a single
 800 .vcf file; data from skin and trunk tissue were separately processed. First,
 801 SelectVariants was used to filter single nucleotide polymorphisms (SNPs), then the
 802 selected SNPs were hard-filtered using Variantfiltration. Specifically, SNPs of 'QUAL
 803 < 30.0, QD < 2, FS > 60, MQ < 40, SOR > 3, MQRankSum < -12.5 and
 804 ReadPosRankSum > -8' as well as non-biallelic SNPs were filtered out. The
 805 remaining SNPs were filtered again using VCFtools (--max-missing 0.8, --maf 0.05).
 806 Finally, SNPs shared by genomes and transcriptomes were selected for the
 807 subsequent allele-specific expression analysis (ASE) using the intersect function of
 808 Bedtools (version 2.30.0)⁷⁹.

809

810 Allele-specific expression analysis

811 Read counts for species-specific SNPs were averaged per gene for each hybrid
 812 transcriptome using GATK ASEReadCounter⁸⁰ with default filters enabled.
 813 Significant allele-specific expression was defined as 'Fold Change' > 2 between
 814 alleles and adjusted p-values (p-adj) < 0.05 from DESeq2 package in R⁸¹. Finally, the
 815 ggplot2⁸² package in R rendered a volcano plot using the data obtained by DESeq2.

816

817 Data availability

818 The authors declare that all data supporting the findings of this study are available
 819 within the article and its supplementary information files or from the corresponding
 820 author upon reasonable request. The dataset generated during this study is available
 821 at The European Nucleotide Archive (ENA) accession number: PRJEB53585.

822

823 Supplementary Table 3: Metadata for transcriptomic analysis

CeGaT ID	short sample description	sex	stage	Egg_lay_date	Sampling_date	Extraction_date	RIN_value	quantity_u g	Concentration_ug_ul
S1906N1	RNA_skin_ento-ascarispp1_pair1_hybrid_1	NA	adult	20190606	20200113	20190114	9.30	0.814	90.4
S1906N2	RNA_trunk_ento-ascarispp1_pair1_hybrid_1	NA	adult	20190606	20200113	20190114	9.30	1.752	219
S1906N3	RNA_skin_ento-ascarispp1_pair1_hybrid_2	NA	adult	20190606	20200113	20190114	8.20	1.548	172
S1906N4	RNA_trunk_ento-ascarispp1_pair1_hybrid_2	NA	adult	20190606	20200113	20190114	8.20	1.656	232
S1906N5	RNA_skin_ento-ascarispp1_pair1_hybrid_3	NA	adult	20190606	20200113	20190114	7.90	1.54	154
S1906N6	RNA_trunk_ento-ascarispp1_pair1_hybrid_3	NA	adult	20190606	20200113	20190114	8.20	4.23	470

29

S1906N7	RNA_skin_rerio-ascacalapii_pair1_hybrid_4	NA	adult	20190606	20201113	20190114	8.50	1.43	130
S1906N8	RNA_skin_rerio-ascacalapii_pair1_hybrid_4	NA	adult	20190606	20201113	20190114	9.30	5.7	570
S1906N9	RNA_skin_rerio-ascacalapii_pair1_hybrid_5	NA	adult	20190606	20201113	20190114	8.20	1.6	160
S1906N10	RNA_skin_rerio-ascacalapii_pair1_hybrid_5	NA	adult	20190606	20201113	20190114	7.80	3.652	332
S1906N11	RNA_skin_rerio-ascacalapii_pair1_hybrid_6	NA	adult	20190606	20201113	20190114	8.50	1.118	93.2
S1906N12	RNA_skin_rerio-ascacalapii_pair1_hybrid_6	NA	adult	20190606	20201113	20190114	9.20	3.204	356
S1906N13	RNA_skin_rerio-ascacalapii_pair1_hybrid_7	NA	adult	20190606	20201113	20190114	9.00	1.232	112
S1906N14	RNA_skin_rerio-ascacalapii_pair1_hybrid_7	NA	adult	20190606	20201113	20190114	9.60	1.76	160
S1906N15	RNA_skin_rerio-ascacalapii_pair2_hybrid_8	NA	adult	20190814	20201113	20190114	9.20	1.56	120
S1906N16	RNA_skin_rerio-ascacalapii_pair2_hybrid_8	NA	adult	20190814	20201113	20190114	9.40	3.77	290
S1906N17	RNA_skin_rerio-ascacalapii_pair2_hybrid_9	NA	adult	20190814	20201113	20190114	7.70	1.596	114
S1906N18	RNA_skin_rerio-ascacalapii_pair2_hybrid_9	NA	adult	20190814	20201113	20190114	9.90	2.288	176
S1906N21	RNA_skin_rerio-ascacalapii_pair2_hybrid_11	NA	adult	20190814	20201113	20190114	8.80	1.644	137
S1906N22	RNA_skin_rerio-ascacalapii_pair2_hybrid_11	NA	adult	20190814	20201113	20190114	9.70	4.296	356
S1906N25	RNA_skin_rerio-ascacalapii_pair2_hybrid_13	NA	adult	20190814	20201113	20190114	9.40	1.365	105
S1906N26	RNA_skin_rerio-ascacalapii_pair2_hybrid_13	NA	adult	20190814	20201113	20190114	10.00	1.728	144
S1906N27	RNA_skin_rerio-ascacalapii_pair2_hybrid_14	NA	adult	20190814	20201113	20190114	9.50	1.508	116
S1906N28	RNA_skin_rerio-ascacalapii_pair2_hybrid_14	NA	adult	20190814	20201113	20190114	9.40	3.406	262
S1906N29	DNA_D_accacalapii_parom3_malo_pair1	malo	adult	NA	20190612	20190612	NA	2.104	11.5
S1906N30	DNA_D_rerio_parrnt1_fomalo_pair1	fomalo	adult	NA	20190612	20190612	NA	5.746	31.4
S1906N31	DNA_D_rerio_parrnt5_malo_pair2	malo	adult	NA	20190816	20190816	NA	7.997	43.7
S1906N32	DNA_D_accacalapii_parom9_fomalo_pair2	fomalo	adult	NA	20190816	20190816	NA	5.124	28

824

825 Acknowledgements

826 We thank Hans-Martin Maischein (now Max Planck Institute for Heart and Lung
827 Research, Bad Nauheim, Germany) and Horst Geiger (Max Planck Institute for
828 Biology, Tübingen, Germany) for help with blastula transplantations, Christian
829 Feldhaus and Aurora Panzera (BioOptics Facility, Max Planck Institute for Biology)
830 for help with imaging of the transgenic lines, Veronika Altmannova and Dorota
831 Rousova (Friedrich Miescher Laboratory, Tübingen, Germany) for help with protein
832 purification, and Silke Geiger-Rudolph, Roberta Occhinegro and Reinhard Albrecht
833 for excellent technical assistance (Max Planck Institute for Biology, Tübingen,
834 Germany). The AlphaFold-Multimer model was generated using the BMBF-funded
835 de.NBI Cloud within the German Network for Bioinformatics Infrastructure (de.NBI)
836 (031A532B, 031A533A, 031A533B, 031A534A, 031A535A, 031A537A, 031A537B,
837 031A537C, 031A537D, 031A538A). This work was supported by an ERC Advanced
838 Grant “DanioPattern” (694289) and the Max Planck Society, Germany.

839

840 **Contributions**

841 M.P., A.P.S., C.M.D., H.G.F., S.W., C.N.V. and U.I. were involved in the design of
842 the experiments. M.P., A.P.S., U.I., H.G.F., and M.F. performed the experiments.
843 U.I., M.P., C.N.V., A.P.S., J.L., Z.F., C.M.D., H.E., S.W., J.R.W. and analysed the
844 data. M.P. made the figures with help from U.I. and C.N.V.; M.P., U.I., A.P.S. and
845 C.N.V. wrote the manuscript. C.N.V. and J.R.W. acquired funding.

846

847 **Ethics declaration**

848 Competing interests

849 The authors declare no competing interests.

850

851 **References**

- 852 1 Parichy, D. M. Advancing biology through a deeper understanding of zebrafish
853 ecology and evolution. *Elife* **4**, doi:10.7554/eLife.05635 (2015).
- 854 2 Singh, A. P. & Nusslein-Volhard, C. Zebrafish stripes as a model for vertebrate colour
855 pattern formation. *Curr Biol* **25**, R81-R92, doi:10.1016/j.cub.2014.11.013 (2015).
- 856 3 Patterson, L. B. & Parichy, D. M. Zebrafish Pigment Pattern Formation: Insights into
857 the Development and Evolution of Adult Form. *Annu Rev Genet* **53**, 505-530,
858 doi:10.1146/annurev-genet-112618-043741 (2019).
- 859 4 Irion, U. & Nusslein-Volhard, C. The identification of genes involved in the evolution
860 of color patterns in fish. *Curr Opin Genet Dev* **57**, 31-38,
861 doi:10.1016/j.gde.2019.07.002 (2019).
- 862 5 Parichy, D. M. Evolution of pigment cells and patterns: recent insights from teleost
863 fishes. *Curr Opin Genet Dev* **69**, 88-96, doi:10.1016/j.gde.2021.02.006 (2021).
- 864 6 McCluskey, B. M. & Postlethwait, J. H. Phylogeny of zebrafish, a "model species,"
865 within Danio, a "model genus". *Mol Biol Evol* **32**, 635-652,
866 doi:10.1093/molbev/msu325 (2015).
- 867 7 Singh, A. P., Schach, U. & Nusslein-Volhard, C. Proliferation, dispersal and patterned
868 aggregation of iridophores in the skin prefigure striped colouration of zebrafish. *Nat*
869 *Cell Biol* **16**, 607-614, doi:10.1038/ncb2955 (2014).
- 870 8 Singh, A. P. *et al.* Pigment Cell Progenitors in Zebrafish Remain Multipotent through
871 Metamorphosis. *Dev Cell* **38**, 316-330, doi:10.1016/j.devcel.2016.06.020 (2016).
- 872 9 Dooley, C. M., Mongera, A., Walderich, B. & Nusslein-Volhard, C. On the embryonic
873 origin of adult melanophores: the role of ErbB and Kit signalling in establishing
874 melanophore stem cells in zebrafish. *Development* **140**, 1003-1013,
875 doi:10.1242/dev.087007 (2013).
- 876 10 Frohnhof, H. G., Krauss, J., Maischein, H. M. & Nusslein-Volhard, C. Iridophores
877 and their interactions with other chromatophores are required for stripe formation in
878 zebrafish. *Development* **140**, 2997-3007, doi:10.1242/dev.096719 (2013).
- 879 11 Patterson, L. B. & Parichy, D. M. Interactions with iridophores and the tissue
880 environment required for patterning melanophores and xanthophores during
881 zebrafish adult pigment stripe formation. *PLoS Genet* **9**, e1003561,
882 doi:10.1371/journal.pgen.1003561 (2013).

- 883 12 Mahalwar, P., Walderich, B., Singh, A. P. & Nusslein-Volhard, C. Local
884 reorganization of xanthophores fine-tunes and colors the striped pattern of zebrafish.
885 *Science* **345**, 1362-1364, doi:10.1126/science.1254837 (2014).
- 886 13 Gur, D. *et al.* In situ differentiation of iridophore crystalotypes underlies zebrafish
887 stripe patterning. *Nat Commun* **11**, 6391, doi:10.1038/s41467-020-20088-1 (2020).
- 888 14 Irion, U. *et al.* Gap junctions composed of connexins 41.8 and 39.4 are essential for
889 colour pattern formation in zebrafish. *Elife* **3**, e05125, doi:10.7554/eLife.05125
890 (2014).
- 891 15 Watanabe, M. *et al.* Spot pattern of leopard Danio is caused by mutation in the
892 zebrafish connexin41.8 gene. *EMBO Rep* **7**, 893-897, doi:10.1038/sj.embor.7400757
893 (2006).
- 894 16 Watanabe, M., Sawada, R., Aramaki, T., Skerrett, I. M. & Kondo, S. The
895 Physiological Characterization of Connexin41.8 and Connexin39.4, Which Are
896 Involved in the Striped Pattern Formation of Zebrafish. *J Biol Chem* **291**, 1053-1063,
897 doi:10.1074/jbc.M115.673129 (2016).
- 898 17 Eom, D. S. *et al.* Melanophore migration and survival during zebrafish adult pigment
899 stripe development require the immunoglobulin superfamily adhesion molecule
900 Igsf11. *PLoS Genet* **8**, e1002899, doi:10.1371/journal.pgen.1002899 (2012).
- 901 18 Eom, D. S., Patterson, L. B., Bostic, R. R. & Parichy, D. M. Immunoglobulin
902 superfamily receptor Junctional adhesion molecule 3 (Jam3) requirement for
903 melanophore survival and patterning during formation of zebrafish stripes. *Dev Biol*
904 **476**, 314-327, doi:10.1016/j.ydbio.2021.04.007 (2021).
- 905 19 Iwashita, M. *et al.* Pigment pattern in jaguar/obelix zebrafish is caused by a Kir7.1
906 mutation: implications for the regulation of melanosome movement. *PLoS Genet* **2**,
907 e197, doi:10.1371/journal.pgen.0020197 (2006).
- 908 20 Parichy, D. M. & Johnson, S. L. Zebrafish hybrids suggest genetic mechanisms for
909 pigment pattern diversification in Danio. *Dev Genes Evol* **211**, 319-328,
910 doi:10.1007/s004270100155 (2001).
- 911 21 Patterson, L. B., Bain, E. J. & Parichy, D. M. Pigment cell interactions and differential
912 xanthophore recruitment underlying zebrafish stripe reiteration and Danio pattern
913 evolution. *Nat Commun* **5**, 5299, doi:10.1038/ncomms6299 (2014).
- 914 22 Spiewak, J. E. *et al.* Evolution of Endothelin signaling and diversification of adult
915 pigment pattern in Danio fishes. *PLoS Genet* **14**, e1007538,
916 doi:10.1371/journal.pgen.1007538 (2018).
- 917 23 Podobnik, M. *et al.* Evolution of the potassium channel gene Kcnj13 underlies colour
918 pattern diversification in Danio fish. *Nat Commun* **11**, 6230, doi:10.1038/s41467-020-
919 20021-6 (2020).
- 920 24 Haffter, P. *et al.* Mutations affecting pigmentation and shape of the adult zebrafish.
921 *Dev Genes Evol* **206**, 260-276, doi:10.1007/s004270050051 (1996).
- 922 25 Maderspacher, F. & Nusslein-Volhard, C. Formation of the adult pigment pattern in
923 zebrafish requires leopard and obelix dependent cell interactions. *Development* **130**,
924 3447-3457, doi:10.1242/dev.00519 (2003).
- 925 26 Inaba, M., Yamanaka, H. & Kondo, S. Pigment pattern formation by contact-
926 dependent depolarization. *Science* **335**, 677, doi:10.1126/science.1212821 (2012).
- 927 27 Henke, K. *et al.* Genetic Screen for Postembryonic Development in the Zebrafish
928 (*Danio rerio*): Dominant Mutations Affecting Adult Form. *Genetics* **207**, 609-623,
929 doi:10.1534/genetics.117.300187 (2017).
- 930 28 Silic, M. R. *et al.* Potassium Channel-Associated Bioelectricity of the Dermomyotome
931 Determines Fin Patterning in Zebrafish. *Genetics* **215**, 1067-1084,
932 doi:10.1534/genetics.120.303390 (2020).
- 933 29 Stern, D. L. Identification of loci that cause phenotypic variation in diverse species
934 with the reciprocal hemizyosity test. *Trends Genet* **30**, 547-554,
935 doi:10.1016/j.tig.2014.09.006 (2014).
- 936 30 Hamada, H. *et al.* Involvement of Delta/Notch signaling in zebrafish adult pigment
937 stripe patterning. *Development* **141**, 318-324, doi:10.1242/dev.099804 (2014).

- 938 31 Bieniossek, C., Imasaki, T., Takagi, Y. & Berger, I. MultiBac: expanding the research
939 toolbox for multiprotein complexes. *Trends Biochem Sci* **37**, 49-57,
940 doi:10.1016/j.tibs.2011.10.005 (2012).
- 941 32 Altmannova, V., Blaha, A., Astrinidis, S., Reichle, H. & Weir, J. R. InteBac: An
942 integrated bacterial and baculovirus expression vector suite. *Protein Sci* **30**, 108-114,
943 doi:10.1002/pro.3957 (2021).
- 944 33 Young, G. *et al.* Quantitative mass imaging of single biological macromolecules.
945 *Science* **360**, 423-427, doi:10.1126/science.aar5839 (2018).
- 946 34 Saunders, L. M. *et al.* Thyroid hormone regulates distinct paths to maturation in
947 pigment cell lineages. *Elife* **8**, doi:10.7554/eLife.45181 (2019).
- 948 35 McCluskey, B. M., Liang, Y., Lewis, V. M., Patterson, L. B. & Parichy, D. M. Pigment
949 pattern morphospace of Danio fishes: evolutionary diversification and mutational
950 effects. *Biol Open* **10**, doi:10.1242/bio.058814 (2021).
- 951 36 Harris, M. P. Bioelectric signaling as a unique regulator of development and
952 regeneration. *Development* **148**, doi:10.1242/dev.180794 (2021).
- 953 37 McCluskey, B. M., Uji, S., Mancusi, J. L., Postlethwait, J. H. & Parichy, D. M. A
954 complex genetic architecture in zebrafish relatives *Danio quagga* and *D. kyathit*
955 underlies development of stripes and spots. *PLoS Genet* **17**, e1009364,
956 doi:10.1371/journal.pgen.1009364 (2021).
- 957 38 Kratochwil, C. F. *et al.* Agouti-related peptide 2 facilitates convergent evolution of
958 stripe patterns across cichlid fish radiations. *Science* **362**, 457-460,
959 doi:10.1126/science.aao6809 (2018).
- 960 39 Jones, F. C. *et al.* The genomic basis of adaptive evolution in threespine
961 sticklebacks. *Nature* **484**, 55-61, doi:10.1038/nature10944 (2012).
- 962 40 Verta, J. P. & Jones, F. C. Predominance of cis-regulatory changes in parallel
963 expression divergence of sticklebacks. *Elife* **8**, doi:10.7554/eLife.43785 (2019).
- 964 41 Hart, J. C., Ellis, N. A., Eisen, M. B. & Miller, C. T. Convergent evolution of gene
965 expression in two high-toothed stickleback populations. *PLoS Genet* **14**, e1007443,
966 doi:10.1371/journal.pgen.1007443 (2018).
- 967 42 Toms, M. *et al.* Phagosomal and mitochondrial alterations in RPE may contribute to
968 KCNJ13 retinopathy. *Sci Rep* **9**, 3793, doi:10.1038/s41598-019-40507-8 (2019).
- 969 43 Toms, M. *et al.* Missense variants in the conserved transmembrane M2 protein
970 domain of KCNJ13 associated with retinovascular changes in humans and zebrafish.
971 *Exp Eye Res* **189**, 107852, doi:10.1016/j.exer.2019.107852 (2019).
- 972 44 Hejtmancik, J. F. *et al.* Mutations in KCNJ13 cause autosomal-dominant snowflake
973 vitreoretinal degeneration. *Am J Hum Genet* **82**, 174-180,
974 doi:10.1016/j.ajhg.2007.08.002 (2008).
- 975 45 Sergouniotis, P. I. *et al.* Recessive mutations in KCNJ13, encoding an inwardly
976 rectifying potassium channel subunit, cause leber congenital amaurosis. *Am J Hum*
977 *Genet* **89**, 183-190, doi:10.1016/j.ajhg.2011.06.002 (2011).
- 978 46 Yin, W. *et al.* The potassium channel KCNJ13 is essential for smooth muscle
979 cytoskeletal organization during mouse tracheal tubulogenesis. *Nat Commun* **9**,
980 2815, doi:10.1038/s41467-018-05043-5 (2018).
- 981 47 Orteu, A. & Jiggins, C. D. The genomics of coloration provides insights into adaptive
982 evolution. *Nat Rev Genet* **21**, 461-475, doi:10.1038/s41576-020-0234-z (2020).
- 983 48 Brand, M., Granato, M. & Nüsslein-Volhard, C. in *Zebrafish: A practical approach* Vol.
984 **7** (eds C Nüsslein-Volhard & R Dahm) 7-37 (2002).
- 985 49 Lister, J. A., Robertson, C. P., Lepage, T., Johnson, S. L. & Raible, D. W. nacre
986 encodes a zebrafish microphthalmia-related protein that regulates neural-crest-
987 derived pigment cell fate. *Development* **126**, 3757-3767,
988 doi:10.1242/dev.126.17.3757 (1999).
- 989 50 Odenthal, J. *et al.* Mutations affecting xanthophore pigmentation in the zebrafish,
990 *Danio rerio*. *Development* **123**, 391-398, doi:10.1242/dev.123.1.391 (1996).
- 991 51 Parichy, D. M., Ransom, D. G., Paw, B., Zon, L. I. & Johnson, S. L. An orthologue of
992 the kit-related gene *fms* is required for development of neural crest-derived

- 993 xanthophores and a subpopulation of adult melanocytes in the zebrafish, *Danio rerio*.
994 *Development* **127**, 3031-3044, doi:10.1242/dev.127.14.3031 (2000).
- 995 52 Parichy, D. M. *et al.* Mutational analysis of endothelin receptor b1 (rose) during
996 neural crest and pigment pattern development in the zebrafish *Danio rerio*. *Dev Biol*
997 **227**, 294-306, doi:10.1006/dbio.2000.9899 (2000).
- 998 53 Dooley, C. M. *et al.* Slc45a2 and V-ATPase are regulators of melanosomal pH
999 homeostasis in zebrafish, providing a mechanism for human pigment evolution and
1000 disease. *Pigment Cell Melanoma Res* **26**, 205-217, doi:10.1111/pcmr.12053 (2013).
- 1001 54 Kelsh, R. N. *et al.* Zebrafish pigmentation mutations and the processes of neural
1002 crest development. *Development* **123**, 369-389, doi:10.1242/dev.123.1.369 (1996).
- 1003 55 Distel, M., Wullimann, M. F. & Koster, R. W. Optimized Gal4 genetics for permanent
1004 gene expression mapping in zebrafish. *Proc Natl Acad Sci U S A* **106**, 13365-13370,
1005 doi:10.1073/pnas.0903060106 (2009).
- 1006 56 Mongera, A. *et al.* Genetic lineage labeling in zebrafish uncovers novel neural crest
1007 contributions to the head, including gill pillar cells. *Development* **140**, 916-925,
1008 doi:10.1242/dev.091066 (2013).
- 1009 57 Bertrand, J. Y. *et al.* Haematopoietic stem cells derive directly from aortic
1010 endothelium during development. *Nature* **464**, 108-111, doi:10.1038/nature08738
1011 (2010).
- 1012 58 Parichy, D. M., Elizondo, M. R., Mills, M. G., Gordon, T. N. & Engeszer, R. E. Normal
1013 table of postembryonic zebrafish development: staging by externally visible anatomy
1014 of the living fish. *Dev Dyn* **238**, 2975-3015, doi:10.1002/dvdy.22113 (2009).
- 1015 59 Yelon, D., Home, S. A. & Stainier, D. Y. Restricted expression of cardiac myosin
1016 genes reveals regulated aspects of heart tube assembly in zebrafish. *Dev Biol* **214**,
1017 23-37, doi:10.1006/dbio.1999.9406 (1999).
- 1018 60 Kawakami, K. & Shima, A. Identification of the Tol2 transposase of the medaka fish
1019 *Oryzias latipes* that catalyzes excision of a nonautonomous Tol2 element in zebrafish
1020 *Danio rerio*. *Gene* **240**, 239-244, doi:10.1016/s0378-1119(99)00444-8 (1999).
- 1021 61 Kwan, K. M. *et al.* The Tol2kit: a multisite gateway-based construction kit for Tol2
1022 transposon transgenesis constructs. *Dev Dyn* **236**, 3088-3099,
1023 doi:10.1002/dvdy.21343 (2007).
- 1024 62 Irion, U., Krauss, J. & Nusslein-Volhard, C. Precise and efficient genome editing in
1025 zebrafish using the CRISPR/Cas9 system. *Development* **141**, 4827-4830,
1026 doi:10.1242/dev.115584 (2014).
- 1027 63 Meeker, N. D., Hutchinson, S. A., Ho, L. & Trede, N. S. Method for isolation of PCR-
1028 ready genomic DNA from zebrafish tissues. *Biotechniques* **43**, 610, 612, 614,
1029 doi:10.2144/000112619 (2007).
- 1030 64 Kane, D. A. & Kishimoto, Y. in *Zebrafish: A practical approach* Vol. 7 (eds C
1031 Nüsslein-Volhard & R Dahm) 95-119 (2002).
- 1032 65 Preibisch, S., Saalfeld, S. & Tomancak, P. Globally optimal stitching of tiled 3D
1033 microscopic image acquisitions. *Bioinformatics* **25**, 1463-1465,
1034 doi:10.1093/bioinformatics/btp184 (2009).
- 1035 66 Waterhouse, A. *et al.* SWISS-MODEL: homology modelling of protein structures and
1036 complexes. *Nucleic Acids Res* **46**, W296-W303, doi:10.1093/nar/gky427 (2018).
- 1037 67 Bertoni, M., Kiefer, F., Biasini, M., Bordoli, L. & Schwede, T. Modeling protein
1038 quaternary structure of homo- and hetero-oligomers beyond binary interactions by
1039 homology. *Sci Rep* **7**, 10480, doi:10.1038/s41598-017-09654-8 (2017).
- 1040 68 Studer, G. *et al.* QMEANDisCo-distance constraints applied on model quality
1041 estimation. *Bioinformatics* **36**, 1765-1771, doi:10.1093/bioinformatics/btz828 (2020).
- 1042 69 Studer, G. *et al.* ProMod3-A versatile homology modelling toolbox. *PLoS Comput Biol*
1043 **17**, e1008667, doi:10.1371/journal.pcbi.1008667 (2021).
- 1044 70 Bienert, S. *et al.* The SWISS-MODEL Repository-new features and functionality.
1045 *Nucleic Acids Res* **45**, D313-D319, doi:10.1093/nar/gkw1132 (2017).
- 1046 71 Evans, R. *et al.* Protein complex prediction with AlphaFold-Multimer. *bioRxiv*,
1047 2021.2010.2004.463034, doi:10.1101/2021.10.04.463034 (2022).

- 1048 72 Jumper, J. *et al.* Highly accurate protein structure prediction with AlphaFold. *Nature*
1049 **596**, 583-589, doi:10.1038/s41586-021-03819-2 (2021).
- 1050 73 Chen, S., Zhou, Y., Chen, Y. & Gu, J. fastp: an ultra-fast all-in-one FASTQ
1051 preprocessor. *Bioinformatics* **34**, i884-i890, doi:10.1093/bioinformatics/bty560 (2018).
- 1052 74 Li, H. Aligning sequence reads, clone sequences and assembly contigs with BWA-
1053 MEM. *arXiv: Genomics* (2013).
- 1054 75 Danecek, P. *et al.* Twelve years of SAMtools and BCFtools. *Gigascience* **10**,
1055 doi:10.1093/gigascience/giab008 (2021).
- 1056 76 Dobin, A. *et al.* STAR: ultrafast universal RNA-seq aligner. *Bioinformatics* **29**, 15-21,
1057 doi:10.1093/bioinformatics/bts635 (2013).
- 1058 77 McKenna, A. *et al.* The Genome Analysis Toolkit: a MapReduce framework for
1059 analyzing next-generation DNA sequencing data. *Genome Res* **20**, 1297-1303,
1060 doi:10.1101/gr.107524.110 (2010).
- 1061 78 Brouard, J. S., Schenkel, F., Marete, A. & Bissonnette, N. The GATK joint genotyping
1062 workflow is appropriate for calling variants in RNA-seq experiments. *J Anim Sci*
1063 *Biotechnol* **10**, 44, doi:10.1186/s40104-019-0359-0 (2019).
- 1064 79 Quinlan, A. R. & Hall, I. M. BEDTools: a flexible suite of utilities for comparing
1065 genomic features. *Bioinformatics* **26**, 841-842, doi:10.1093/bioinformatics/btq033
1066 (2010).
- 1067 80 Castel, S. E., Levy-Moonshine, A., Mohammadi, P., Banks, E. & Lappalainen, T.
1068 Tools and best practices for data processing in allelic expression analysis. *Genome*
1069 *Biol* **16**, 195, doi:10.1186/s13059-015-0762-6 (2015).
- 1070 81 Love, M. I., Huber, W. & Anders, S. Moderated estimation of fold change and
1071 dispersion for RNA-seq data with DESeq2. *Genome Biol* **15**, 550,
1072 doi:10.1186/s13059-014-0550-8 (2014).
- 1073 82 Wickham, H. *ggplot2 : elegant graphics for data analysis*. 2nd edn, (Springer
1074 International Publishing, 2016).
- 1075

REFERENCES

- 1 Cuthill, I. C. *et al.* The biology of color. *Science* **357**, doi:10.1126/science.aan0221 (2017).
- 2 Orteu, A. & Jiggins, C. D. The genomics of coloration provides insights into adaptive evolution. *Nat Rev Genet* **21**, 461-475, doi:10.1038/s41576-020-0234-z (2020).
- 3 Fujii, R. The regulation of motile activity in fish chromatophores. *Pigment Cell Res* **13**, 300-319, doi:10.1034/j.1600-0749.2000.130502.x (2000).
- 4 Wucherer, M. F. & Michiels, N. K. A fluorescent chromatophore changes the level of fluorescence in a reef fish. *PLoS One* **7**, e37913, doi:10.1371/journal.pone.0037913 (2012).
- 5 Krishnan, J. & Rohner, N. Cavefish and the basis for eye loss. *Philos Trans R Soc Lond B Biol Sci* **372**, doi:10.1098/rstb.2015.0487 (2017).
- 6 O'Gorman, M. *et al.* Pleiotropic function of the *oca2* gene underlies the evolution of sleep loss and albinism in cavefish. *Curr Biol* **31**, 3694-3701 e3694, doi:10.1016/j.cub.2021.06.077 (2021).
- 7 Gould, S. J. *The structure of evolutionary theory.* (Belknap Press of Harvard University Press, 2002).
- 8 Irion, U. & Nüsslein-Volhard, C. Developmental genetics with model organisms. *Proceedings of the National Academy of Sciences* **119**, e2122148119, doi:doi:10.1073/pnas.2122148119 (2022).
- 9 Salzburger, W. Understanding explosive diversification through cichlid fish genomics. *Nat Rev Genet* **19**, 705-717, doi:10.1038/s41576-018-0043-9 (2018).
- 10 Gerwin, J., Urban, S., Meyer, A. & Kratochwil, C. F. Of bars and stripes: A Malawi cichlid hybrid cross provides insights into genetic modularity and evolution of modifier loci underlying colour pattern diversification. *Mol Ecol* **30**, 4789-4803, doi:10.1111/mec.16097 (2021).
- 11 Kratochwil, C. F. *et al.* An intronic transposon insertion associates with a trans-species color polymorphism in Midas cichlid fishes. *Nat Commun* **13**, 296, doi:10.1038/s41467-021-27685-8 (2022).
- 12 Kon, T. *et al.* The Genetic Basis of Morphological Diversity in Domesticated Goldfish. *Curr Biol* **30**, 2260-2274 e2266, doi:10.1016/j.cub.2020.04.034 (2020).
- 13 Klann, M. *et al.* Variation on a theme: pigmentation variants and mutants of anemonefish. *Evodevo* **12**, 8, doi:10.1186/s13227-021-00178-x (2021).
- 14 Salis, P. *et al.* Thyroid hormones regulate the formation and environmental plasticity of white bars in clownfishes. *Proc Natl Acad Sci U S A* **118**, doi:10.1073/pnas.2101634118 (2021).
- 15 Paris, J. R. *et al.* A large and diverse autosomal haplotype is associated with sex-linked colour polymorphism in the guppy. *Nat Commun* **13**, 1233, doi:10.1038/s41467-022-28895-4 (2022).
- 16 Schartl, M. *et al.* The Developmental and Genetic Architecture of the Sexually Selected Male Ornament of Swordtails. *Curr Biol* **31**, 911-922 e914, doi:10.1016/j.cub.2020.11.028 (2021).
- 17 Powell, D. L. *et al.* The Genetic Architecture of Variation in the Sexually Selected Sword Ornament and Its Evolution in Hybrid Populations. *Curr Biol* **31**, 923-935 e911, doi:10.1016/j.cub.2020.12.049 (2021).

- 18 Wang, L. *et al.* Genomic Basis of Striking Fin Shapes and Colors in the Fighting Fish. *Mol Biol Evol* **38**, 3383-3396, doi:10.1093/molbev/msab110 (2021).
- 19 Kwon, Y. M. *et al.* Genomic consequences of domestication of the Siamese fighting fish. *Sci Adv* **8**, eabm4950, doi:10.1126/sciadv.abm4950 (2022).
- 20 Kelsh, R. N. *et al.* The Tomita collection of medaka pigmentation mutants as a resource for understanding neural crest cell development. *Mech Dev* **121**, 841-859, doi:10.1016/j.mod.2004.01.004 (2004).
- 21 Singh, A. P. & Nusslein-Volhard, C. Zebrafish stripes as a model for vertebrate colour pattern formation. *Curr Biol* **25**, R81-R92, doi:10.1016/j.cub.2014.11.013 (2015).
- 22 Patterson, L. B. & Parichy, D. M. Zebrafish Pigment Pattern Formation: Insights into the Development and Evolution of Adult Form. *Annu Rev Genet* **53**, 505-530, doi:10.1146/annurev-genet-112618-043741 (2019).
- 23 Parichy, D. M. Evolution of pigment cells and patterns: recent insights from teleost fishes. *Curr Opin Genet Dev* **69**, 88-96, doi:10.1016/j.gde.2021.02.006 (2021).
- 24 Irion, U. & Nusslein-Volhard, C. The identification of genes involved in the evolution of color patterns in fish. *Curr Opin Genet Dev* **57**, 31-38, doi:10.1016/j.gde.2019.07.002 (2019).
- 25 Streisinger, G., Walker, C., Dower, N., Knauber, D. & Singer, F. Production of clones of homozygous diploid zebra fish (*Brachydanio rerio*). *Nature* **291**, 293-296, doi:10.1038/291293a0 (1981).
- 26 Creaser, C. W. The Technic of Handling the Zebra Fish (*Brachydanio rerio*) for the Production of Eggs Which Are Favorable for Embryological Research and Are Available at Any Specified Time Throughout the Year. *Copeia* **4**, 159-161, doi:10.2307/1435845 (1934).
- 27 Haffter, P. *et al.* Mutations affecting pigmentation and shape of the adult zebrafish. *Dev Genes Evol* **206**, 260-276, doi:10.1007/s004270050051 (1996).
- 28 Odenthal, J. *et al.* Mutations affecting xanthophore pigmentation in the zebrafish, *Danio rerio*. *Development* **123**, 391-398, doi:10.1242/dev.123.1.391 (1996).
- 29 Lister, J. A., Robertson, C. P., Lepage, T., Johnson, S. L. & Raible, D. W. nacre encodes a zebrafish microphthalmia-related protein that regulates neural-crest-derived pigment cell fate. *Development* **126**, 3757-3767, doi:10.1242/dev.126.17.3757 (1999).
- 30 Irion, U. *et al.* Gap junctions composed of connexins 41.8 and 39.4 are essential for colour pattern formation in zebrafish. *Elife* **3**, e05125, doi:10.7554/eLife.05125 (2014).
- 31 Henke, K. *et al.* Genetic Screen for Postembryonic Development in the Zebrafish (*Danio rerio*): Dominant Mutations Affecting Adult Form. *Genetics* **207**, 609-623, doi:10.1534/genetics.117.300187 (2017).
- 32 Johnson, S. L., Africa, D., Walker, C. & Weston, J. A. Genetic control of adult pigment stripe development in zebrafish. *Dev Biol* **167**, 27-33, doi:10.1006/dbio.1995.1004 (1995).
- 33 Eskova, A., Frohnhof, H. G., Nusslein-Volhard, C. & Irion, U. Galanin Signaling in the Brain Regulates Color Pattern Formation in Zebrafish. *Curr Biol* **30**, 298-303 e293, doi:10.1016/j.cub.2019.11.033 (2020).

- 34 Parichy, D. M. Advancing biology through a deeper understanding of zebrafish ecology and evolution. *Elife* **4**, doi:10.7554/eLife.05635 (2015).
- 35 McCluskey, B. M. & Postlethwait, J. H. Phylogeny of zebrafish, a "model species," within *Danio*, a "model genus". *Mol Biol Evol* **32**, 635-652, doi:10.1093/molbev/msu325 (2015).
- 36 Parichy, D. M. & Johnson, S. L. Zebrafish hybrids suggest genetic mechanisms for pigment pattern diversification in *Danio*. *Dev Genes Evol* **211**, 319-328, doi:10.1007/s004270100155 (2001).
- 37 Patterson, L. B., Bain, E. J. & Parichy, D. M. Pigment cell interactions and differential xanthophore recruitment underlying zebrafish stripe reiteration and *Danio* pattern evolution. *Nat Commun* **5**, 5299, doi:10.1038/ncomms6299 (2014).
- 38 Spiewak, J. E. *et al.* Evolution of Endothelin signaling and diversification of adult pigment pattern in *Danio* fishes. *PLoS Genet* **14**, e1007538, doi:10.1371/journal.pgen.1007538 (2018).
- 39 McCluskey, B. M., Uji, S., Mancusi, J. L., Postlethwait, J. H. & Parichy, D. M. A complex genetic architecture in zebrafish relatives *Danio quagga* and *D. kyathit* underlies development of stripes and spots. *PLoS Genet* **17**, e1009364, doi:10.1371/journal.pgen.1009364 (2021).
- 40 Hoekstra, H. E. Genetics, development and evolution of adaptive pigmentation in vertebrates. *Heredity (Edinb)* **97**, 222-234, doi:10.1038/sj.hdy.6800861 (2006).
- 41 Braasch, I., Brunet, F., Volff, J. N. & Schartl, M. Pigmentation pathway evolution after whole-genome duplication in fish. *Genome Biol Evol* **1**, 479-493, doi:10.1093/gbe/evp050 (2009).
- 42 Lorin, T., Brunet, F. G., Laudet, V. & Volff, J. N. Teleost Fish-Specific Preferential Retention of Pigmentation Gene-Containing Families After Whole Genome Duplications in Vertebrates. *G3 (Bethesda)* **8**, 1795-1806, doi:10.1534/g3.118.200201 (2018).
- 43 Kratochwil, C. F. *et al.* Agouti-related peptide 2 facilitates convergent evolution of stripe patterns across cichlid fish radiations. *Science* **362**, 457-460, doi:10.1126/science.aao6809 (2018).
- 44 Stern, D. L. & Orgogozo, V. The loci of evolution: how predictable is genetic evolution? *Evolution* **62**, 2155-2177, doi:10.1111/j.1558-5646.2008.00450.x (2008).
- 45 Stern, D. L. & Orgogozo, V. Is genetic evolution predictable? *Science* **323**, 746-751, doi:10.1126/science.1158997 (2009).
- 46 Martin, A. & Orgogozo, V. The Loci of repeated evolution: a catalog of genetic hotspots of phenotypic variation. *Evolution* **67**, 1235-1250, doi:10.1111/evo.12081 (2013).
- 47 Ohno, S. *Evolution by gene duplication*. (Springer-Verlag, 1970).
- 48 Pasquier, J. *et al.* Evolution of gene expression after whole-genome duplication: New insights from the spotted gar genome. *J Exp Zool B Mol Dev Evol* **328**, 709-721, doi:10.1002/jez.b.22770 (2017).
- 49 Braasch, I. *et al.* The spotted gar genome illuminates vertebrate evolution and facilitates human-teleost comparisons. *Nat Genet* **48**, 427-437, doi:10.1038/ng.3526 (2016).
- 50 Thompson, A. W. *et al.* The bowfin genome illuminates the developmental evolution of ray-finned fishes. *Nat Genet* **53**, 1373-1384, doi:10.1038/s41588-021-00914-y (2021).

- 51 Abitua, P. B., Wagner, E., Navarrete, I. A. & Levine, M. Identification of a rudimentary neural crest in a non-vertebrate chordate. *Nature* **492**, 104-107, doi:10.1038/nature11589 (2012).
- 52 Hall, B. K. The neural crest as a fourth germ layer and vertebrates as quadroblastic not triploblastic. *Evolution & Development* **2**, 3-5, doi:<https://doi.org/10.1046/j.1525-142x.2000.00032.x> (2000).
- 53 Richardson, J. *et al.* Leader Cells Define Directionality of Trunk, but Not Cranial, Neural Crest Cell Migration. *Cell Rep* **15**, 2076-2088, doi:10.1016/j.celrep.2016.04.067 (2016).
- 54 Alhashem, Z. *et al.* Notch controls the cell cycle to define leader versus follower identities during collective cell migration. *Elife* **11**, doi:10.7554/eLife.73550 (2022).
- 55 Lencer, E., Prekeris, R. & Artinger, K. B. Single-cell RNA analysis identifies pre-migratory neural crest cells expressing markers of differentiated derivatives. *Elife* **10**, doi:10.7554/eLife.66078 (2021).
- 56 Nord, H., Kahsay, A., Denhag, N., Pedrosa Domellof, F. & von Hofsten, J. Genetic compensation between Pax3 and Pax7 in zebrafish appendicular muscle formation. *Dev Dyn* **251**, 1423-1438, doi:10.1002/dvdy.415 (2022).
- 57 Elworthy, S., Lister, J. A., Carney, T. J., Raible, D. W. & Kelsh, R. N. Transcriptional regulation of mitfa accounts for the sox10 requirement in zebrafish melanophore development. *Development* **130**, 2809-2818, doi:10.1242/dev.00461 (2003).
- 58 Curran, K. *et al.* Interplay between Foxd3 and Mitf regulates cell fate plasticity in the zebrafish neural crest. *Dev Biol* **344**, 107-118, doi:10.1016/j.ydbio.2010.04.023 (2010).
- 59 Petratou, K., Spencer, S. A., Kelsh, R. N. & Lister, J. A. The MITF paralog tfec is required in neural crest development for fate specification of the iridophore lineage from a multipotent pigment cell progenitor. *PLoS One* **16**, e0244794, doi:10.1371/journal.pone.0244794 (2021).
- 60 Jang, H. S. *et al.* Epigenetic dynamics shaping melanophore and iridophore cell fate in zebrafish. *Genome Biol* **22**, 282, doi:10.1186/s13059-021-02493-x (2021).
- 61 Krauss, J. *et al.* transparent, a gene affecting stripe formation in Zebrafish, encodes the mitochondrial protein Mpv17 that is required for iridophore survival. *Biol Open* **2**, 703-710, doi:10.1242/bio.20135132 (2013).
- 62 Parichy, D. M. & Turner, J. M. Temporal and cellular requirements for Fms signaling during zebrafish adult pigment pattern development. *Development* **130**, 817-833, doi:10.1242/dev.00307 (2003).
- 63 Parichy, D. M., Rawls, J. F., Pratt, S. J., Whitfield, T. T. & Johnson, S. L. Zebrafish sparse corresponds to an orthologue of c-kit and is required for the morphogenesis of a subpopulation of melanocytes, but is not essential for hematopoiesis or primordial germ cell development. *Development* **126**, 3425-3436, doi:10.1242/dev.126.15.3425 (1999).
- 64 O'Reilly-Pol, T. & Johnson, S. L. Kit signaling is involved in melanocyte stem cell fate decisions in zebrafish embryos. *Development* **140**, 996-1002, doi:10.1242/dev.088112 (2013).
- 65 Dooley, C. M., Mongera, A., Walderich, B. & Nusslein-Volhard, C. On the embryonic origin of adult melanophores: the role of ErbB and Kit signalling in establishing melanophore stem cells in zebrafish. *Development* **140**, 1003-1013, doi:10.1242/dev.087007 (2013).

- 66 Dorsky, R. I., Raible, D. W. & Moon, R. T. Direct regulation of nacre, a zebrafish MITF homolog required for pigment cell formation, by the Wnt pathway. *Genes Dev* **14**, 158-162 (2000).
- 67 Mo, E. S., Cheng, Q., Reshetnyak, A. V., Schlessinger, J. & Nicoli, S. Alk and Ltk ligands are essential for iridophore development in zebrafish mediated by the receptor tyrosine kinase Ltk. *Proc Natl Acad Sci U S A* **114**, 12027-12032, doi:10.1073/pnas.1710254114 (2017).
- 68 Fadeev, A. *et al.* ALKALs are in vivo ligands for ALK family receptor tyrosine kinases in the neural crest and derived cells. *Proc Natl Acad Sci U S A* **115**, E630-E638, doi:10.1073/pnas.1719137115 (2018).
- 69 Parichy, D. M. *et al.* Mutational analysis of endothelin receptor b1 (rose) during neural crest and pigment pattern development in the zebrafish *Danio rerio*. *Dev Biol* **227**, 294-306, doi:10.1006/dbio.2000.9899 (2000).
- 70 Krauss, J. *et al.* Endothelin signalling in iridophore development and stripe pattern formation of zebrafish. *Biol Open* **3**, 503-509, doi:10.1242/bio.20148441 (2014).
- 71 Brombin, A. *et al.* Tfp2b specifies an embryonic melanocyte stem cell that retains adult multifate potential. *Cell Rep* **38**, 110234, doi:10.1016/j.celrep.2021.110234 (2022).
- 72 Budi, E. H., Patterson, L. B. & Parichy, D. M. Post-embryonic nerve-associated precursors to adult pigment cells: genetic requirements and dynamics of morphogenesis and differentiation. *PLoS Genet* **7**, e1002044, doi:10.1371/journal.pgen.1002044 (2011).
- 73 Singh, A. P. *et al.* Pigment Cell Progenitors in Zebrafish Remain Multipotent through Metamorphosis. *Dev Cell* **38**, 316-330, doi:10.1016/j.devcel.2016.06.020 (2016).
- 74 Mahalwar, P., Walderich, B., Singh, A. P. & Nusslein-Volhard, C. Local reorganization of xanthophores fine-tunes and colors the striped pattern of zebrafish. *Science* **345**, 1362-1364, doi:10.1126/science.1254837 (2014).
- 75 Saunders, L. M. *et al.* Thyroid hormone regulates distinct paths to maturation in pigment cell lineages. *Elife* **8**, doi:10.7554/eLife.45181 (2019).
- 76 McMenamain, S. K. *et al.* Thyroid hormone-dependent adult pigment cell lineage and pattern in zebrafish. *Science* **345**, 1358-1361, doi:10.1126/science.1256251 (2014).
- 77 Parichy, D. M., Ransom, D. G., Paw, B., Zon, L. I. & Johnson, S. L. An orthologue of the kit-related gene *fms* is required for development of neural crest-derived xanthophores and a subpopulation of adult melanocytes in the zebrafish, *Danio rerio*. *Development* **127**, 3031-3044, doi:10.1242/dev.127.14.3031 (2000).
- 78 Mills, M. G., Nuckels, R. J. & Parichy, D. M. Deconstructing evolution of adult phenotypes: genetic analyses of kit reveal homology and evolutionary novelty during adult pigment pattern development of *Danio* fishes. *Development* **134**, 1081-1090, doi:10.1242/dev.02799 (2007).
- 79 Singh, A. P., Schach, U. & Nusslein-Volhard, C. Proliferation, dispersal and patterned aggregation of iridophores in the skin prefigure striped colouration of zebrafish. *Nat Cell Biol* **16**, 607-614, doi:10.1038/ncb2955 (2014).
- 80 Gur, D. *et al.* In situ differentiation of iridophore crystalotypes underlies zebrafish stripe patterning. *Nat Commun* **11**, 6391, doi:10.1038/s41467-020-20088-1 (2020).

- 81 Eskova, A. *et al.* Gain-of-function mutations in Aqp3a influence zebrafish pigment pattern formation through the tissue environment. *Development* **144**, 2059-2069, doi:10.1242/dev.143495 (2017).
- 82 Lang, M. R., Patterson, L. B., Gordon, T. N., Johnson, S. L. & Parichy, D. M. Basonuclin-2 requirements for zebrafish adult pigment pattern development and female fertility. *PLoS Genet* **5**, e1000744, doi:10.1371/journal.pgen.1000744 (2009).
- 83 Patterson, L. B. & Parichy, D. M. Interactions with iridophores and the tissue environment required for patterning melanophores and xanthophores during zebrafish adult pigment stripe formation. *PLoS Genet* **9**, e1003561, doi:10.1371/journal.pgen.1003561 (2013).
- 84 McCluskey, B. M., Liang, Y., Lewis, V. M., Patterson, L. B. & Parichy, D. M. Pigment pattern morphospace of Danio fishes: evolutionary diversification and mutational effects. *Biol Open* **10**, doi:10.1242/bio.058814 (2021).
- 85 Lewis, V. M. *et al.* Fate plasticity and reprogramming in genetically distinct populations of Danio leucophores. *Proc Natl Acad Sci U S A* **116**, 11806-11811, doi:10.1073/pnas.1901021116 (2019).
- 86 Huang, D. *et al.* Development and genetics of red coloration in the zebrafish relative Danio albolineatus. *Elife* **10**, doi:10.7554/eLife.70253 (2021).
- 87 Bagnara, J. T., Fernandez, P. J. & Fujii, R. On the blue coloration of vertebrates. *Pigment Cell Res* **20**, 14-26, doi:10.1111/j.1600-0749.2006.00360.x (2007).
- 88 Goda, M. *et al.* Integumental reddish-violet coloration owing to novel dichromatic chromatophores in the teleost fish, *Pseudochromis diadema*. *Pigment Cell Melanoma Res* **24**, 614-617, doi:10.1111/j.1755-148X.2011.00861.x (2011).
- 89 Scharl, M. *et al.* What is a vertebrate pigment cell? *Pigment Cell Melanoma Res* **29**, 8-14, doi:10.1111/pcmr.12409 (2016).
- 90 Frohnhof, H. G., Krauss, J., Maischein, H. M. & Nusslein-Volhard, C. Iridophores and their interactions with other chromatophores are required for stripe formation in zebrafish. *Development* **140**, 2997-3007, doi:10.1242/dev.096719 (2013).
- 91 Watanabe, M., Sawada, R., Aramaki, T., Skerrett, I. M. & Kondo, S. The Physiological Characterization of Connexin41.8 and Connexin39.4, Which Are Involved in the Striped Pattern Formation of Zebrafish. *J Biol Chem* **291**, 1053-1063, doi:10.1074/jbc.M115.673129 (2016).
- 92 Mahalwar, P., Singh, A. P., Fadeev, A., Nusslein-Volhard, C. & Irion, U. Heterotypic interactions regulate cell shape and density during color pattern formation in zebrafish. *Biol Open* **5**, 1680-1690, doi:10.1242/bio.022251 (2016).
- 93 Usui, Y., Aramaki, T., Kondo, S. & Watanabe, M. The minimal gap-junction network among melanophores and xanthophores required for stripe pattern formation in zebrafish. *Development* **146**, doi:10.1242/dev.181065 (2019).
- 94 Watanabe, M. *et al.* Spot pattern of leopard Danio is caused by mutation in the zebrafish connexin41.8 gene. *EMBO Rep* **7**, 893-897, doi:10.1038/sj.embor.7400757 (2006).
- 95 Hultman, K. A., Bahary, N., Zon, L. I. & Johnson, S. L. Gene Duplication of the zebrafish kit ligand and partitioning of melanocyte development functions to kit ligand a. *PLoS Genet* **3**, e17, doi:10.1371/journal.pgen.0030017 (2007).

- 96 Zhang, Y. M. *et al.* Distant Insulin Signaling Regulates Vertebrate Pigmentation through the Sheddase Bace2. *Dev Cell* **45**, 580-594 e587, doi:10.1016/j.devcel.2018.04.025 (2018).
- 97 Eom, D. S. *et al.* Melanophore migration and survival during zebrafish adult pigment stripe development require the immunoglobulin superfamily adhesion molecule Igsf11. *PLoS Genet* **8**, e1002899, doi:10.1371/journal.pgen.1002899 (2012).
- 98 Eom, D. S., Patterson, L. B., Bostic, R. R. & Parichy, D. M. Immunoglobulin superfamily receptor Junctional adhesion molecule 3 (Jam3) requirement for melanophore survival and patterning during formation of zebrafish stripes. *Dev Biol* **476**, 314-327, doi:10.1016/j.ydbio.2021.04.007 (2021).
- 99 Fadeev, A., Krauss, J., Frohnhof, H. G., Irion, U. & Nusslein-Volhard, C. Tight Junction Protein 1a regulates pigment cell organisation during zebrafish colour patterning. *Elife* **4**, doi:10.7554/eLife.06545 (2015).
- 100 Sawada, R., Aramaki, T. & Kondo, S. Flexibility of pigment cell behavior permits the robustness of skin pattern formation. *Genes Cells* **23**, 537-545, doi:10.1111/gtc.12596 (2018).
- 101 Eom, D. S., Bain, E. J., Patterson, L. B., Grout, M. E. & Parichy, D. M. Long-distance communication by specialized cellular projections during pigment pattern development and evolution. *Elife* **4**, doi:10.7554/eLife.12401 (2015).
- 102 Hamada, H. *et al.* Involvement of Delta/Notch signaling in zebrafish adult pigment stripe patterning. *Development* **141**, 318-324, doi:10.1242/dev.099804 (2014).
- 103 Eom, D. S. & Parichy, D. M. A macrophage relay for long-distance signaling during postembryonic tissue remodeling. *Science* **355**, 1317-1320, doi:10.1126/science.aal2745 (2017).
- 104 Iwashita, M. *et al.* Pigment pattern in jaguar/obelix zebrafish is caused by a Kir7.1 mutation: implications for the regulation of melanosome movement. *PLoS Genet* **2**, e197, doi:10.1371/journal.pgen.0020197 (2006).
- 105 Yamanaka, H. & Kondo, S. In vitro analysis suggests that difference in cell movement during direct interaction can generate various pigment patterns in vivo. *Proc Natl Acad Sci U S A* **111**, 1867-1872, doi:10.1073/pnas.1315416111 (2014).
- 106 Inaba, M., Yamanaka, H. & Kondo, S. Pigment pattern formation by contact-dependent depolarization. *Science* **335**, 677, doi:10.1126/science.1212821 (2012).
- 107 Lanni, J. S. *et al.* Integrated K⁺ channel and K⁺Cl⁻ cotransporter functions are required for the coordination of size and proportion during development. *Dev Biol* **456**, 164-178, doi:10.1016/j.ydbio.2019.08.016 (2019).
- 108 Inoue, S., Kondo, S., Parichy, D. M. & Watanabe, M. Tetraspanin 3c requirement for pigment cell interactions and boundary formation in zebrafish adult pigment stripes. *Pigment Cell Melanoma Res* **27**, 190-200, doi:10.1111/pcmr.12192 (2014).
- 109 Frohnhof, H. G. *et al.* Spermidine, but not spermine, is essential for pigment pattern formation in zebrafish. *Biol Open* **5**, 736-744, doi:10.1242/bio.018721 (2016).
- 110 Watanabe, M., Watanabe, D. & Kondo, S. Polyamine sensitivity of gap junctions is required for skin pattern formation in zebrafish. *Sci Rep* **2**, 473, doi:10.1038/srep00473 (2012).

- 111 Hirata, M., Nakamura, K., Kanemaru, T., Shibata, Y. & Kondo, S. Pigment cell organization in the hypodermis of zebrafish. *Dev Dyn* **227**, 497-503, doi:10.1002/dvdy.10334 (2003).
- 112 Hirata, M., Nakamura, K. & Kondo, S. Pigment cell distributions in different tissues of the zebrafish, with special reference to the striped pigment pattern. *Dev Dyn* **234**, 293-300, doi:10.1002/dvdy.20513 (2005).
- 113 Turing, A. M. The chemical basis of morphogenesis. *Phil. Trans. R. Soc. Lond. B* **237**, 37-72 (1952).
- 114 Walderich, B., Singh, A. P., Mahalwar, P. & Nusslein-Volhard, C. Homotypic cell competition regulates proliferation and tiling of zebrafish pigment cells during colour pattern formation. *Nat Commun* **7**, 11462, doi:10.1038/ncomms11462 (2016).
- 115 Stern, D. L. Identification of loci that cause phenotypic variation in diverse species with the reciprocal hemizyosity test. *Trends Genet* **30**, 547-554, doi:10.1016/j.tig.2014.09.006 (2014).
- 116 Jinek, M. *et al.* A programmable dual-RNA-guided DNA endonuclease in adaptive bacterial immunity. *Science* **337**, 816-821, doi:10.1126/science.1225829 (2012).
- 117 Ding, Y., Berrocal, A., Morita, T., Longden, K. D. & Stern, D. L. Natural courtship song variation caused by an intronic retroelement in an ion channel gene. *Nature* **536**, 329-332, doi:10.1038/nature19093 (2016).
- 118 Barrett, R. D. H. *et al.* Linking a mutation to survival in wild mice. *Science* **363**, 499-504, doi:10.1126/science.aav3824 (2019).
- 119 Cal, L. *et al.* Countershading in zebrafish results from an *Asip1* controlled dorsoventral gradient of pigment cell differentiation. *Sci Rep* **9**, 3449, doi:10.1038/s41598-019-40251-z (2019).
- 120 Cal, L. *et al.* Loss-of-function mutations in the melanocortin 1 receptor cause disruption of dorso-ventral countershading in teleost fish. *Pigment Cell Melanoma Res* **32**, 817-828, doi:10.1111/pcmr.12806 (2019).
- 121 Meyer, A., Biermann, C. H. & Orti, G. The phylogenetic position of the zebrafish (*Danio rerio*), a model system in developmental biology: an invitation to the comparative method. *Proc Biol Sci* **252**, 231-236, doi:10.1098/rspb.1993.0070 (1993).
- 122 Endoh, M. *et al.* Hybrid between *Danio rerio* female and *Danio nigrofasciatus* male produces aneuploid sperm with limited fertilization capacity. *PLoS One* **15**, e0233885, doi:10.1371/journal.pone.0233885 (2020).
- 123 Quigley, I. K. *et al.* Evolutionary diversification of pigment pattern in *Danio* fishes: differential *fms* dependence and stripe loss in *D. albolineatus*. *Development* **132**, 89-104, doi:10.1242/dev.01547 (2005).
- 124 Meyer, A., Ritchie P. A., Witte, K.-E. Predicting developmental processes from evolutionary patterns: a molecular phylogeny of the zebrafish (*Danio rerio*) and its relatives. *Phil. Trans. R. Soc. Lond. B* **349**, 103-111, doi:<https://doi.org/10.1098/rstb.1995.0096> (1995).
- 125 Gould, S. J. *Ontogeny and phylogeny*. (Belknap Press of Harvard University Press, 1977).
- 126 Hall, B. K. *Evolutionary developmental biology*. 2nd ed edn, (Kluwer Academic Publ., 1999).
- 127 Toms, M. *et al.* Phagosomal and mitochondrial alterations in RPE may contribute to KCNJ13 retinopathy. *Sci Rep* **9**, 3793, doi:10.1038/s41598-019-40507-8 (2019).

- 128 Toms, M. *et al.* Missense variants in the conserved transmembrane M2 protein domain of KCNJ13 associated with retinovascular changes in humans and zebrafish. *Exp Eye Res* **189**, 107852, doi:10.1016/j.exer.2019.107852 (2019).
- 129 Darwin, C. *The Descent of Man, and Selection in Relation to Sex.* John Murray, London. (1871).